GAS PERMSELECTIVITY IN AMORPHOUS LINEAR AND CROSSLINKED POLY(ARYLENE ETHER KETONES)

by

Silvia Parisi Skischally

Thesis submitted to the Faculty of the
Virginia Polytechnic Institute and State University
in partial fulfillment of the requirements for the degree of

MASTER OF SCIENCE

in

Chemistry (Polymer Science)

APPROVED:

J. E. McGrath, Chairman

T. C. Ward

H. M. McNair

September, 1990

Blacksburg, Virginia

GAS PERMSELECTIVITY
IN AMORPHOUS LINEAR AND CROSSLINKED
POLY(ARYLENE ETHER KETONES)

by

Silvia Parisi Skischally

Committee Chairman: James E. McGrath

Chemistry (Polymer Science)

(ABSTRACT)

The present study addresses a systematic evaluation of the effect of crosslinking via terminal maleimide units on the gas transport properties through a dense polymer film of amorphous Poly(Arylene Ether Ketones) or PEK. The methodology for the preparation of crosslinked Maleimide terminated PEK (or MIPEK) films from several blend ratios of different molecular weights of MIPEK is discussed in detail.

The primary focus of this work has been to investigate the influence of different degrees of crosslinking on gas permeabilities and selectivities, with an objective of producing a highly selective membrane. It has been demonstrated that crosslinking markedly decreases the permeation of methane, without changing the values for molecules such as helium.

ACKNOWLEDGEMENTS

The author wishes to express her most sincere appreciation to Prof. James E. McGrath for his valuable support, guidance and understanding. She would also like to thank Prof. Harold M. McNair for his infinite help and moral support. In addition, she would like to thank Prof. T. C. Ward for participating in her advisory committee and for his valuable suggestions.

She would like to extend her special thanks to Greg Lyle, Jeff Hedrick, Jim Senger, Niranjan Patel and Maria Spinu for their suggestions in the experimental work and for their friendship.

The author would also like to express her gratitude to INTEVEP (Venezuelan Petroleum Institute for Research and Development) for the financial support she received during the past few years.

Also, she would like to express her thanks to her husband for his love and infinite patience during her research.

TABLE OF CONTENTS

Table of Contents (Continued)

Table of Contents (Continued)

LIST OF TABLES

List of Tables (Continued)

LIST OF FIGURES

List of Figures (Continued)

List of Figures (Continued)

List of Figures (Continued)

LIST OF APPENDIX

CHAPTER I

INTRODUCTION AND LITERATURE REVIEW

I.A. Introduction to Polymeric Membranes.

Polymeric membranes are highly attractive materials for gas separation due to the versatility of polymers to produce thin and strong films with a wide range of chemical and physical characteristics [1].

The history of polymeric membranes is long. The first known work on permeability of gases was reported in 1831 by Mitchell [2] in his work with natural rubber membranes. The area of synthetic membranes began with the invention in 1846 of cellulose nitrate, the first semisynthetic polymer. Since then and for approximately one hundred years, most of the work that was done was related to cellulosic type membranes. More recently a great variety of new synthetic polymeric membranes has been evaluated and used for commercial applications. Moreover, the developments made in configuration and packing design of membrane systems as well as the significant advances made in membrane preparation or physical structure have made the polymeric membranes very effective separating systems that can be highly competitive to the more traditional separation processes for several gas treatment applications.

Some examples of membrane materials are listed in Table 1 [3].

Table 1. Some Membrane Materials [3].

Modified Natural Products.

- Cellulose Acetate
- Cellulose Acetobutyrate
- Cellulose Nitrate

Synthetic Polymers

- Polyamides
- Poly (vinyl alcohol)
- Vinyl Polymers
- Polysulfones
- Polyimides

Others

- Porous Glass
- Graphite Oxide
- Aluminium Oxide

Research in this area is directed to the development of gas separation membranes with:

- high permeability and selectivity
- high flux for an extended period of time
- mechanical stability
- temperature stability
- chemical resistance
- absence of pinholes or mechanical defects

conditions that are necessary characteristics in order to obtain an economically feasible membrane.

I.B. Applications of Membrane-Based Gas Separation Technology.

The great interest in membranes separation technology is mainly due to the fact that these are highly energy-efficient devices compared to the traditional separation technologies. Also, the required process equipment is very simple, compact and easy to operate and control. In addition, one of the biggest advantages over the conventional processes is that the equipment is modular and can be easily scaled-up or operated by reduced capacity if needed.

The most important applications of membrane-based gas separation technology have been in general classified, according to the ease of the gas separation involved, into three major areas [2]:

i - Hydrogen separation from slower permeating gases such as CO, CH_4 and N_2.

ii - Separation of acid gases such as H_2S, CO_2 and water from natural gas.

iii - O_2 and N_2 enrichment from air.

The first separation (i) is possible due to the very small molecular size of the hydrogen molecule which makes it more permeable than the more bulky gases. Most of the commercially installed operating plants today are for the separation of hydrogen from different industrial gas streams. Typical applications of this separation are:

- **H_2 recovery in:**
  - . Synthesis of ammonia
  - . Hydrotreatment of purge gas
  - . Synthesis of methanol
- **H_2 enrichment in:**
  - . Naphta catalytic reformers
  - . Fluid catalytic cracking
  - . Hydrocrackers

The second separation (ii) is possible due to the high solubility of CO_2, H_2S and H_2O in membranes at low partial pressures and to the bulky CH_4 which has low solubility and diffusivity coefficients. Examples of this application are:

- . Gas Sweetening (CO_2 and/or H_2S removal)
- . CO_2 reclamation for Enhanced Oil Recovery

. Dehydration of Natural Gas (CH_4)

. CO_2 removal from low BTU gas

The most difficult of the three separations is the third one (iii), since the polymer membranes available up to date have relative low separation factors for O_2/N_2 ($O_2/N_2 < 6$). The difficulty of this separation is because N_2 and O_2 are very similar in size and shape as well as their solubilities in most membranes are similar. Thus, the permeability of these two gases is almost the same. Selectivities for O_2/N_2 of 30 have been reported [4] with a facilitated-transport membrane for O_2 yielding over 80% of O_2. However, it has not found practical applications since the metal-organic complex used as the carrier oxidized irreversibly and consequently the lifetime of this membrane is very limited. Nevertheless, there is a large potential market involving these separations, e.g.:

- Oxygen enrichment of air for medical and furnace applications.
- Nitrogen enrichment of air for blanketing of fuels and chemical storage.

Membranes processes for O_2/N_2 separations have been developed and commercialized that can for some applications, economically perform this separation. However, research in this area is still been conducted with emphasis in facilitated-transport membranes in order to achieve better O_2/N_2 separations.

Besides the three previously mentioned separations, there are other areas that can be named as non-conventional applications such as:

- Separation of ethane, ethylene and methane in the direct conversion of methane (C1 Chemistry).

- Separation of olefins in the petrochemical industry.
- Membrane reactors by which it is possible to shift equilibrium controlled reactions by removal of product(s) to achieve higher conversions.

I.C. Factors Affecting Gas Permeability Through Polymers.

The rate at which gases permeate through different polymers can vary over many orders of magnitude and depends on several factors which are gas and polymer related. The factors that govern the gas flux and the permselectivity are listed in Table 2.

In order to understand the influence of these factors, the fundamental principles that control the membrane-based gas separation processes will be briefly described. The permeation of gases through dense polymer films is the result of two processes [5-7]:

. Diffusion of the penetrant in the polymer matrix, and

. Solubility of the penetrant into the polymer material.

The first process or diffusion is a kinetic quantity and it is a measure of the gas mobility in the free volume within the polymer. The diffusion process is a function of the physical and chemical structure of the membrane and the size, shape and polarity of the penetrant. Thus, this process is largely determined by the dynamics between polymer and penetrant.

Table 2. Factors Affecting Gas Permeability through Polymers [8-10].

- <u>Penetrant Related</u>
    - . Chemical Composition
    - . Physical Characteristics (Size and Shape) of the Penetrant Molecule.

- <u>Polymer Related</u>
    - . Chemical Composition
    - . Physical Structure:
        - Polymer Porosity
        - Packing Density
        - Side Chains
        - Crosslinking
        - Additives (plasticizers and fillers)
        - Degree of Crystallinity and Orientation
    - . Physical Aging

- <u>Temperature and Pressure</u>

The second process or solubility is controlled by thermodynamics and is a measure of the affinity between the penetrant and polymer. The solubility process is a function of polymer-penetrant interactions and of the amount of excess voids or interchain gaps in the polymer.

The permeability is a statistical process that may be understood as a thermal motion of the polymer chains creating a microvoid large enough to allow the passage of a penetrant molecule. The probability of the formation of this microvoid is higher in the direction of the concentration gradient and will result in a net flux through the film. The expression for the local flux of the penetrant at any point in the polymer film is given by:

$$F = - D (- dC/dx) \quad (1)$$

where: F = Flux of the penetrant in unit of time per unit of area

D = Diffusion Coefficient

C = Concentration of penetrant

The gas molecule will move from one microvoid to another. This process is commonly referred as "diffusion jump" and requires certain amount of energy (activation energy potential barrier) to be localized next to the penetrant to permit the molecule to execute the jump. The diffusion coefficient, D, can then be expressed in terms of a pre-exponential factor, D_o and of the activation energy for the diffusion process, E_d:

$$D = D_o \exp(-E_d/RT) \quad (2)$$

The value of E_d will depend on the degree of interaction between the polymer and the penetrant and determines the energy associated with the formation of the microvoid. The value of D_o is related to the number of microvoids in the polymer. Thus, the net flux of diffusion depends on the number and size distribution of the microvoids and how easy they can be formed.

The number of existing microvoids depends on the polymer chain packing and is a function of the free volume and density of the polymer. The easiness of formation of the microvoids depends on the mobility of the polymer chains and is a function of chain stiffness and cohesive energy of the polymer. Then, the presence of crosslinking, crystalline regions and additives affect the diffusion process by changing the size and the distribution of these microvoids.

I.D. Mechanism of Gas Separation.

A membrane or permeable medium can be defined as a phase between two phases [11]. In the case of a membrane gas separation process, the role of the membrane is to change the composition of the mixture based on the relative permeation rates of the different components to obtain a concentrated stream in one component and a residue stream or non-permeate.

The accepted process for the permeation of gases through nonporous polymer membranes is a "solution-diffusion" mechanism [5-7]. This mechanism can be explained with a cross-section through a planar membrane. If a film of thickness "l" and area "A" separates two chambers which contain a permeable gas at different pressures, the gas will permeate from the high pressure chamber to the low pressure chamber. The application of gas pressure in one chamber will produce the absorption of the gas in the membrane at this side of the interphase, then the molecular diffusion of the gas through the membrane and the desorption of this gas at the other interphase. This situation is the basis of the time-lag method for the determination of diffusion coefficients (Appendix C).

In general, for most of the membrane gas separations, molecular diffusion is the slower or the rate-determining step in gas permeation. The absorption and desorption steps are very fast and the equilibrium is established at the interphases.

The diffusion of gases through polymer membranes are described by Fick's first and second laws. From practical experimental considerations, the rate of gas permeation is determined under steady-state conditions, that is where concentration is not varying with time. The steady state is achieved when constant pressures P_1 and P_2 are constantly maintained at the two sides of the membrane at a constant temperature. Fick's first law is the fundamental law of diffusion for the steady state rate of gas

permeation through a planar membrane. It states that the flux is proportional to the concentration gradient:

$$J = - D \, (dc/dx) \qquad (3)$$

where: J = amount of substance diffusing across unit area per unit time

D = proportionality factor or diffusion coefficient

If at zero time, a gas pressure of P_1 is applied in chamber 1 in a system that was initially free of gas, the amount of gas that will permeate the membrane (Q) is given by:

$$Q/l.C_1 = f \, (D,t,l) \qquad (4)$$

where: C_1 = concentration of gas at the interphase adjacent to chamber 1

assuming that an instantaneous equilibrium is established at the interphase. A plot of this equation is shown in Appendix C where the y axis represents $J/l.C_1$ and the x axis is equal to $D.t/l$. After an initial build-up period (θ = time lag), a linear relationship is developed as $t \rightarrow \infty$. Under these last conditions, the previous equation simplifies to:

$$Q = (D.C_1/l) \, . \, (t - l^2/6D) \qquad (5)$$

where the time-lag is the intercept on the time axis: $\theta = l^2/6D$

In the linear region of this curve, the concentrations are static or $(dC/dt) = 0$. Then, the flux is given by:

$$J = - D (C_2 - C_1)/l \tag{6}$$

and the total permeant that diffused through a film of area A is:

$$Q = - D.A.t (C_2 - C_1)/l \tag{7}$$

Assuming that Henry's law applies at the interphases, the solubility coefficient, S is given by:

$$S = C_1/p_1 = C_2/p_2 \tag{8}$$

and

$$Q = - D.S.A.t (p_2 - p_1)/l \tag{9}$$

Thus, if $D.S = P$ = permeability coefficient, then:

$$Q = - P.A.t \Delta p/l \tag{10}$$

When $p_1 >> p_2$ under the normal experimental conditions:

$$Q = P.A.t p_1/l \tag{11}$$

The selectivity of a nonporous membrane towards two components A and B in a gas mixture is expressed as the ideal separation factor α :

$$\alpha_{AB} = P_A/P_B \qquad (12)$$

I.E. Dense Polymeric Membranes.

An homogeneous, non-porous membrane is a dense film which is capable of transporting penetrants under driving forces of pressure, concentration or electrical potential. Table 3 shows the separation processes associated with each one of these driving forces.

Dense polymeric membranes are high-polymer-density films with almost no voids in a colloidal structure. In general, transport rates are higher for amorphous polymers than in crystalline or crosslinked polymers.

There is a compromise between the transport rate and the physical strength of the material, since although crosslinking and crystallinity reduce the transport of penetrants, they give proper mechanical strength to the film.

Mainly, two basic membrane configurations are used:

i - Flat sheets, prepared by extrusion of the melted polymer or by casting a film from a polymer solution.

ii - Hollow Fibers, prepared by extrusion.

Table 3. Driving Forces in Membrane Separations [12].

. <u>Pressure Driven Processes.</u>

- Microporous Filtration
- Ultrafiltration
- Reversed Osmosis or Hyperfiltration

. <u>Concentration Driven Processes.</u>

- Dialysis
- Gas Separation

. <u>Applied Voltage</u>

- Electrodialysis

Dense polymeric films are normally prepared by the three following methods:

- Solvent Cast
- Melt - Extruded
- Direct Polymerization (dense membranes formed during polymerization).

The factors in membrane preparation that influence its final characteristics are listed in Table 4. A fairly detailed description of these factors can be found in the work of Govind [13].

I.F. Literature Review.

The following review corresponds to gas transport literature related to the crosslinking effect in polymer films. For reviews regarding to other areas like:

- History of Membrane Technology [2,12,14,15]
- Gas Transport through Polymers/Polymers Permeability [5-7]
- Dual Mode Transport and other Theories [16-23]

the reader is referred to the references specified above.

Table 5 provides brief descriptions of the references concerning gas permeabilities through crosslinked polymeric systems. The references in the table are presented in order of their date of publication and represent the information obtained through an on-line search using

Table 4. Factors that Affect Dense Membrane Preparation by Solvent-Casting.

Film Formation.

i - Solvent Characteristics:

- Polymer - Solvent interactions (dispersion)
- Polymer - Polymer interactions (aggregation)
- Solvent Vapor Pressure

ii - Rate of Solvent Evaporation

iii - Casting Surface

iv - Relative Humidity

v - Contamination with Atmospheric Particles

Film Treatments.

i - Thermal Annealing (T > Tg)

ii - Presence of Plasticizers by Exposure to Solvents.

Table 5. List of References on the Effects of Polymer Crosslinking on Gas Transport Properties.

REFERENCE No.	SUMMARY COMMENTS
27	Study of Gas Diffusion and Solution in highly crosslinked copolymers membranes.
24	Crosslinking caused by air and vacuum-irradiated Polyethylene. Irradiation decreased the total permeability and separation factor of CH_4-N_2 gas mixtures.
25	Gamma-Irradiated Teflon FEP copolymer films. Diffusion and permeability coefficients of CH_4 and N_2 decreased with the irradiation dose whereas solubility coefficients were not greatly affected.
41	Gas permeation of collagen films afffected by crosslinking, moisture and plasticizer content.
30	Diffusion of gases in crosslinked polysiloxanes.

Table 5 (continued).

28	Anomalous O_2 and CO_2 permeabilities of m-divinylbenzene-styrene copolymer films on the degree of crosslinking and temperature.
42	O_2 permeation indicates crosslink density, chain flexibility and bulkiness of linker.
31	Effect of crosslink density on gas permeability of styrene-cured polyester networks.
32	H_2, CO_2, O_2, N_2 and CH_4 permeation through covalently-bonded, crosslinked poly(arylene oxide) dense film membranes.
33,34	Gas permeation through Amino Ketone crosslinked polyphenylene oxide polymers.
47	Mechanical and gas transport properties of poly-epsilon-caprolactone model networks. Gas permeability decreased with increasing crosslinking density in non-crystalline networks.

Table 5 (continued).

37	Swelling study of crosslinked PHEMA.
39	Effects of crosslinking on polymer swelling for polystyrene-cyclohexane system.
43	Crosslinking from photooxidation in poly(ether amides).
44	Sorption overshoot for cyclohexane (20-50°C) in crosslinked PS due to relaxation mechanisms.
29	O_2/N_2 gas permselectivity through novel crosslinked polyorganosiloxane-base copolymers.
38	Swelling of crosslinked PHEMA.
40	Effects of crosslinking on polymer swelling for polystyrene-cyclohexane system.
35	O_2/N_2 gas permselectivity through fluorine-containing acrylate, methacrylate or a crosslinked compound of the polymer.

Table 5 (continued).

45	Effect of UV radiation on the permeation of He, H_2, CO_2, Ar and N_2 through poly(ethylene terephthalate).
36	Gas permeation through Ammonium salts crosslinked membranes.
26	Electron-beam-irradiated polymer films. The permeability coefficients of CO_2, CH_4, O_2, N_2, SF_6 and He decreased with increasing irradiation dose.

Chemical Abstracts as the data base by covering the period from 1970 to April 1990.

Initial studies on the effect of crosslinks on gas permeation were carried out with rubber of different degrees of vulcanization [8]. These studies showed that as the degree of crosslinking increased the diffusion constants decreased and the change was greater, the larger the molecule of the penetrant. Several studies have been reported on radiation crosslinked polymers [8, 24-26, 45, 46]. As in the case of crosslinking in rubber, it was found that there is a reduction in the diffusion constants and the permeability coefficients with irradiation dose.

The diffusion and solution of gases in crosslinked copolymers have been also studied. A study performed with a copolymer system of ethylacrylate (EA) and different compositions of tetraethyleneglycoldimethacrylate (TEGDM) as crosslinking agent [27] suggested that high permeation rates are obtained at the expense of the permselectivity.

An anomalous behavior for the dependance of O_2 and CO_2 permeabilities on the degree of crosslinking was reported for membranes of m-divinylbenzene-styrene copolymers. For several cases, the permeabilities increased with increasing the degree of crosslinking [28].

Crosslinked polyorganosiloxane - based copolymers capable of providing suitable permselectivities and mechanical strength have been patented for O_2/N_2 separation [29]. Studies of highly crosslinked polysiloxanes showed that the diffusion of gases depended on the structure of the polymer used. The addition of alkylalkoxysilanes to

poly(methylphenylsiloxane) decreased the diffusion and solubility coefficients of gases. The decrease was attributed to an increase in the density of three-dimensional crosslinks [30].

The effect of crosslinking density on the gas permeability of crosslinked polyesters in the glassy state has been evaluated. The study reported that the permeability coefficient increased with decreasing the total number of crosslinks and the content of elastic-active and inactive crosslinks [31].

Crosslinked phenylene oxide polymer compositions comprising the reaction product of an alkyl halogenated phenylene oxide polymer and ammonia have been patented by Monsanto. These crosslinked polymers have crosslinks between phenyl groups represented by the structural formula $-CH_2-NH-CH_2-$. O_2/N_2 selectivities up to 5.5 were reported [32].

Crosslinked phenylene oxide polymer compositions comprising the reaction product of a haloacylated phenylene oxide and a primary monoamine have been also patented by Monsanto [33,34] as membrane materials. O_2/N_2 selectivities of 4.7 were found for the example composition given by the authors.

Gas separating membranes from fluorine- containing acrylates or methacrylates polymers or a crosslinked compound of this polymer have been patented for O_2/N_2 separations [35]. Selectivities of 3.0 to 4.1 were obtained.

The separation of ethylene from methane and ethane has been reported [36] by using membranes prepared with crosslinked hydrophilic

polyvinyl alcohol and nylon and the films contain complex forming metal components active in the presence of water.

The swelling behavior of poly (2-hydroxyethylmethacrylate) (PHEMA) has been modified by changing the crosslinking density. The swelling studies of crosslinked PHEMA [37,38] showed that increasing the amount of crosslinker increased the elastic retractive force and reduced the degree of swelling. The swelling rate of the polymer decreased with increasing crosslinker, since crosslinking decreased diffusivity of the penetrant and relaxation of the polymer chains. The same complex effects of crosslinking on polymer swelling have been also reported for polystyrene-cyclohexane system [39,40].

No gas transport studies regarding crosslinked maleimide terminated Poly(Arylene Ether Ketones) have yet been reported.

I.G. Research Objectives.

The primary purpose of this research was to study the influence of different degrees of crosslinking on gas permeabilities and selectivities through amorphous linear and model terminally end-linked or crosslinked Poly(Arylene Ether Ketones) or PEK. This system would have the advantage of excellent chemical resistance and mechanical properties. Moreover, the crosslinking could produce a high selective membrane. In order to achieve this objective it was necessary to develop a work methodology for the preparation of Poly(Arylene Ether Ketones) films and to design a work scheme capable to produce different degrees of crosslinking by thermal

reaction of maleimide terminated PEK blends of different molecular weights and compositions.

The effects of polymer crosslinking on gas transport properties have been previously studied by several investigators (Section II). However, the work in this particular area has been questioned [8] since these previous studies were performed by:

- Introducing sulphur into a rubber, which could change the cohesive energy of the polymer, or by
- Radiation induced crosslinking that could also produce changes in crystallinity or chemical structure, or by
- Introducing different crosslinkers to form the network.

Therefore it has been argued that it could be difficult to separate these various factors from the net effect of polymer crosslinking on gas permeation. The final objective of this research was then to perform a systematic evaluation of the crosslinking effect on gas transport properties through a dense polymer film.

CHAPTER II

EXPERIMENTAL PROCEDURE

This chapter contains a detailed description of the procedure followed for the synthesis of the polymeric materials used in this work, the methodology developed for the preparation of films and the crosslinking experimental procedure. A general overview of the gas permeation equipment, the gas permeabilities calculations and the technique used in the characterization of the samples are also presented.

II. A. Synthesis of the Polymeric Systems Studied.

This section contains a description of the synthesis of the control linear high molecular weight polymer and the oligomers used for the free radical crosslinking studies.

II. A.1. Synthesis of the Control Polymer.

Amorphous linear end capped Poly (Arylene Ether Ketone) or PEK was used as a control thermoplastic oligomer. A sample of number average molecular weights of approximately 20,000 g/mol (or 0.551 dl/gm intrinsic viscosity at 25°C in chloroform) was synthesized by nucleophilic aromatic substitution, step polymerization of bisphenol-A(phenolate) with 4,4′-di-fluorobenzophenone as the activated aromatic

halide and mono-fluorobenzophenone was used as the monofunctional end capper. This synthesis was performed by colleagues of the author in our laboratories at VPI & SU [48]. The schematic representation of this reaction is shown in Figure 1.

II. A.2. Synthesis of the Oligomers for Crosslinking Studies.

Maleimide terminated amorphous Poly(Arylene Ether Ketones) or MIPEK of controlled molecular weights and end group functionalities were also synthesized in our laboratories at VPI & SU by nucleophilic aromatic substitution, step polymerization of bis-phenol-A with di-fluoro-benzophenone in the presence of m-aminophenol or 2,2′ (4-aminophenyl-4-hydroxyphenyl) propane. The synthesis of the MIPEK oligomers used in the present work was carried out as a two step reaction. The first step involved the synthesis of amine terminated oligomers of predictable molecular weight and in the second step the amine was converted to the maleimide. For this conversion, the terminal amines were reacted with maleic anhydride in the presence of chlorobenzene as a co-solvent. The schematic diagram of the complete polymerization procedure is shown in Figure 2. For more specific details on the synthesis of the MIPEK oligomers others than the ones provided above, the reader is referred to the work of Lyle, et al [48].

The titrated molecular weights of the MIPEK oligomers synthesized for this work are reported in Table 6 and will be referred from now on in the text as 5K, 10K, 16K and 20K g/mol.

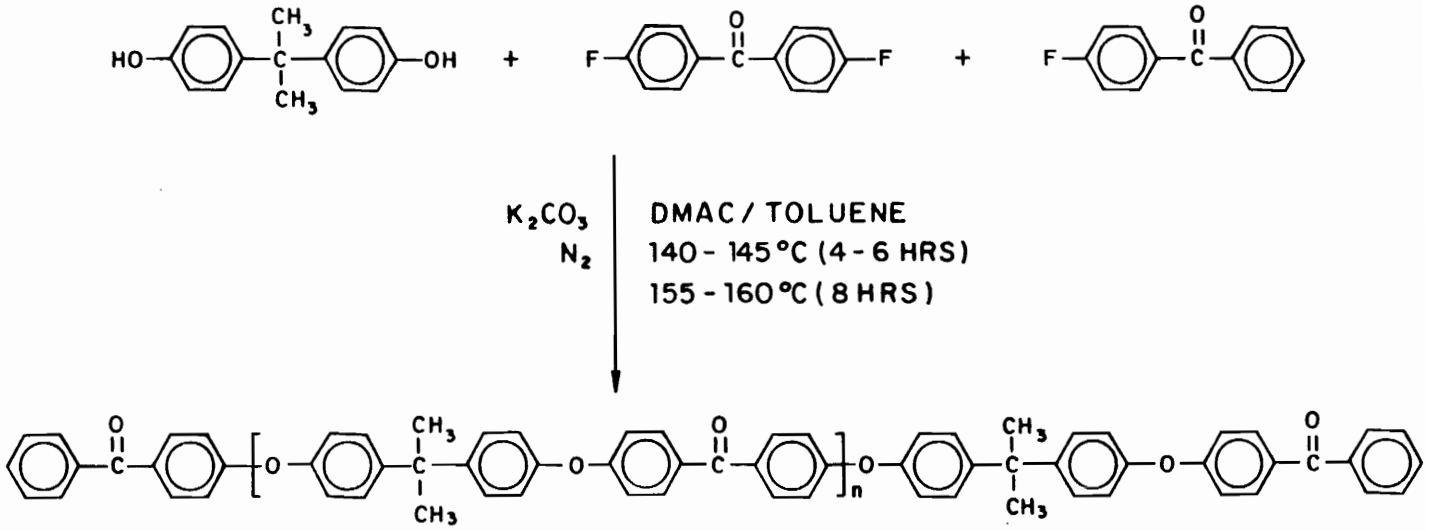

Figure 1. Synthesis of an Amorphous Poly(Ether Ketone)

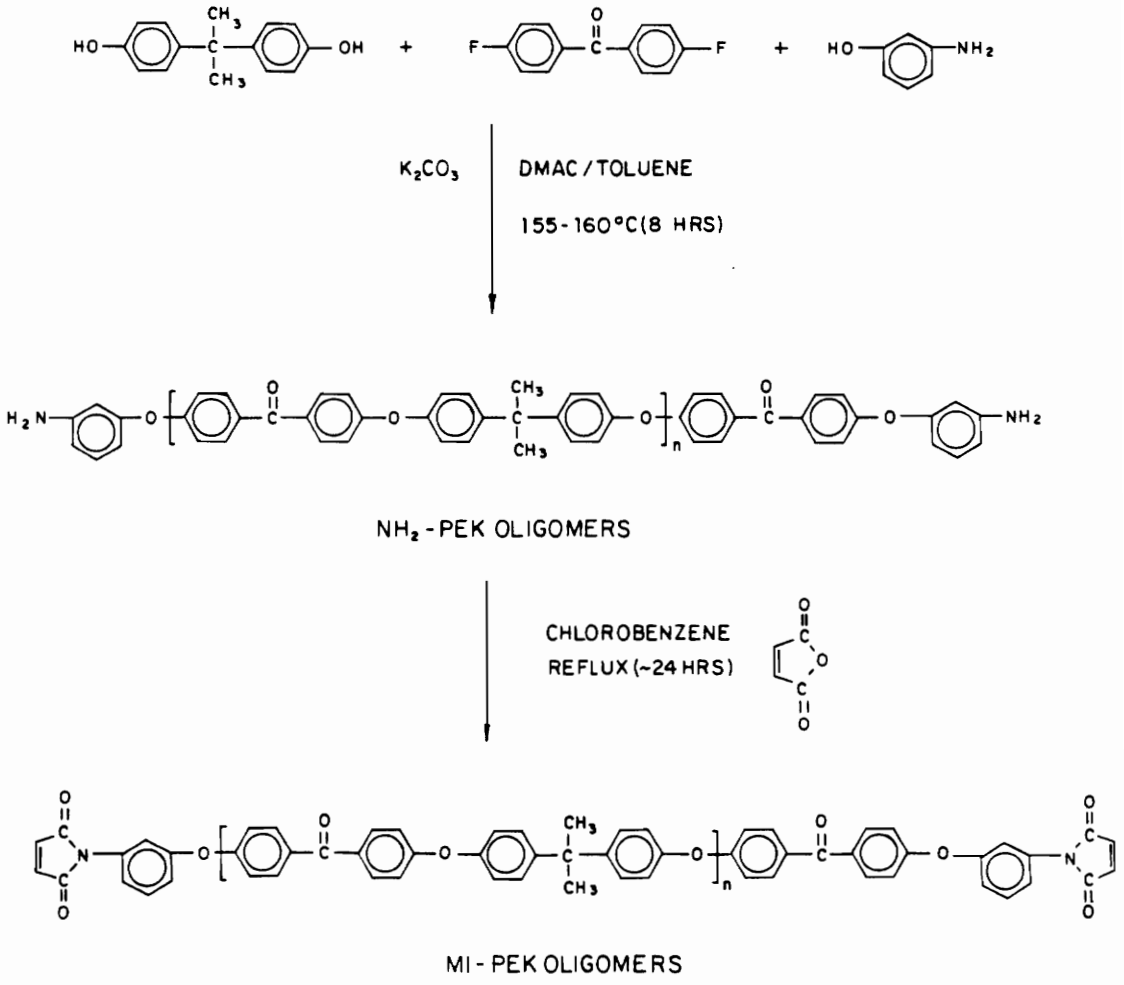

Figure 2. Synthesis of Maleimide Terminated Poly(Arylene Ether Ketone) Oligomers.

Table 6. Titrated Number Average Molecular Weights ($\bar{M}n$) of the MIPEK Oligomers.

Molecular Weight*	Titrated $\bar{M}n$
20K	22300
16K	16200
10K	10600
5K	5900

* As referred in the text.

Amine terminated Poly (Arylene Ether Ketone) oligomers were titrated with an acid-base potentiometric titrator (COSA Instrument Corporation, MCI-Automatic Titrator, Model GT-05) in order to determine their number average molecular weights ($\overline{Mn}$) before imidization.

The titration procedure consisted in the dissolution of about 0.3 gms of the polymer in 50 mls of chlorobenzene and the addition of 10 mls of acetic acid. HBr dissolved in glacial acetic acid was used as the titrant in the potentiometric titration. The titrant was previously standardized with potassium hydrogen phthalate (KHP).

II. B. Materials Systems.

The effects of the degree of crosslinking and crosslink density on the gas permselectivities through amorphous maleimide terminated Poly(Arylene Ether Ketones) were studied by varying the molecular weights of the MIPEK oligomers, the weight ratio of the different molecular weight oligomers and reaction time of the thermally induced crosslinking reaction. The systematic research scheme developed by the author for this thesis is schematically shown in Table 7. The combination of different molecular weight oligomers and different weight ratios were selected so that a non-brittle, self-supporting polymer films were obtained (e.g. experimentation with films prepared from 20K/5K, 25/75 ratios were too brittle for reproducible gas permeability measurements).

Table 7. Molecular Weights and Blend Ratios of Maleimide Terminated Poly (Arylene Ether Ketones) utilized for Dense Film Solution Fabrication (a).

MIPEK Oligomers ($\overline{M}n$)x 10^3 gm/mole	Oligomer Weight Ratio w/w
20	100%
16	100%
10	100%
20/10	95/5
	75/25
	50/50
20/5	95/5
	75/25
	50/50
16/5	95/5
	75/25
	50/50

(a) For each composition, the films were carefully dried and then thermally crosslinked @ 250°C for 10, 30 and 120 minutes.

II. C. Preparation of Polymer Membranes.

This section contains a detailed description of the methodology developed by the author for the preparation of polymeric membranes suitable for gas permeation characterization. The procedure consisted of several steps as shown in Figure 3:

- Oligomer(s) solution preparation
- Substrate surface modification and conditioning
- Solution casting
- Film drying
- Film crosslinking
- Film removal
- Film cutting and thickness determination

This steps are individually discussed below.

II. C.1 Oligomer(s) Solutions Preparation:

The preparation of the oligomer solutions was performed according to the following steps:

a. Reprecipitation of the oligomers

b. Solution preparation

c. Solution filtration

a. Reprecipitation of the Oligomer(s):

Oligomers were precipitated first in methanol from chlorobenzene which was the co-solvent used in the synthesis, then filtered and dried under vacuum below than 60°C for several days until the solvents were

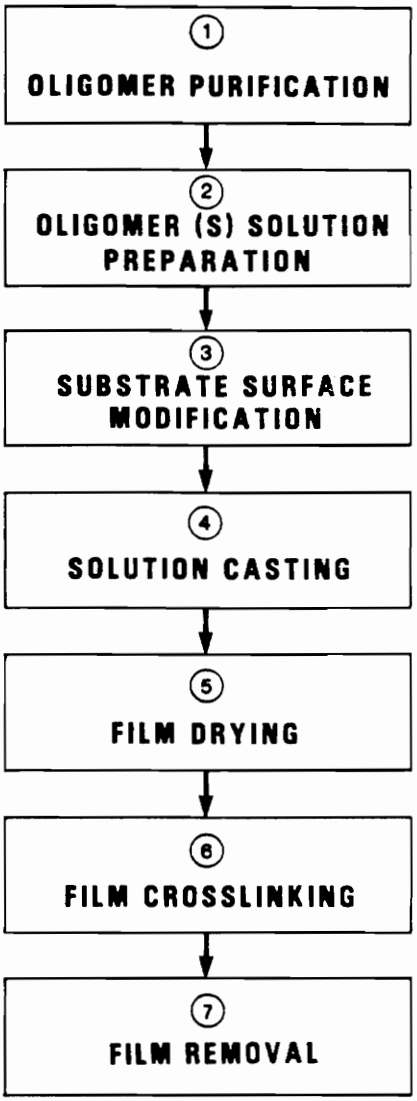

Figure 3. Film Preparation Procedure

essentially removed. Next, the oligomers were reprecipitated in methanol from a 10% (w/w) solution of the oligomer in chloroform. For each ml of polymer solution used, approximately 7 ml of methanol were used in the precipitation. The precipitated polymer was again dried under vacuum at about 60°C for several days. The absence of solvent in the sample was determined by thermogravimetric analysis (TGA) using a Dupont Thermogravimetric analyzer.

The oligomers were kept in a dessicator under vacuum prior to use in order to avoid possible moisture sorption from the environment.

b. Solution Preparation.

Oligomer(s) solutions of 23-25% (w/w) of the oligomer(s) (total solids content) in dry chloroform as a solvent were used for film preparation. An example of the calculation procedure is presented in Appendix A. Approximately 40-45 mls of total solution were prepared each time. Solutions were shaken in an "orbit shaker" until complete dissolution of the oligomer(s) was observed.

c. Solution Filtration.

The oligomer(s) were filtered through PTFE (Teflon) filters of 10.0 microns pore size and 47 mm of diameter (MSI) prior to solution casting. A stainless steel pressure filtration funnel (Gelman Sciences, Inc. Product No. 4280) was used for filtration as illustrated in Figure 4 by applying approximately 40 psig of inlet nitrogen gas pressure. The filtration was performed at room temperature and the filtrated solutions

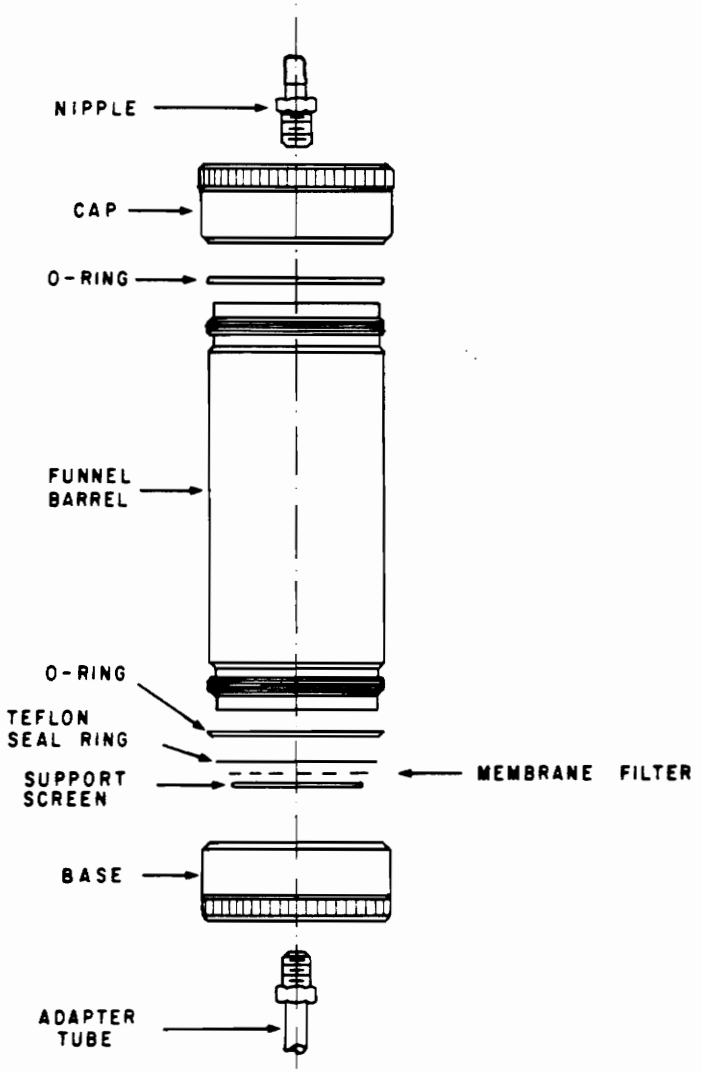

Figure 4. Pressure Filtration Funnel.

were collected in previously carefully cleaned small jars (~ 60 mls). The filtered solutions were again agitated in an "orbit shaker" until use, in order to eliminate any gas bubbles prior to the film casting procedure.

II. C.2 Substrate Surface Modification.

Glass plates of 8" x 12" and 1/8" thick were carefully cleaned with an abrasive soap, washed with water, flushed with acetone and finally air dried at room temperature. The plates were then immersed in a concentrated solution of dichlorodimethylsilane or chlorotrimethylsilane in toluene and placed in an air convection oven at 250°C for 1 hour. The plates were then carefully removed from the oven and allowed to cool to room temperature. Next, they were rinsed and cleaned with pure toluene by using a soft cloth. Once again, the glass plates were placed in the oven at 250°C for 1 hour in order to eliminate traces of residual solvent. The glass plates were then removed from the oven, cooled to room temperature and immediately used for casting the films. The previous procedure was repeated prior to each individual membrane film preparation.

II. C.3 Solution Casting.

A 23-25% (w/w) filtered solution of the oligomer(s) in chloroform (see Section II. C.1) was cast on the previously treated glass plates (see Section II. C.2) using the "Doctor blade" technique. An adjustable micrometer aluminum film applicator (Paul N. Gardner Company,Inc. Cat No.

AP-M06) with a path width of 6" and a gate clearance adjustable from 0 to 1/4" increments of 1 mil with resolution to 1/2 mil was used to cast the films on the glass plates as illustrated in Figure 5. The clean applicator was placed at the upper end of the glass plate and approximately 15 mls of the oligomer solution were poured directly in front of the blade. The applicator was then drawn in a slow and uniform fashion toward the lower end of the glass plate. The applicator was immediately cleaned with chloroform after use. Films of uniform thickness (see Section II. C.7 for a more detailed discussion) were cast with this technique by setting the gate clearance in approximately 1.5 mils.

The complete procedure of film casting was conducted inside a glove bag to eliminate any possible contamination of the film with dust particles.

II. C.4 Film Drying.

Films prepared as specified in the previous section were allowed to air dry at room temperature for 1 hour. The glass plates with films were then placed in an air convection oven (Microprocessor Oven-Imperial IV, Lab-Line Instruments, Inc.) under the following conditions:

- 40°C for 1 hour
- 60 - 160°C @ <0.5°C/min.
- 160 - 250°C @ 1-2°C/min.

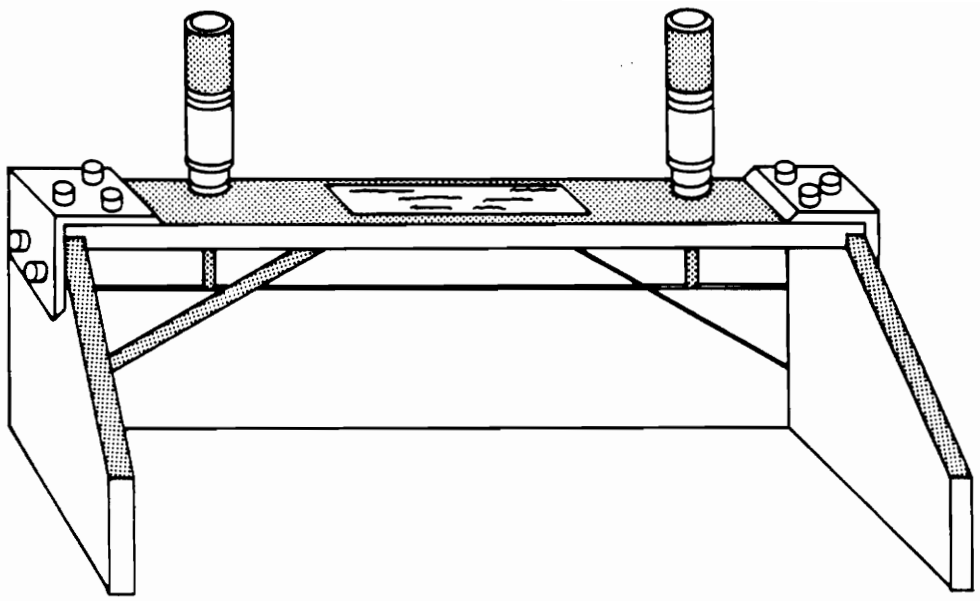

Figure 5. Micron Film Applicator (adjustable knife-blade).

II. C.5 Film Crosslinking Procedure.

The oligomers were crosslinked through a thermally induced free radical reaction across the double bonds of the two maleimide end groups (f = 4) in order to form the crosslinked network. Figure 6 shows the schematic representation of an idealized crosslinking reaction. Since the reaction takes place at the end groups, a high molecular weight network between the crosslinking sites can be attained.

Experimentally, the films were crosslinked according to the following procedure: when the oven reached 250°C as described in section II. C.4, three different films were quenched at different times. The quench times of films A, B and C from 250°C were 10, 30 and 120 minutes, respectively.

Films specimen were then fast cooled to room temperature by removing the glass plates, together with the oven tray in order to avoid cracking and breaking of the glass plates due to the abrupt change in temperature.

II. C.6 Film Removal.

Once the films were cooled to room temperature as described in section II. C.5, the films were then trimmed along their edges with a razor blade. This procedure instantaneously released the films from the glass plates. This step was meticulously performed to avoid any possible rupture of the films. The films were then lifted and stored on clean tissues until their use.

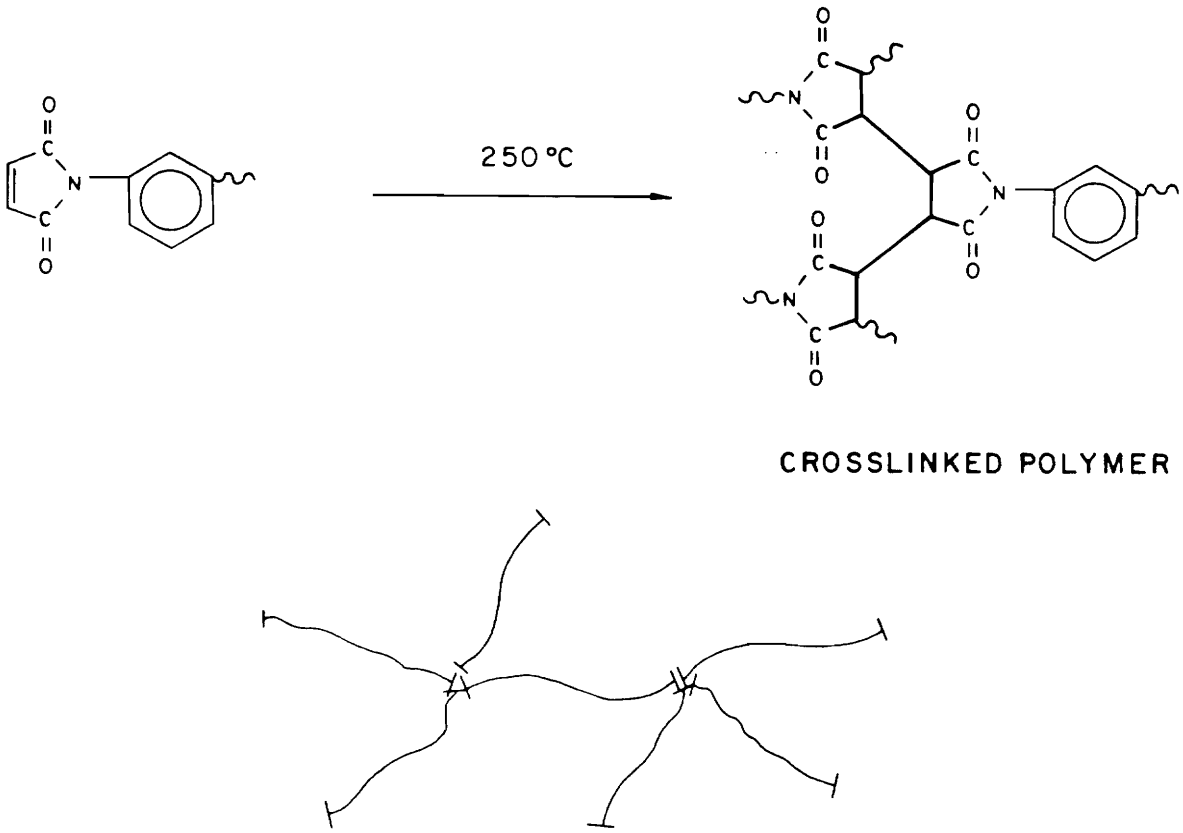

Figure 6. Curing of Maleimide Capped Polyether Ketone Oligomer.

II. C.7 Film Cutting and Thickness Measurement.

Films prepared in section II. C.6 were then cut to approximately 88 mm diameter with a razor blade attached to a compass by using a flat rubber piece in the center position of the compass. This procedure needed to be carefully accomplished so as to avoid any damage of the polymeric membrane.

The remaining portions of the film were saved and stored for additional characterization (i.e. % insolubles, crosslinking density, etc.).

Membranes obtained by the previous procedure were usually about 25.4 to 50.8 microns (1 to 2 mils) thick with a relative standard deviation (RSD) of less than 5%, as determined by an average of 56 readings across the diameter of the film. The thickness of the films was determined with a Minitest FD (ElektroPhysik, Model SM-10) having an accuracy of ± 3%. In order to avoid possible damage of the membrane to be used in the gas permeation analysis, a preliminary and approximate thickness was measured before the permeation test by using the average of 2 thickness readings. After the gas permeation measurements were completed, the final film thickness was determined by using the average of the 56 readings (see Appendix B for an example). The schematic diagram of the complete film preparation procedure is shown in Figure 7.

1- OLIGOMER(S) SOLUTIONS PREPARATION:

- 23-25% (W/W) TOTAL SOLIDS OLIGOMER(S) SOLUTION IN $CHCl_3$
- SOLUTION FILTRATION THROUGH 10 μm TEFLON FILTER

2- SOLUTION CASTING:

- SOLUTION CASTING ON TREATED GLASS PLATES WITH ADJUSTABLE BLADE.
- GLASS SURFACE TREATMENT:
  - $(CH_3)_2$ $SICl_2$ AND $(CH_3)_3$ SICl/TOLUENE
  - 250° C/1 hr.
  - COOLING TO ROOM TEMPERATURE
  - RINSE WITH TOLUENE

3- FILM DRYING CONDITIONS:

- AIR DRIED @ ROOM TEMPERATURE/1 hr.
- AIR CONVECTION OVEN:
  - 40° C/1 hr.
  - 60° C -160° C @ < 1°C/min.
  - 160° C - 250° C @ 1-2° C/min.

Figure 7. Film Preparation Procedure.

4- FILM X-LINKING

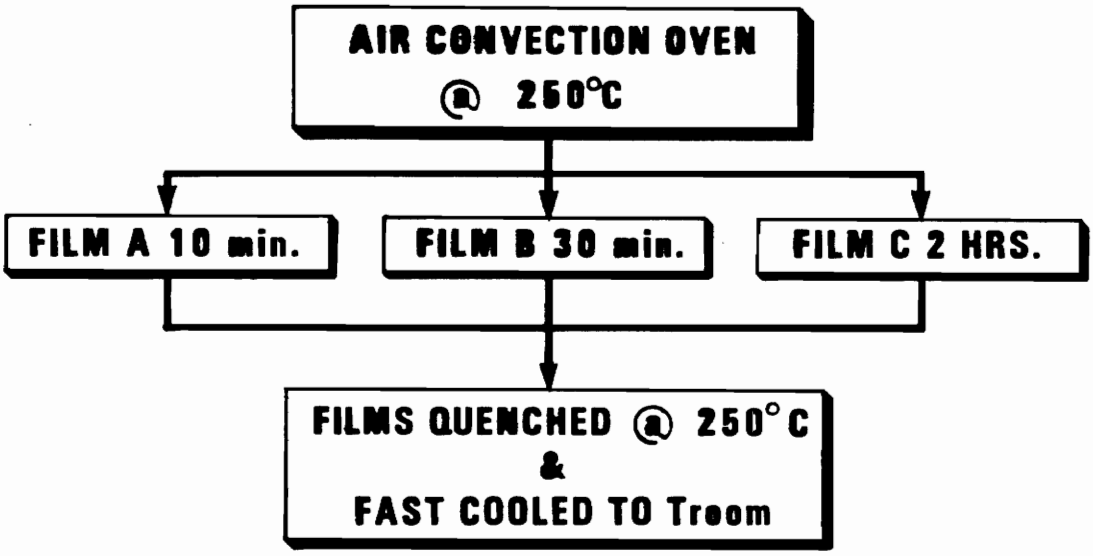

5- FILM REMOVAL

FILMS WERE REMOVED FROM GLASS PLATES BY TRIMMING THE EDGES

Figure 7. Film Preparation Procedure (Continued).

II. D. Film Characterization Techniques.

II. D.1 Percent Insolubles Determination Procedure.

The amount of insoluble portion in the crosslinked films was determined by extraction studies performed in chloroform. The percent of insolubles or the gel fraction in the sample was used as an indicator of the degree of crosslinking attained by the thermally induced reaction.

The steps in the extraction procedure for the determination of the percent of insolubles [49] are described below:

1 - Thimbles pre-treatment:

Paper thimbles were soaked in chloroform for at least 12 hours and later placed in numbered 150 mls beakers which were then heated in a vacuum oven at 110-120°C for about 18 hours. The thimbles were cooled inside the vacuum oven for 4 hours and then removed for their weight determination. The weight was recorded using an analytical balance (± 0.0001 g), the weighing procedure was as rapid as possible, to avoid moisture sorption and weight gain. Each thimble weight was recorded to a 1.0 mg accuracy.

2 - Sample weight (before extraction):

Approximately 0.5 - 0.8 g of the sample (crosslinked polymeric film) were weighed on an analytical balance (± 0.0001 g) and this value recorded to a 1.0 mg accuracy (e.g. 0.553 g). The sample was then placed in a pretreated thimble.

3 - Extraction Procedure:

Soxhlets with a round bottom flask of 500 mls capacity were used for the extraction of the samples in chloroform. The thimble with the sample was placed in the Soxhlet apparatus containing about 350 mls of chloroform. Samples were extracted for 5 days.

4 - Drying Procedure:

After extraction, the thimbles were removed from the Soxhlets and given the same drying procedure described in step 1 (thimbles pre-treatment).

5 - Sample Weight (after extraction):

Thimbles containing the extracted samples were weighted as described before and their weight recorded again with a 1.0 mg accuracy.

6 - % Insolubles Calculation:

The calculation procedure is as follows:

$$W\ (\text{polymer after}) = W\ (\text{polymer + thimble})_{\text{after}} - W\ (\text{thimble})$$

$$\%\ \text{Insolubles} = \frac{W\ (\text{polymer after})}{W\ (\text{polymer before})} \times 100$$

The procedure described before was appropriate to achieve a constant weight of the samples and was reproducible.

II. D.2 Swelling of Network Polymer Films.

The degree of swelling of the previously extracted films (section II. D.1) was determined in order to approximate the number of effective network chains (crosslinks) per unit volume of polymer, the crosslink

density per unit volume of the polymer and the molecular weight between crosslinks.

A. Procedure

The swelling procedure described here was performed by using chloroform as the swelling solvent and the following gravimetric technique was followed.

Approximately 0.300 g of a previously extracted and dried polymer film was cut and weighed. The weighed samples were then placed in small stoppered vials containing enough chloroform to cover the films. The samples were soaked in chloroform for 7 days and weighed. The procedure was repeated after 14 days and 30 days and the samples weighed again until constant weight was achieved. When the sample was removed from the solvent, it was blot dried with a kimwipe paper and rapidly weighed. This step was performed rapidly to minimize the loss of chloroform by evaporation.

B. Calculations

The crosslink density dc (network chains/cc) and the number average molecular weight of the network chain, $\bar{M}c$ (gms/mol) were calculated according to the following procedure [50]:

B. 1. Number Average Molecular Weight of Network Chain ($\bar{M}c$).

$$V_\infty = \text{final swollen volume} = \frac{w_o}{d_p} + \frac{w_\infty - w_o}{d_s} \ (=) \ cc$$

where: w_o = initial polymer weight in gms

w_∞ = weight of swollen polymer in gms

d_p = polymer density = 1.25 gms/cc

d_s = solvent density (1.484 gms/cc for chloroform)

$$C = \text{relative concentration} = \frac{w_o}{d_p V_\infty} \ (=) \ \text{dimensionless}$$

$$\bar{M}c = \frac{-V_s d_p (C^{1/3} - C/2)}{\ln(1-C) + C + XC^2} \ (=) \ g/mol$$

where: V_s = molar volume of solvent = $\frac{MW_s}{d_s} = \frac{119.39 \text{ gms/mol}}{1.484 \text{ gms/cc}}$

V_s = 80.45 cc/mole for chloroform

X = Flory-Huggins constant = 0.388 for MIPEK - chloroform @ 25°C [50]

B.2 CROSSLINK DENSITY (dc)

$$dc = \frac{d_p \times N_{AV}}{Mc} \ (=) \ \text{network chains/cc}$$

where: d_p = polymer density = 1.25 gms/cc

$N_{AV} = 6.023 \times 10^{23}$

$\bar{M}c$ = Number Average MW of network chain

B.3. Swelling Ratio (Q)

$$Q = \frac{w_\infty}{w_o} \ (=) \ \text{dimensionless}$$

II. D.3. Differential Scanning Calorimetry (DSC).

All the DSC characterizations utilized in this research were performed on a DSC DuPont Model 2100 Differential Scanning Calorimeter. This instrument was installed and operated in Dr. T. C. Ward's laboratory. The thin films were submitted for DSC analysis after the crosslinking procedure and before the permeation experiments. First and second heats were recorded from 50 to 250°C at 10°C/min. DSC were used to detect any possible change in the glass transition temperatures (Tg) of the crosslinked samples with different degrees of crosslinking.

II. E. Gas Permeability Measurements.

II. E.1. Gas Permeation Equipment.

The permeability instrument utilized in this research was a low pressure manometric device developed at VPI & SU [19]. A simplified scheme of the gas permeation equipment is shown in Figure 8 and its schematic diagram in Figure 9. The permeability system consisted of the following main integrated components:

a. Automated control and data acquisition system.

b. Gas supply and regulating system.

c. Pressure measuring device.

d. Permeation cell.

e. Vacuum supply system.

f. Thermostated Bath.

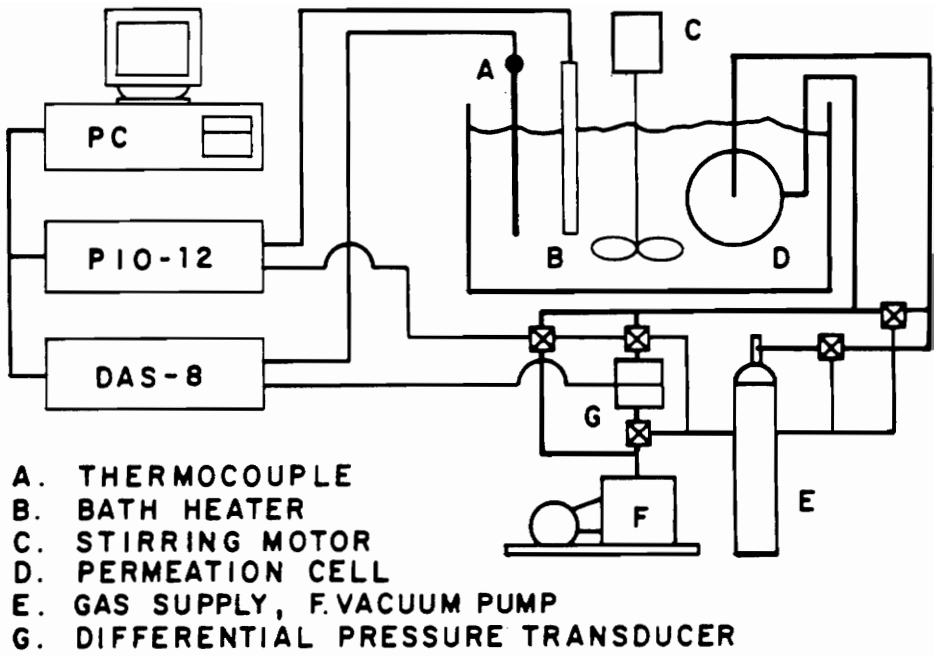

Figure 8. Permeability Instrumentation Scheme. [19]

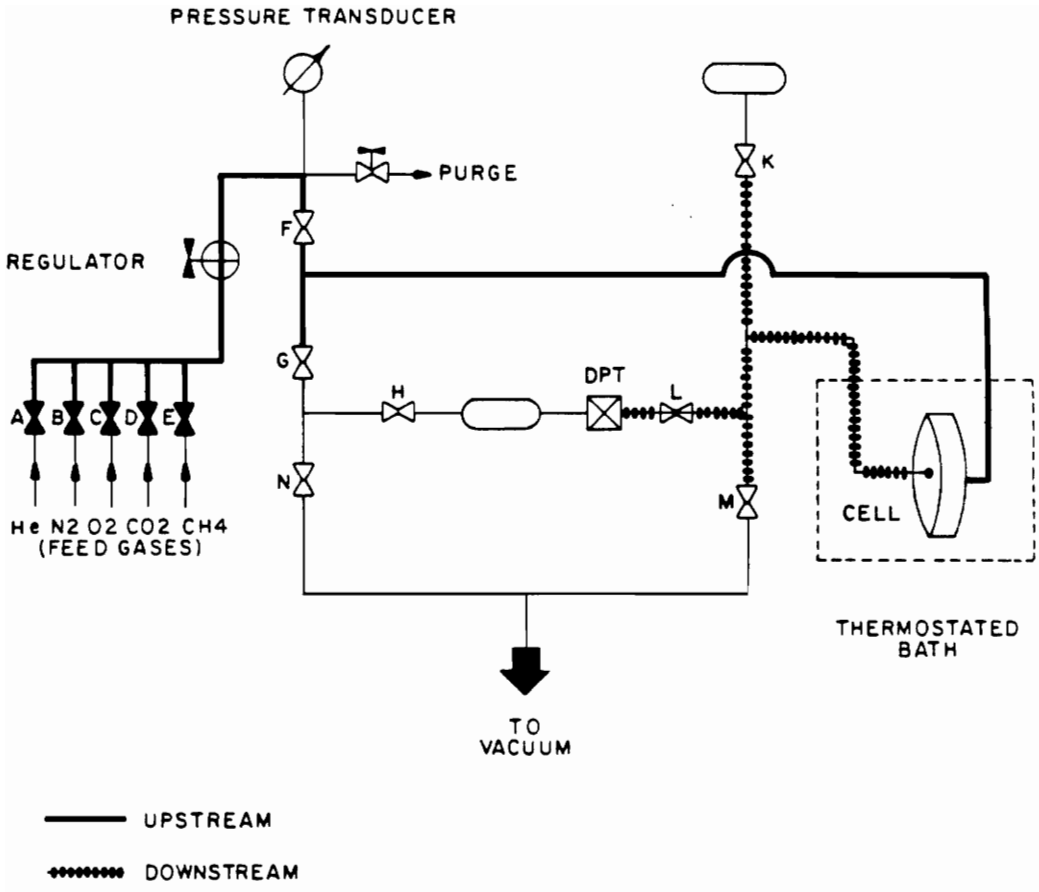

Figure 9. Gas Permeation Device.

Each one of these components is described below in a general fashion. For the design specifications and for a more detailed discussion on this system, the reader is referred to the thesis of J.M. Hoover [19].

a. Automated Control and Data Acquisition System.

Automated control and data acquisition of the gas permeability experiments were performed in an IBM PC-AT interfaced to 12 bits A/D and 24 channel digital output boards (Metrabyte DASH-8 and PIO-12). The system was responsible for the following functions:

i - Operating the valves

ii - Maintaining the desired constant temperature of a water bath

iii - Data acquisition from two pressure transducers.

All these functions and a clock were commanded from the computer through LABTECH NOTEBOOK software. The schematic diagram of the control and data acquisition system is presented in Figure 10.

a.i. Valve Operation.

In a simplified way, the valves were operated by a sequence of electronic and mechanical switches where the digital open /close signals were generated by the PIO-12 digital output board in the IBM-PC-AT and then sent to the ERB-24 mechanical relay board (equipped with 24 double throw relays). The relays acted as ON-OFF switches for 16 solenoid valves, 2 quartz heaters and two transducers protection valves. The solenoid valves served as ON-OFF air switches for 13 bellows valves. An open valve command from the LABTECH NOTEBOOK software was converted to a digital signal by the PIO-12 board. This signal actuated one of the

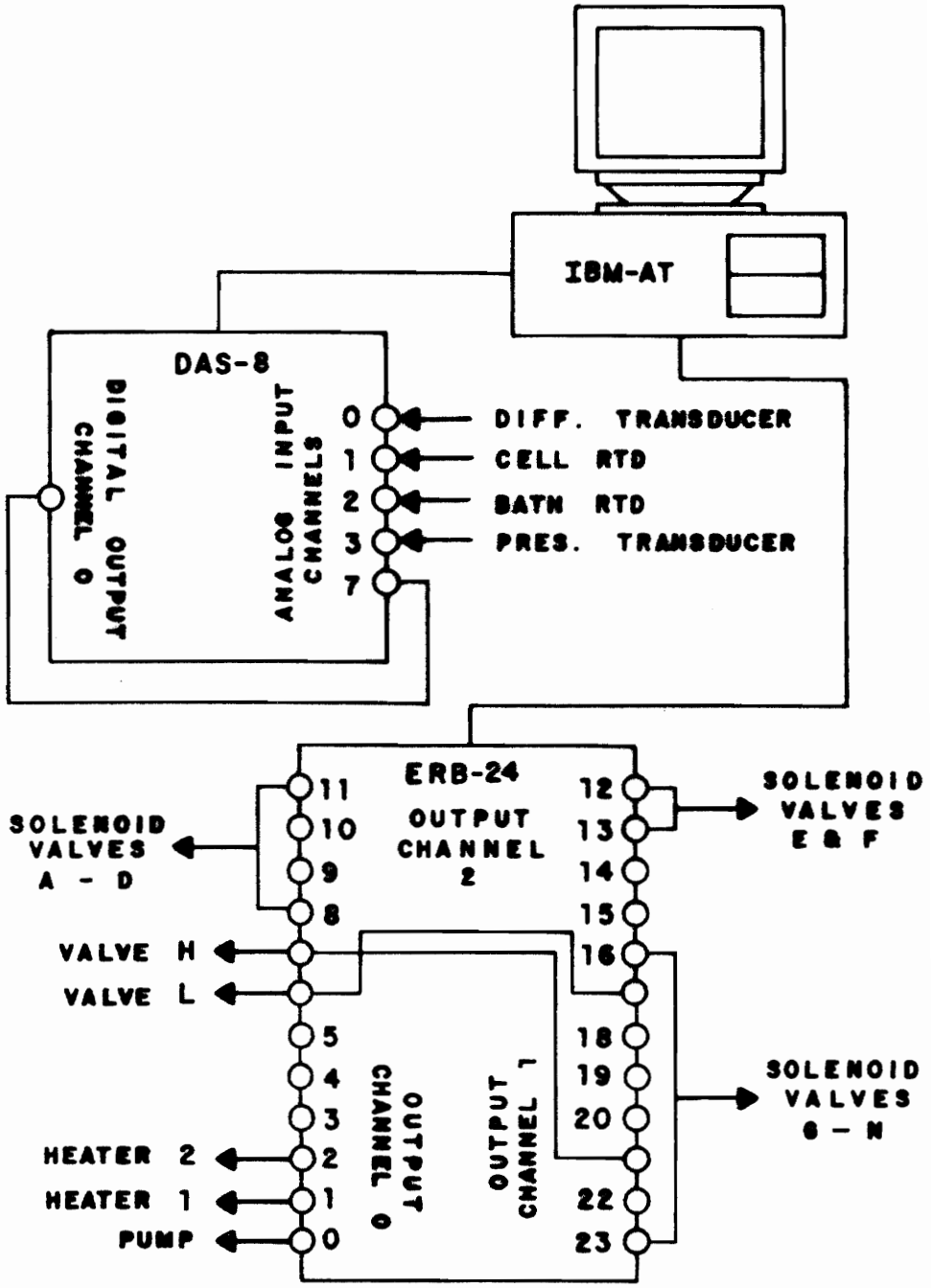

Figure 10. Data Acquisition and Control Scheme. [19]

corresponding solenoid valves. The solenoid valve provided air (50 psig) to the appropriate bellow valve and caused it to open.

Table 8 shows the position of each one of the valves during the system pre-conditioning methods (-RDY1) and during the gas permeation experiments (-PERM1). Table 9 explains the nomenclature used to name the methods.

a.ii. Temperature Control.

The system was responsible for measuring and controlling the temperature of the permeation equipment and is illustrated in Figure 11. The measuring system consisted of two platinum resistance thermocouples (RTD) connected to three three-wire platinum RTD probes which were in charge of measuring the temperature of the water bath, the permeation cell and the instrument plumbing exposed to the laboratory temperature. Temperatures were digitally displayed in tenths of degrees Celsius (i.e. 30.0°C) and were controlled via the computer by a connector of each RTD to the input channel on the DASH-8 A/D board.

The heating of the water bath was accomplished by immersing two 700 watts quartz heating elements which were connected to solid state relays attached to the PIO-12 digital output board of the IBM computer.

Labtech Notebook data acquisition and control software was used to specify the parameters to control the operations of the DASH-8 A/D (temperature reading) board and of the PIO-12 (bath heating) digital output board. The resulting controlled temperatures varied less than 0.1°C.

Table 8. Valve Operation in LABTECH NOTEBOOK Methods.

	VALVE POSITION (O=OPEN ; C=CLOSED)												
METHOD NAME	A	B	C	D	E	F	G	N	H	I	K	L	M
HRDY1	O	C	C	C	C	C	O	O	O	C	O	O	O
NRDY1	C	O	C	C	C	C	O	O	O	C	O	O	O
ORDY1	C	C	O	C	C	C	O	O	O	C	O	O	O
CDRDY1	C	C	C	O	C	C	O	O	O	C	O	O	O
MDRY1	C	C	C	C	O	C	O	O	O	C	O	O	O
HPERM1	O	C	C	C	C	O	C	O	O	C	C	O	C
NPERM1	C	O	C	C	C	O	C	O	O	C	C	O	C
OPERM1	C	C	O	C	C	O	C	O	O	C	C	O	C
CDPERM1	C	C	C	O	C	O	C	O	O	C	C	O	C
MPERM1	C	C	C	C	O	O	C	O	O	C	C	O	C

Table 9. LABTECH NOTEBOOK Methods.

Method Type	Method Name	Gas
Pre-conditioning	HRDY1	Helium
	NRDY1	Nitrogen
	ORDY1	Oxygen
	CDRDY1	Carbon Dioxide
	MRDY1	Methane
Gas Permeation Data Acquisition	HPERM1	Helium
	NPERM1	Nitrogen
	OPERM1	Oxygen
	CDPERM1	Carbon Dioxide
	MPERM1	Methane

A. PLATINUM RTD PROBES (2)
B. QUARTZ HEATERS (2)
C. PERMEATION CELL
D. STIRRING MOTOR
E. RTD THEMOMETERS (2)
F. 25 AMP RELAYS (2)

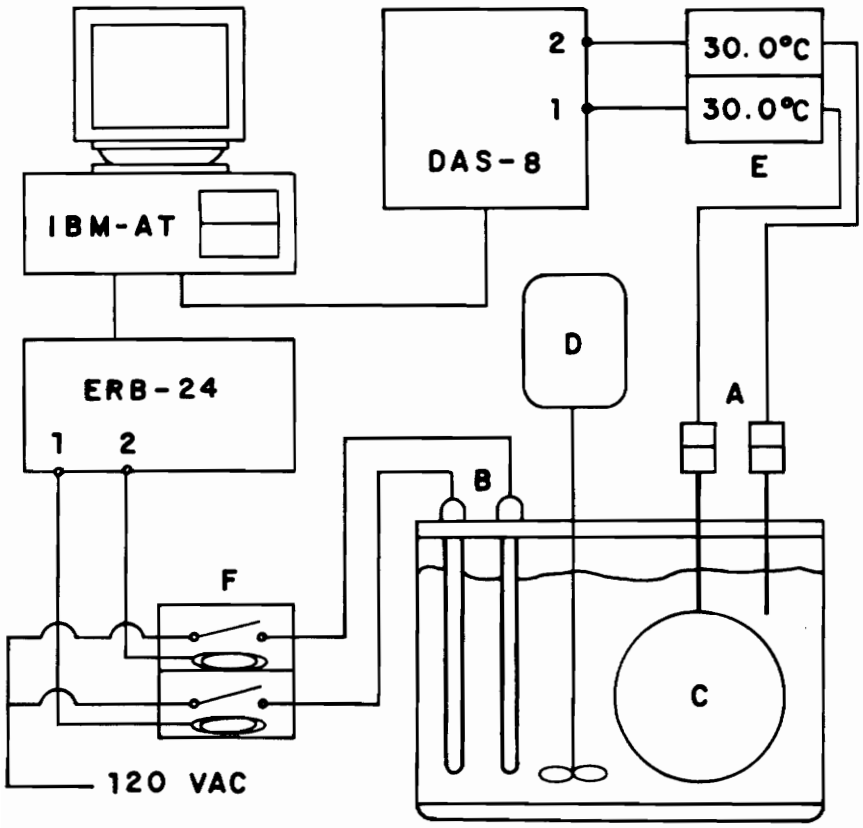

Figure 11. Temperature Control Scheme. [19]

a.iii. Data Acquisition.

This system was responsible for acquiring data from 2 pressure transducers and a clock. Data acquisition from the differential pressure transducer (DPT), the gas supply pressure transducer (PT) and the internal clock was performed by Labtech Notebook Software (LNS) according to specified parameters in the setup channels of this software. These parameters were specified through two different sets of methods in LNS. One series of methods (-RDY1) was used to set the gas permeation instrument ready for the permeability experiments using the smaller control volume available (32.31 mls). The empty space in the name of the method corresponds to the first initial of the probe gas to be analyzed. Table 9 lists the names of all methods used. Ready methods were used to evacuate the cell, pressurize the gas supply manifold and set up the desired constant temperature of the bath for the permeability experiment.

The other set of methods (-PERM1) was used to conduct the gas permeation experiments with the smaller control volume (32.31 mls) and the gas whose first initial appeared in the blank. For a listing of the set up conditions the reader is referred to the work of J.M. Hoover [19].

Data acquisition was performed as follows:

DPT by channel 1

Clock by channel 14

PT by channel 16

An example of the file for a typical permeation experiment is shown in Table 10 and the frequency for data acquisition is presented in Table 11. The frequency of data acquisition was chosen such that approximately 1000

Table 10. Example of a file for a typical permeation experiment.

```
"PERMEABILITY DATA"
"FOR OXYGEN"
"OMI1A-1"
"1.00 ATM"
"PRESSURE" "TIME" "PRESSURE"
"(hPa)""(s)""(psig)"
      0.0168        0.000      14.6030
      0.0168        2.000      14.4591
      0.0168        4.000      14.5311
      0.0168        6.000      14.4591
      0.0000        8.000      14.3153
      0.0168       10.000      14.5311
      0.0168       12.000      14.5311
      0.0168       14.000      14.4591
      0.0337       16.000      14.5311
      0.0168       18.000      14.5311
      0.0337       20.000      14.5311
      0.0000       22.000      14.6030
      0.0337       24.000      14.5311
      0.0337       26.000      14.8188
      0.0337       28.000      14.0995
      0.0168       30.000      14.5311
      0.0337       32.000      14.6030
      0.0505       34.000      14.5311
      0.0673       36.000      14.6030
```

Table 11. Data Acquisition Frequency.

Gas	Frequency (Hz)
Helium	2
Oxygen	0.5
Nitrogen	0.1
Carbon Dioxide	0.5
Methane	0.1

data points were acquired during an experiment. The graphic (plot) representing the data obtained is presented in Figure 12. The analysis of the data was performed by a data analysis program (ANALYZE.BAS) which can process a maximum of 1200 data points from the Labtech Notebook - PERM1 data files. The basis for the permeability and selectivity calculations are detailed in Appendix C as well as a computer copy of the ANALYZE.BAS program (Appendix D) written by a co-worker of the author [19] which was used for the calculations.

b. Gas Supply and Regulating System.

The gas supply and regulating system consisted of 5 high pressure gas cylinders of high purity gases (Table 12) equipped with gas regulators. A precision in-line, 0-100 psi gas regulator was connected to the gas manifold for a fine pressure regulation of the inlet gases. A 0-300 psi pressure transducer (Omega Engineering) with a power supply and a digital display was used to measure the gas inlet pressure. Five air-operated helium leak tested bellows valves allowed the selection and supply of the analysis gas to the up-stream or pressure side of the permeation cell at a desired and constant pressure rate.

The manifold was carefully purged with the selected probe gas prior to the permeation experiments. The pressure of the gas cylinder regulators was kept at approximately 10-15 psig. The pressure of the gas

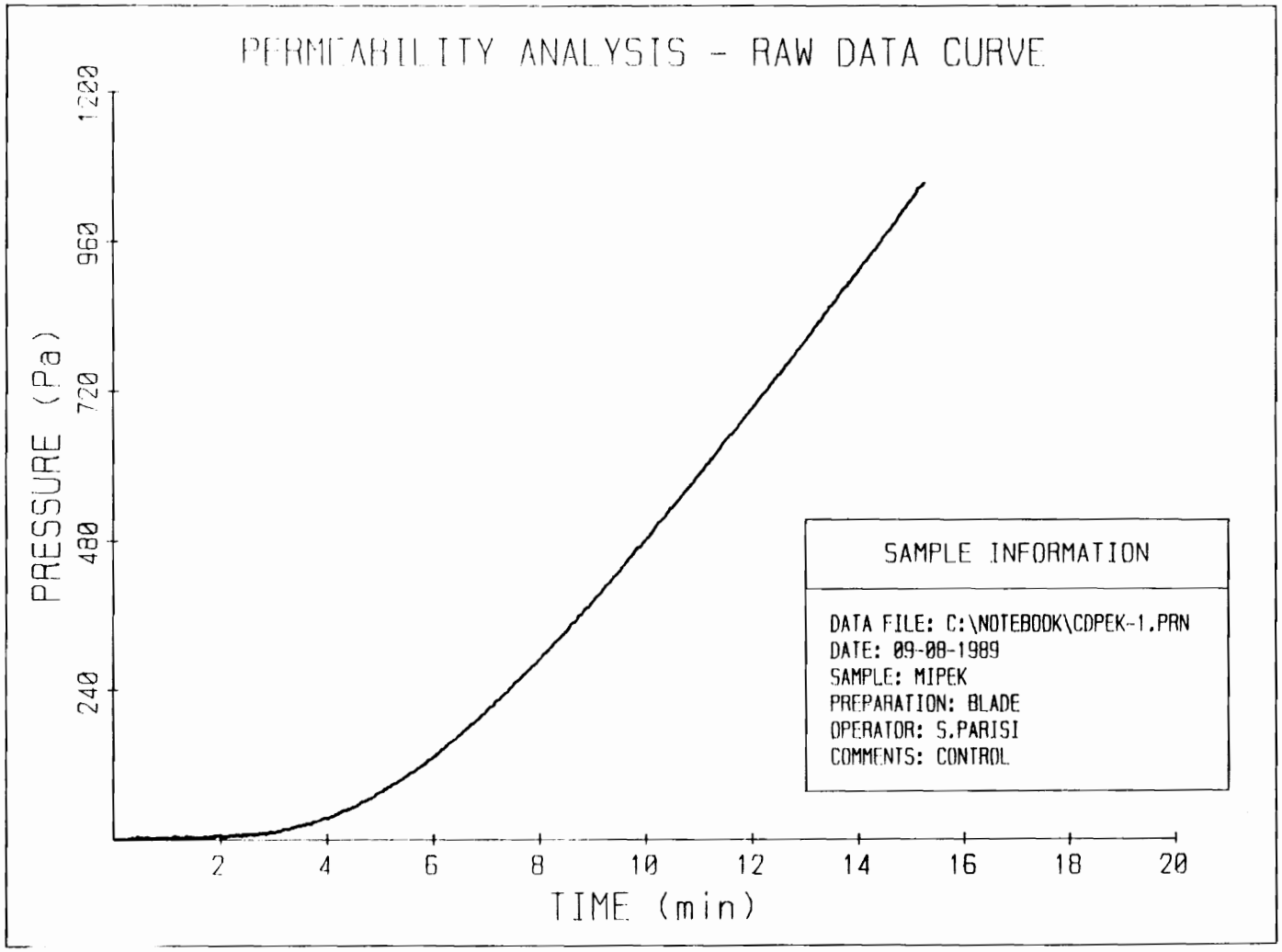

Figure 12. Graphic Representation of the Results of a Permeation Run.

Table 12. Specifications of the Gases Utilized in the Gas Permeation Experiments.

Gas	Grade*	Minimun Purity*
Helium	5	99.999
Oxygen	4.3	99.993
Nitrogen	5	99.999
Methane	4.2	99.992
Carbon Dioxide	4	99.99

* From AIRCO, Inc.

required for the experiment was measured by the transducer (PT). The output signal from the transducer was sent to a digital d.c. voltage meter and also to the DASH-8 A/D board in the computer. The display indicated the pressure in atmospheres. Once the gas was selected and its pressure regulated, the experiment was started by opening the cell supply valve F directing the gas stream to the pressure side of the permeation cell.

c. Pressure Measuring Device.

A very sensitive (1.0 psid or 6.9 kPa full scale) differential pressure transducer or DPT (Celesco P7D-LCCD-110) with a low cost carrier demodulator (LCCD) and a digital display to indicate the pressure in the down stream side (vacuum side) of the permeation cell, were used to measure the pressure of the gas that permeated through the membranes. The digital display indicated the permeated gas pressure in kilopascal (kPa) units. The reference side (-) of the DPT was connected to the vacuum supply system side and the sampling side (+) of the DPT was connected to the vacuum side (or down-stream side) of the permeation cell. Thus, the DPT measured the difference in pressure between the vacuum produced by the vacuum supply system and the pressure that was build-up in the control volume of the permeation cell (gas that permeated through the film).

This pressure increase relative to vacuum was detected by the transducer which produced an output signal of 10 volts d.c. at a full scale reading of 1.0 psi (6.9 kPa). This signal went to the DASH-8 board and to the digital d.c. voltage meter scaled so that a 5.0 volt d.c.

signal (for 0.25 psi) produced a reading of 1.72 kPa on the display. The pressure measuring device is schematically represented in Figure 13.

The span calibration of the transducer was checked monthly using a manometer filled with distilled water. The calibration set-up is shown in Figure 14.

The DPT was calibrated against atmospheric pressure. An example of one calibration curve is presented in Figure 15. Several pressure readings were recorded from the DPT digital display in kPa by applying different pressures to the water manometer. Then, the data obtained was regressed, the experimental slope calculated and compared to the theoretical slope. The calculations of the theoretical slope are shown in Appendix E.

The span on the LCCD was adjusted and the calibration procedure repeated until the measured error was 0.1% or less. The zero adjustment on the LCCD was adjusted when necessary, normally before each permeation run.

d. Permeation Cell.

After the removal of the film from its glass plate and its thickness estimation, the membrane was placed in the permeation cell which is schematically shown in Figures 16 and 17.

The cell was designed by a co-worker of the author at VPI & SU with the objective to provide as high a ratio possible of membrane surface area to down-stream volume so that low permeabilities can be accurately measured. For a more detailed description than the one presented below, the reader is referred to the work of Hoover [19].

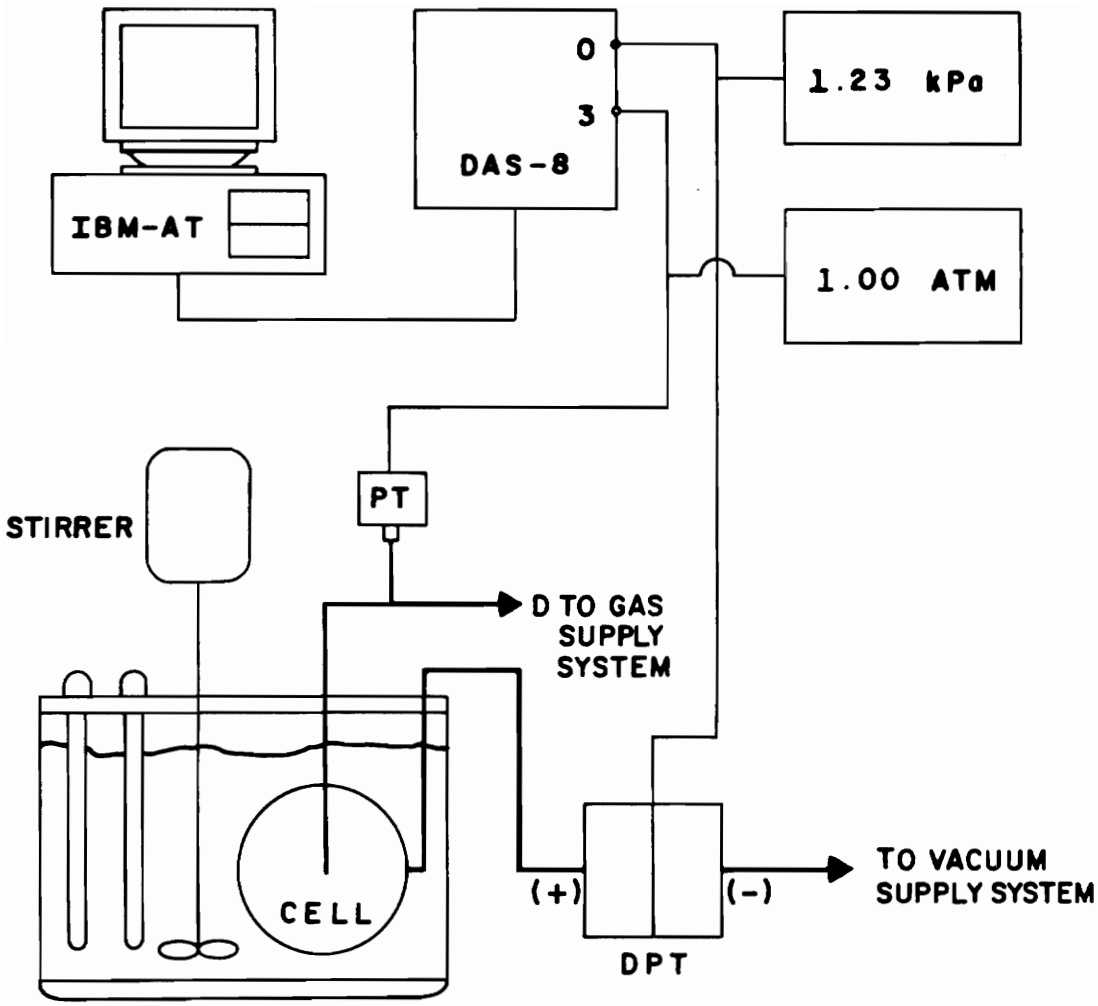

Figure 13. Pressure Measurement Scheme. [19].

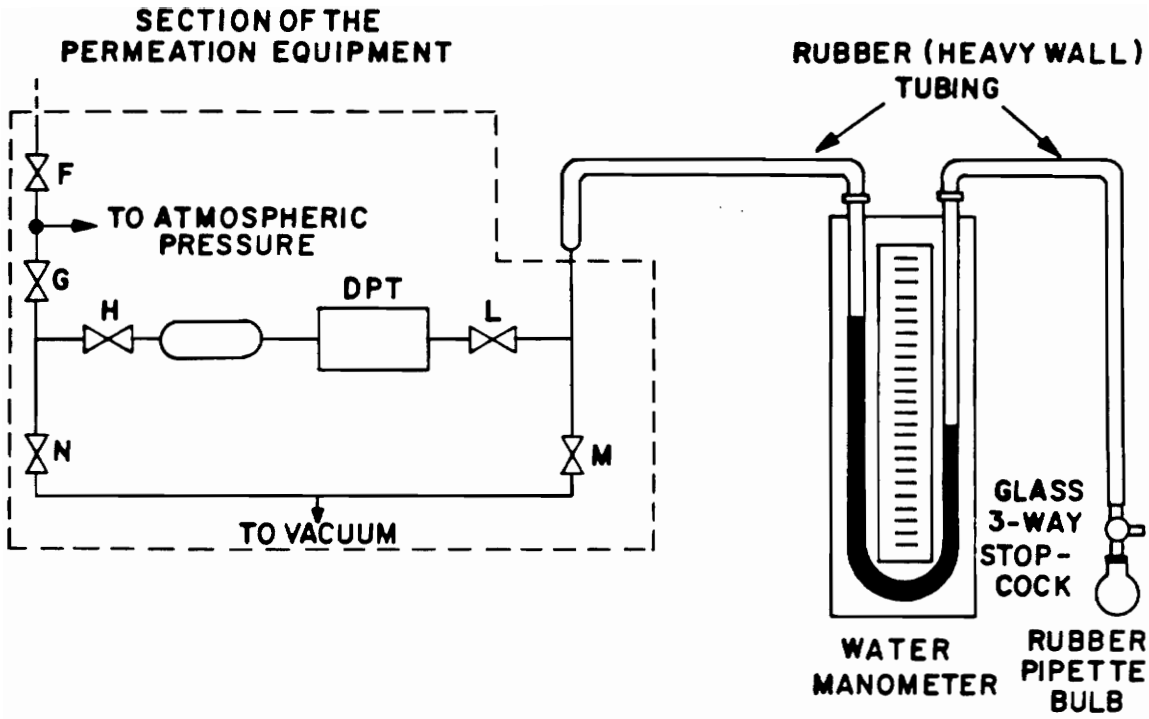

Figure 14. Differential Pressure Transducer Calibration Set-up.

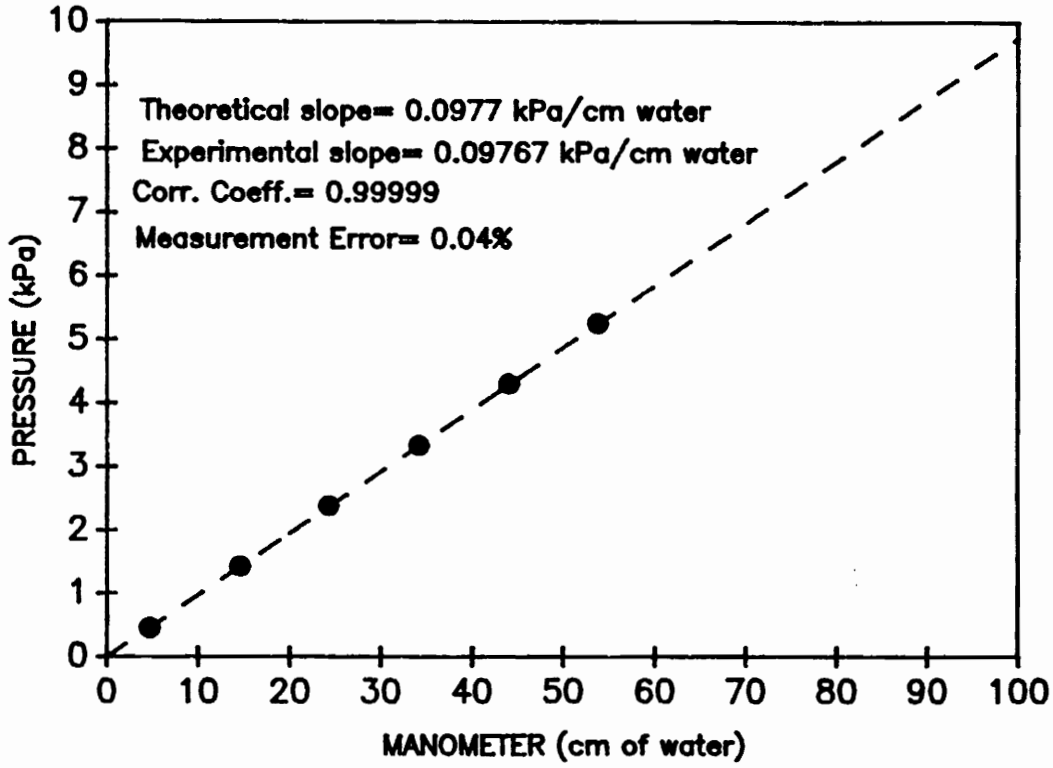

Figure 15. Calibration Curve for the Differential Pressure Transducer.

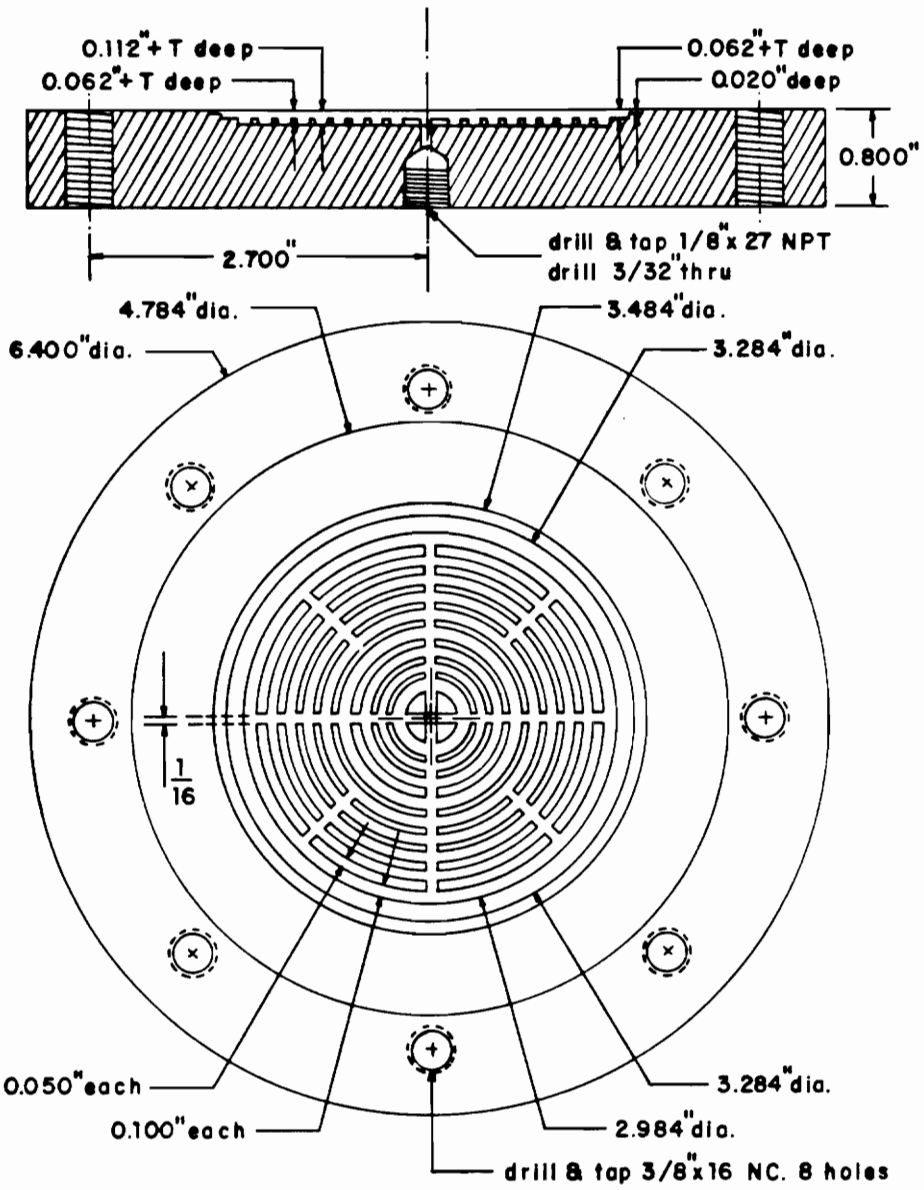

Figure 16. Drawing of Permeability Cell, Bottom Plate or Vacuum Side. [19]

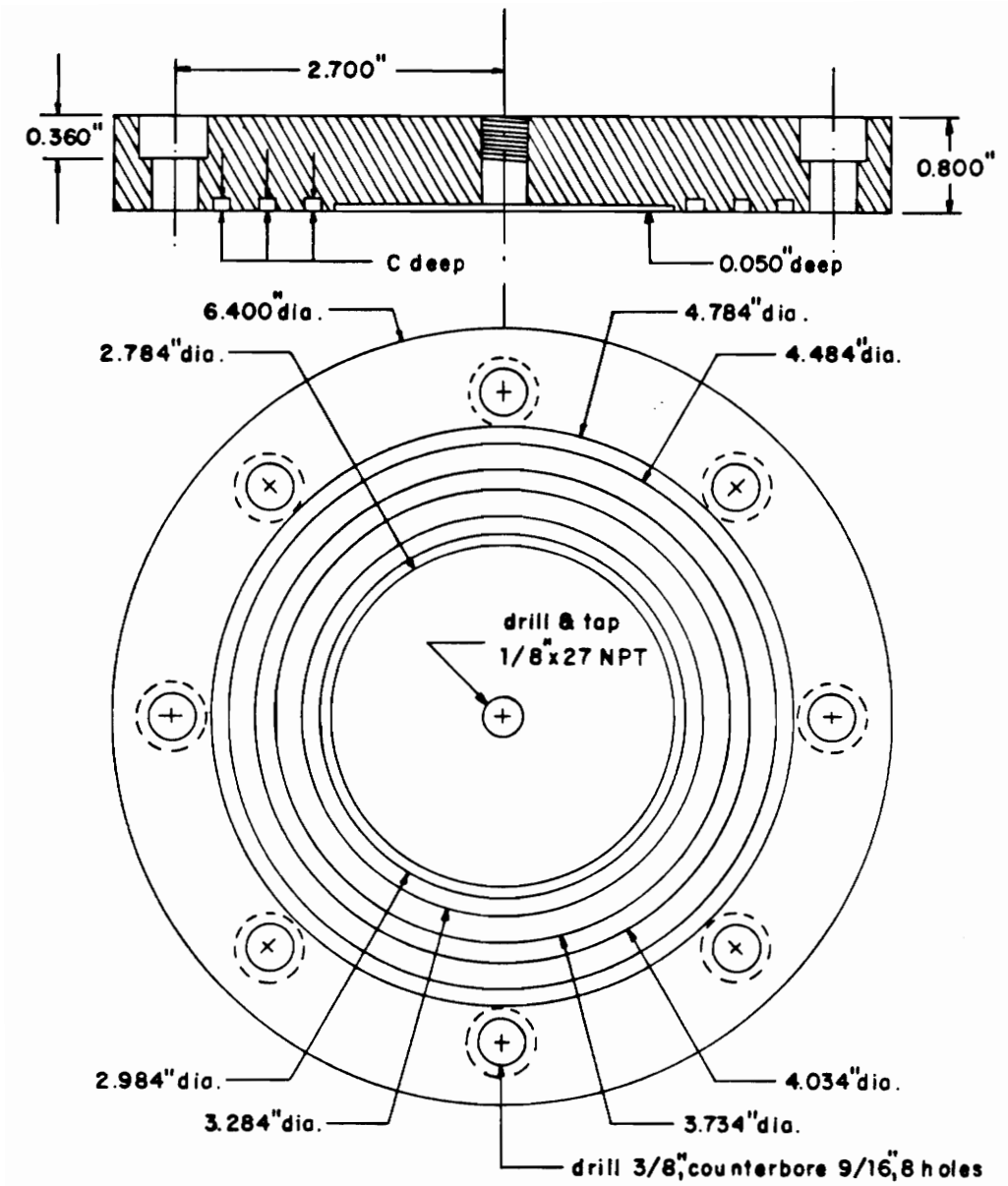

Figure 17. Drawing of Permeability Cell, Top Plate or Pressure Side. [19]

The permeation cell consisted of two stainless steel disks (upper and down stream sections) and of a 5 microns pore size stainless steel porous plate to provide support to the membrane. Figure 16 shows the scaled drawing of the down-stream section (bottom plate and vacuum side). Figure 17 shows the scaled diagram of the up-stream disk (top plate or pressure side). The two disks were separated by three nitrile rubber o-ring seals as illustrated in this figure. This design provided a gas tight chamber on each side of the membrane and isolated the vacuum seal from any contact with water from the thermostated water bath. The schematic view of the head of the cell is presented in Figure 18.

A fairly detailed description of the procedure for positioning the film on the porous SS plate and inside the permeation cell can be found in the work of Hoover [19].

e. Vacuum Supply System.

The vacuum supply system is schematically represented in Figure 19 and consisted of a vacuum pump (Sargent-Welch, model 1401), a glass vapor trap and a Dewar, a vacuum transducer and a vacuum gauge. The system was connected trough rubber (vacuum type) and SS tubings. A vacuum a 50-55 militorr was sustained constant during the permeation runs and the pump operated almost continuously during the course of this research.

f. Thermostated Bath.

The thermostated bath consisted of a glass container filled with distilled water, a stirrer, two bath electrical heaters and two thermocouples (RTD) already described in Section II. E.aii as well as the temperature control setup.

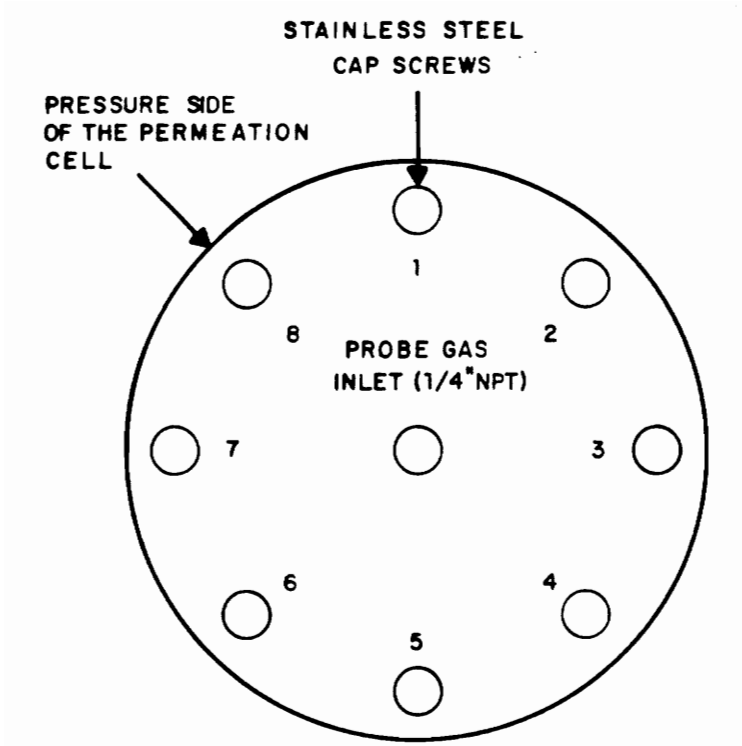

Figure 18. Schematic View of Cell Head. [19]

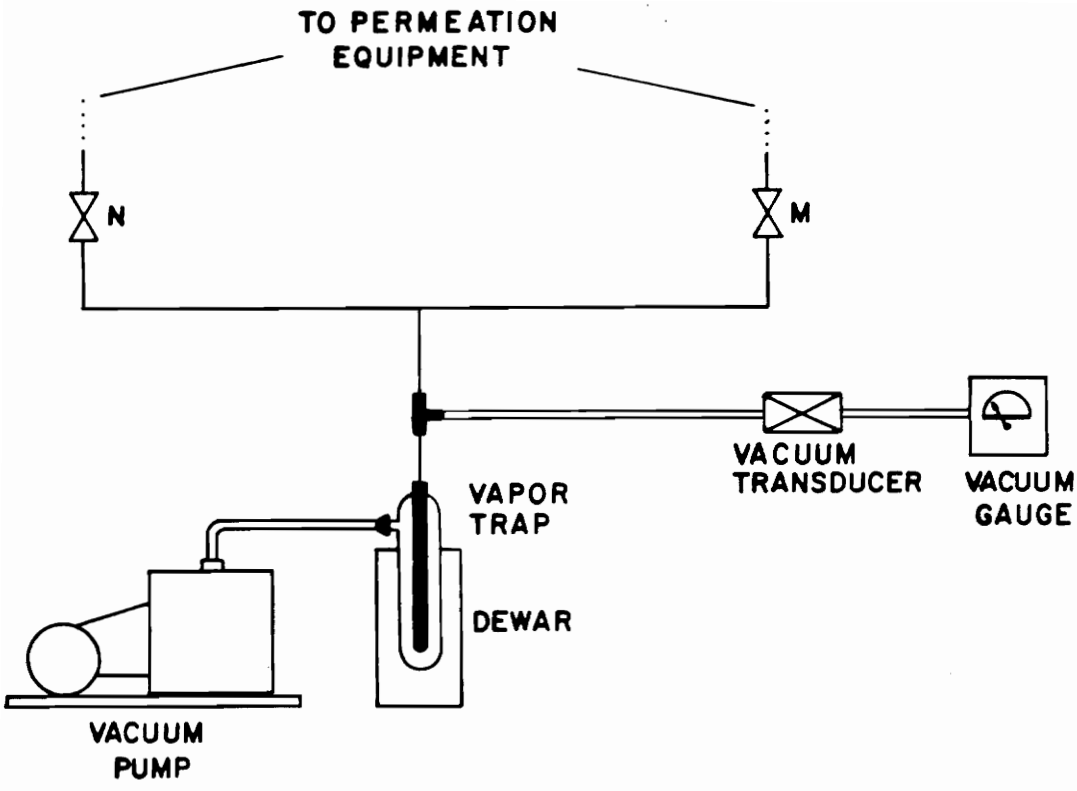

Figure 19. Vacuum Supply System.

II. E.2. Permeability Measurements.

After positioning the film in the permeation cell and its installation in the gas permeation equipment, the system was evacuated at 30-75 militorr for 12-18 hours prior to the first permeation measurement of a film. A preliminary study was carried out in order to estimate the optimum degassing time needed for a complete evacuation of the permeated gas through MIPEK films. Different degassing times were tested until the permeabilities values differing only in the third decimal figure and the time lag obtained was fairly reproducible.

The gases were analyzed in the following sequence: 1. Helium, 2. Nitrogen, 3. Oxygen, 4. Methane and 5. Carbon Dioxide. Due to evidence of a history effect when a gas was run after Carbon Dioxide [5], this gas was analyzed last.

Table 13 shows the degassing times used between runs when switching from one gas to another.

Table 13. Degassing times between runs of different gases.

GAS	DEGASSING TIME (hrs)
He	6
N2	12
O2	6
CH4	12-18

CHAPTER III

RESULTS AND DISCUSSION

This section contains the results obtained through the application of the procedures and techniques described in Chapter II. The results presented here are described, tabulated and discussed. The relationship between the crosslinking time under thermal conditions and the corresponding percentage of insolubles in the films are first presented. Also, the correlations between the Number Average Molecular Weight of the network chains ($\overline{M}c$), the crosslink density (dc) and the swelling ratio (Q) with the crosslinking time are presented. They are followed by the results on membrane thickness characterization and the results of the gas permselectivities. The gas permeation results are discussed as a function of the insoluble fraction in the films, the crosslink density dc (and $\overline{M}c$) and the swelling ratio (Q).

III. A. Crosslinking Time and Percentage of Insolubles.

The percentage of insolubles present in the evaluated films as a result of three different crosslinking times is schematically represented in Figures 20 and 21. Within the same blend (e.g. 20K, 100%), longer crosslinking times (@ 250°C) increase the insoluble content of the films. The assumption can be made that long periods of time at 250°C increases

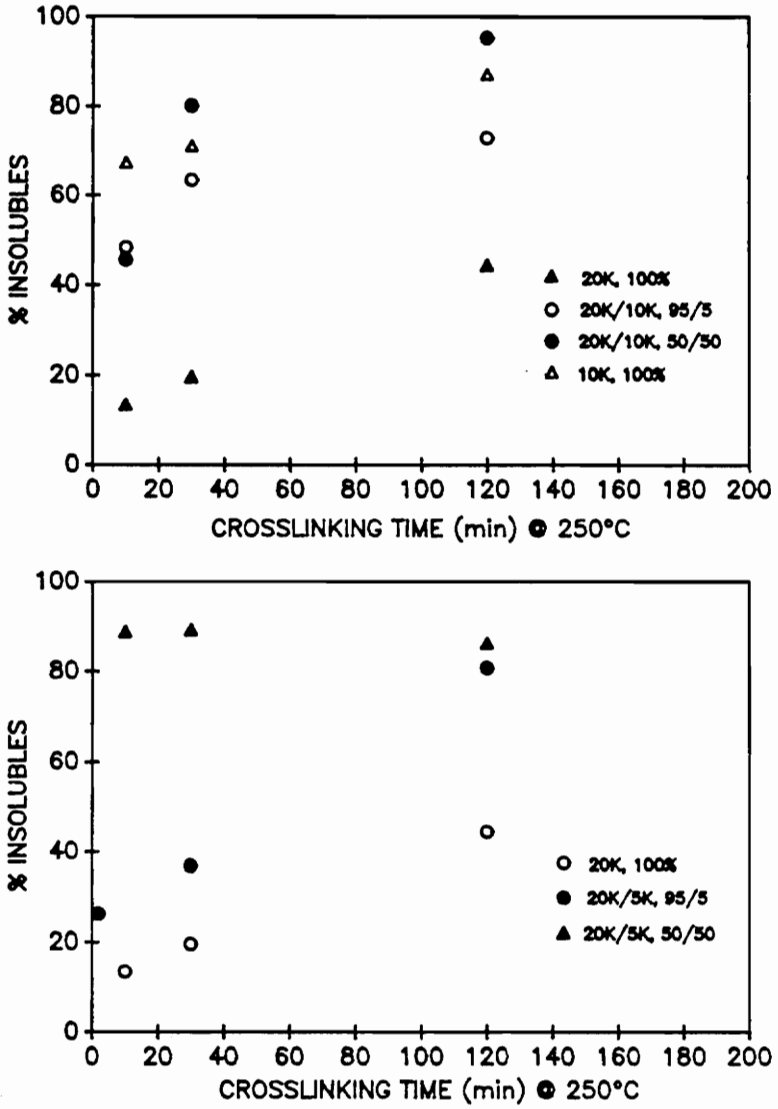

Figure 20. Percentage of Insolubles and Crosslinking Time for Blends of MIPEK.

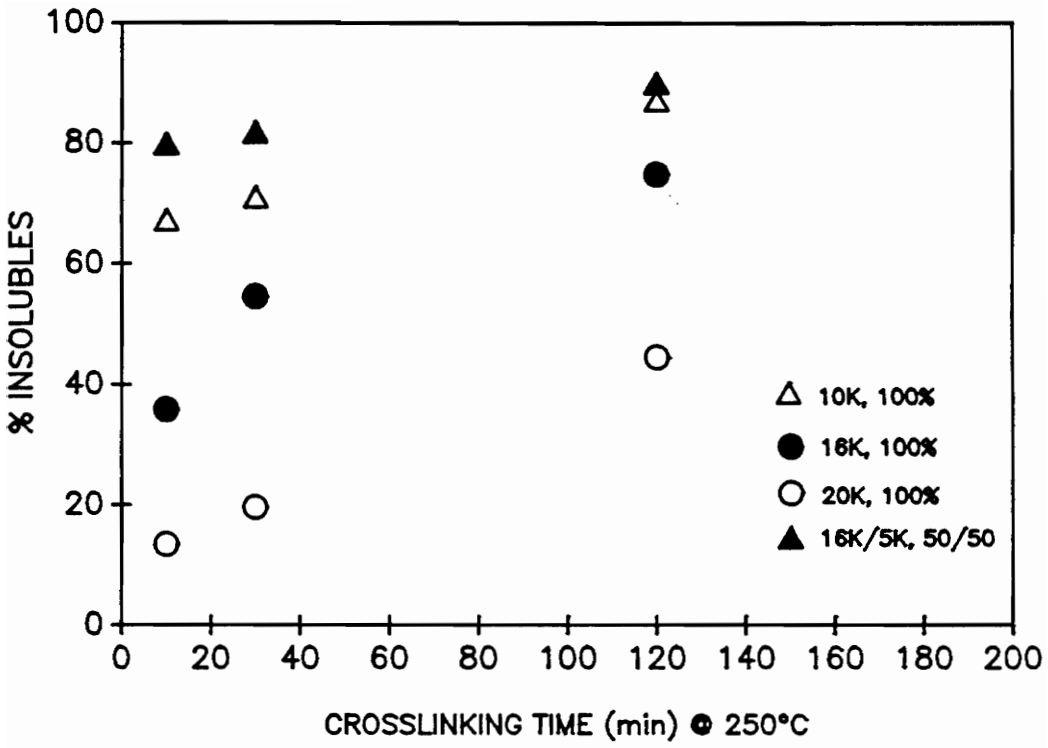

Figure 21. Percentage of Insolubles and Crosslinking Time for Blends of MIPEK.

the probability of two chain ends to react. This could explain why these films show a higher content of insoluble portion.

For a given crosslinking time (e.g. 2 hours), the percentage of insolubles increases at higher contents of low molecular weight oligomers in the blend. Thus, for a thermal treatment of 2 hours with films of 10K, all show a higher percentage of insolubles than those of pure 20,000 $\bar{M}n$ (20K) films. This trend may be explained by considering a higher probability to crosslink for those chains of lower molecular weights as a result of a high crosslinking concentration sites. Thus, the chance for the chain ends to encounter each other and react would be higher.

The results summarized in Figures 20 and 21 can be used to estimate the experimental conditions needed in order to obtain the desired film characteristics (e.g. a certain content of insolubles for a given blend).

III.B. Crosslinking Time, Number Average Molecular Weight ($\bar{M}c$), Crosslinking Density (dc) and Swelling Ratio (Q).

The dependance of the number average molecular weight of the network chains ($\bar{M}c$) with the crosslinking time at 250°C for the different blends of MIPEK evaluated is illustrated in Figures 22 and 23. The experimental values for Mc are also reported in Appendix F.

For an individual blend composition (e.g. 16K, 100%), the shorter crosslinking times correlate well with higher $\bar{M}c$ values. The same kind of behavior was observed for all the series evaluated. This trend could

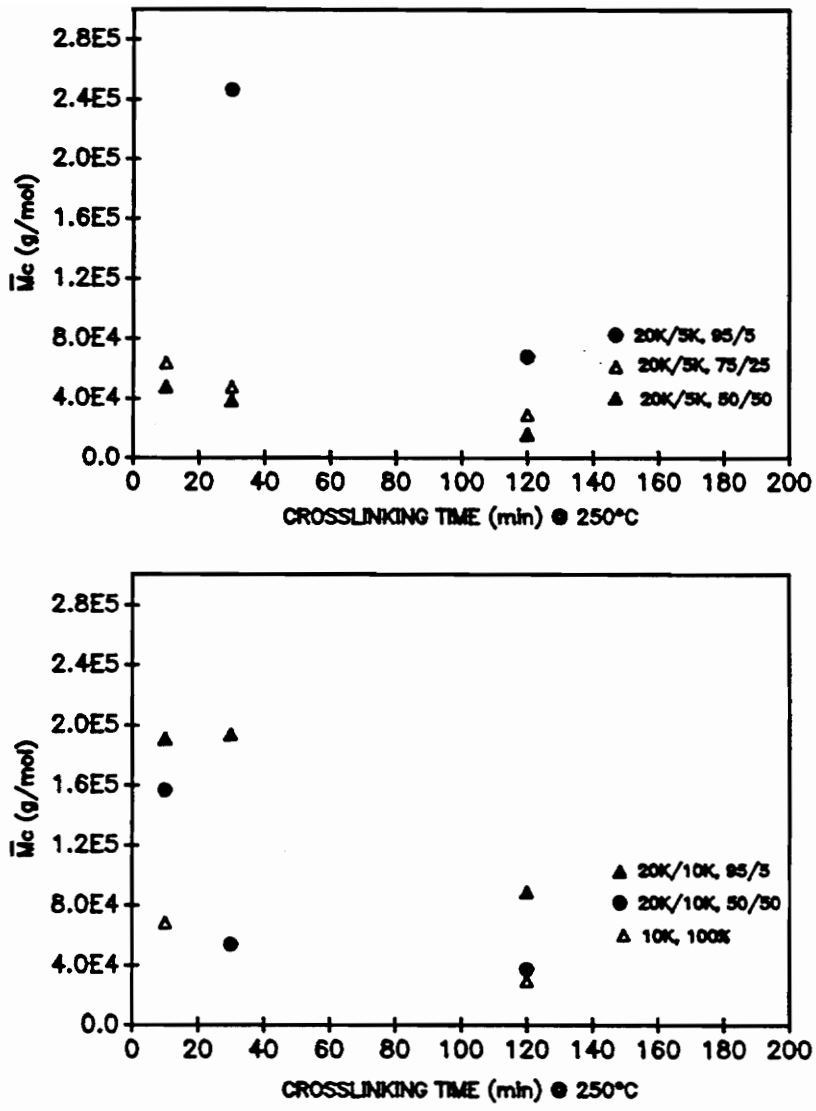

Figure 22. Number Average Molecular Weight of the Network Chains ($\overline{M}c$) and Crosslinking Time for Series of MIPEK.

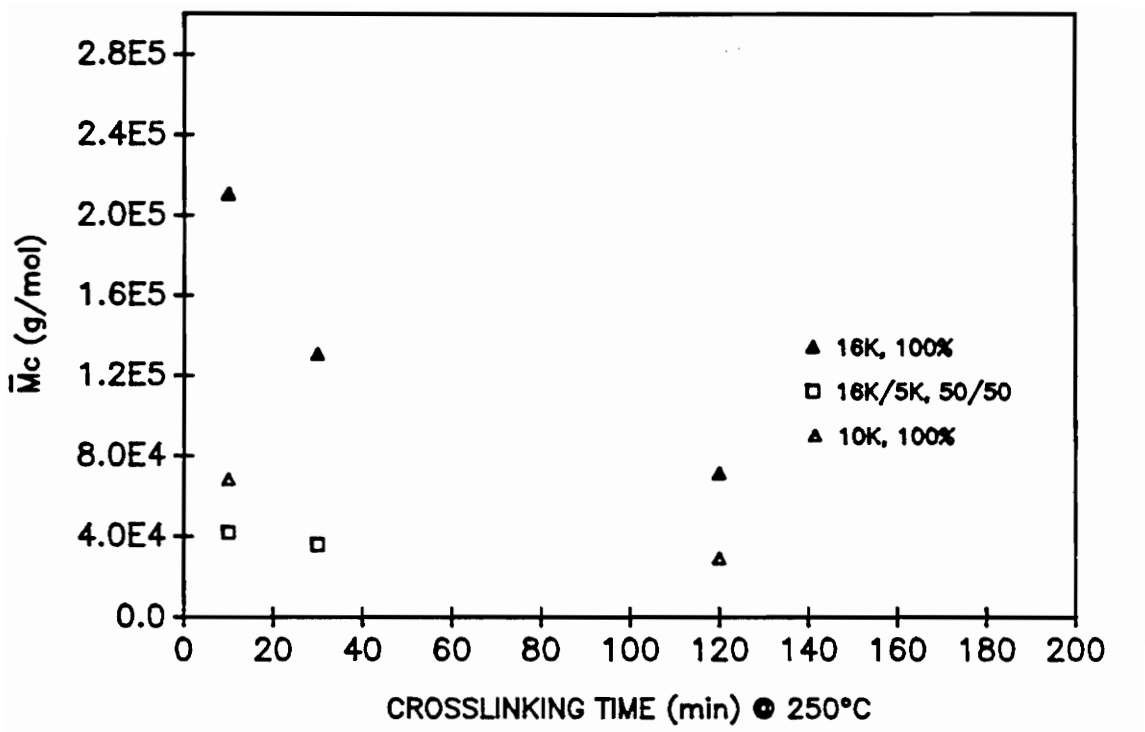

Figure 23. Number Average Molecular Weight of the Network Chains ($\bar{M}c$) and Crosslinking Time for Series of MIPEK.

be explained by considering that initially (at short crosslinking times), the free radical reactions between the chain ends could take place mostly in a linear or modestly branched fashion. Thus, under these conditions the $\bar{M}c$ to be observed between the network chains would be large. Figure 24.a shows an idealized representation of this behavior. Consequently, at longer crosslinking times (e.g. 2 hours), there is a higher probability for the chain ends to encounter each other and the resulting network chain would show a lower $\bar{M}c$. This idealized situation is represented in Figure 24.b. The effects of the presence of low MW oligomers in the blend and of the low MW films on $\bar{M}c$ could be explained by considering the possibility of additional reactions due to the presence of shorter more highly functional chains. Then, the $\bar{M}c$ will be lower at higher contents of low MW oligomers in the blends (Figure 24.b).

Since the crosslinking density (dc) is inversely proportional to $\bar{M}c$ (See Section II.D.2 B.2 for calculations), the results for dc and the corresponding crosslinking times for the evaluated samples were also tabulated (Appendix F). An inverse dependance was observed for dc. Thus, when $\bar{M}c$ is small at long crosslinking times, the value of dc is large.

The swelling ratios (Q) for all the samples evaluated are also summarized in Appendix F. At long crosslinking times (e.g. 2 hours), the value of Q is lower, representing a small degree of swelling and a higher crosslink density value for the polymer network.

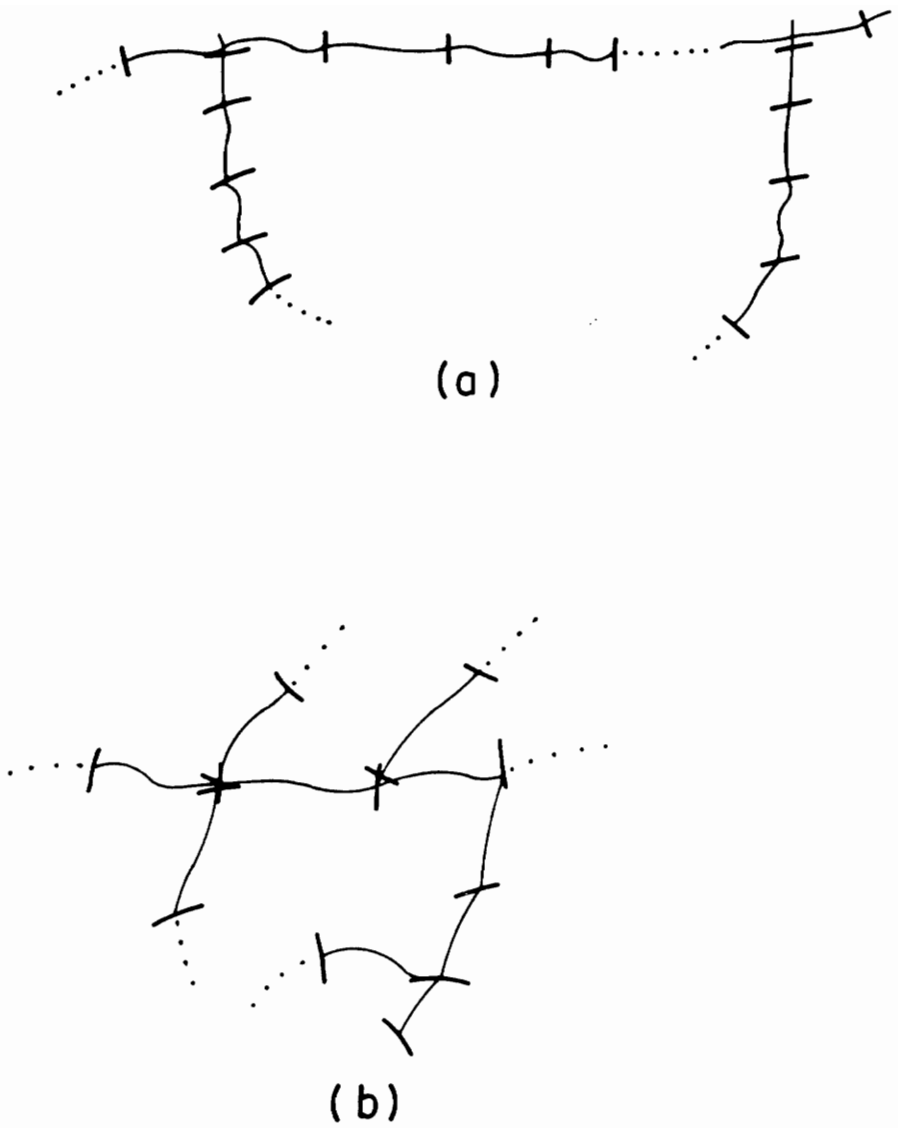

Figure 24. Idealized Schematic Representation of the Crosslinking Reaction.

(a) At short crosslinking times;
(b) Long crosslinking times.

III.C. Number Average Molecular Weight ($\overline{M}c$) and Percentage of Insolubles.

The relationship between the $\overline{M}c$ of the network chains and the insoluble portion in the evaluated blends is illustrated in Figures 25 and 26. The general trend observed is that low molecular weights of the network chains ($\overline{M}c$) correlate with large percentages of insolubles, as expected.

At relative low content of insolubles (e.g. 40%), the observed $\overline{M}c$ values differ depending upon the composition of the blend (Figure 26.b). Those blends with a higher content of oligomers of low MW showed the lower $\overline{M}c$. However, at high percentage of insolubles the differences in $\overline{M}c$ become smaller and the observed $\overline{M}c$ values are of the same order, independently of the sample composition.

III.D. Film Preparation Procedure and Membrane Thickness Characterization.

The gas permeability value is directly proportional to the thickness of the polymer membrane. Therefore, the selection of the film preparation technique is a critical step to consider.

The "Dr. blade" or "Dr. knife" technique was the methodology chosen in this research for the preparation of the membranes. This method was selected after a preliminary study performed in order to determine the best procedure suitable to make films with MIPEK blends.

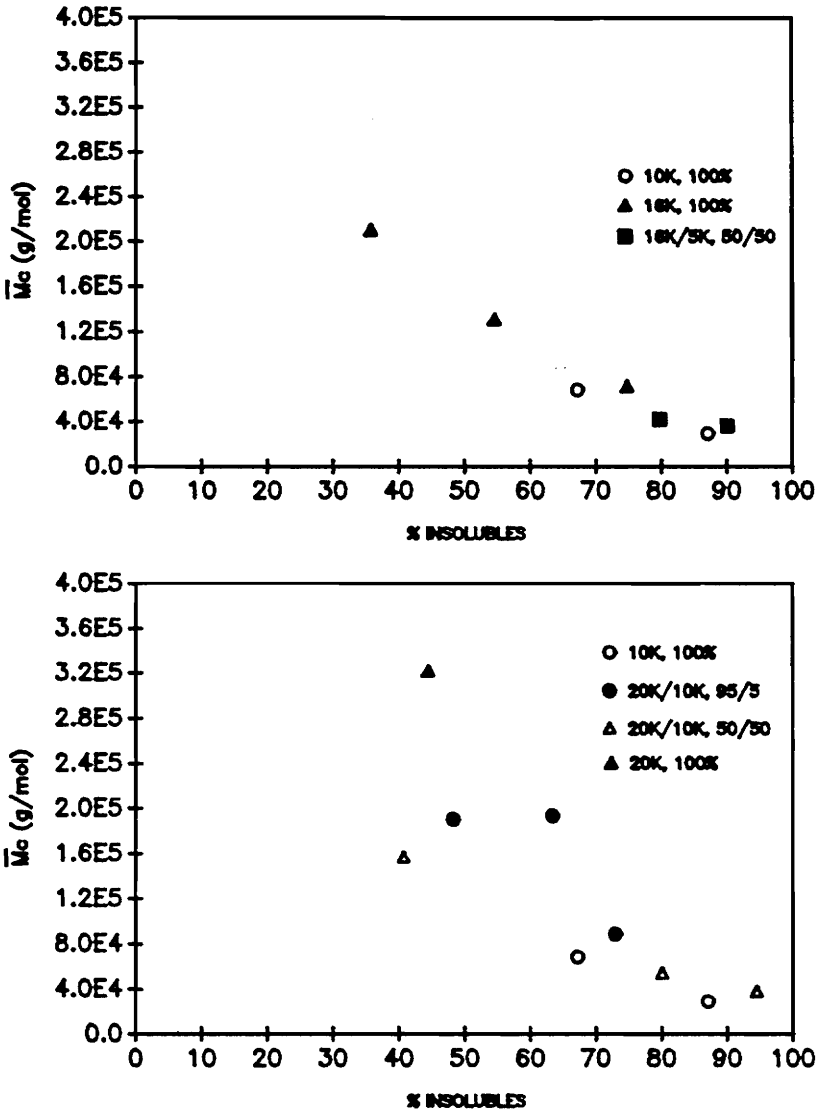

Figure 25. Number Average Molecular Weight ($\bar{M}c$) of the Network Chains and the Percentage of Insolubles for Series of MIPEK Blends.

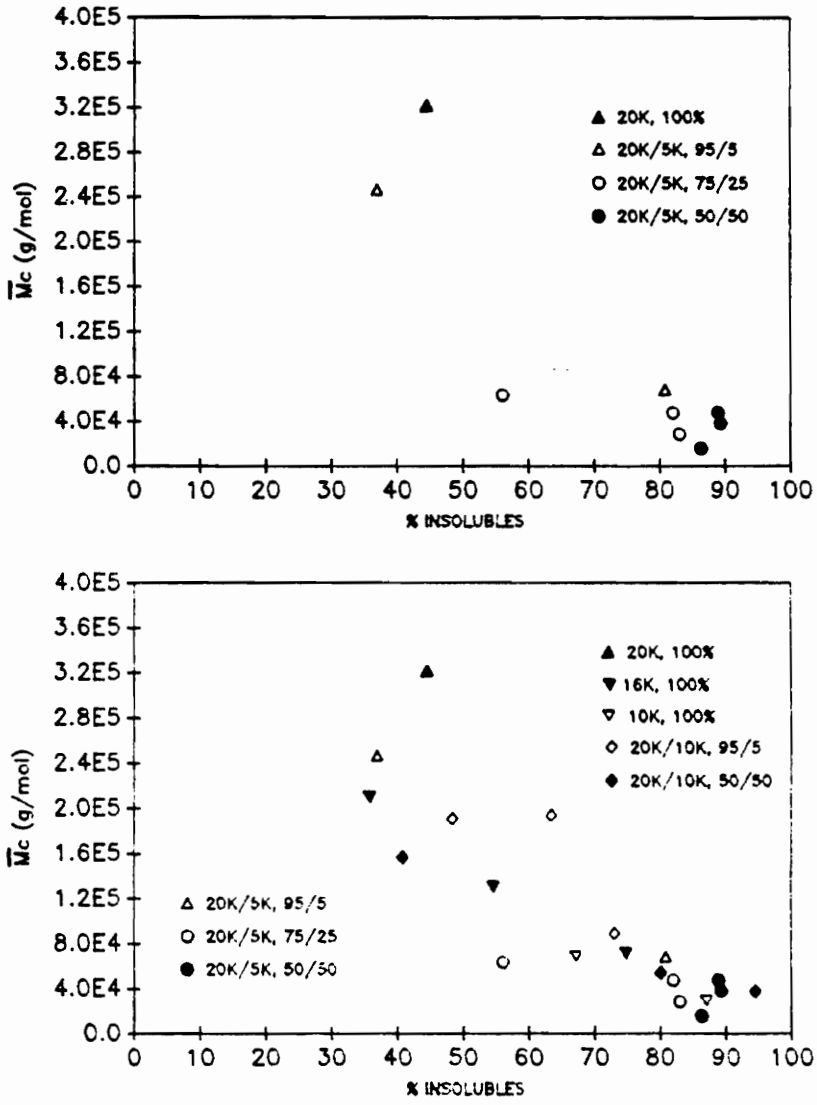

Figure 26. Number Average Molecular Weight ($\overline{M}c$) of the Network Chains and the Percentage of Insolubles for Series of MIPEK Blends.

The slow spin-casting technique was the first procedure evaluated since it is known to produce films of very uniform thickness. Standard deviations in thickness in the range of 1 to 5 percent of the total film thickness has been previously reported for graft copolymer films [19]. The slow spin-casting procedure is accomplished by pouring a polymer solution on a substrate and rotating it at a constant speed (200-1000 rpm) until the solvent has been evaporated. The thickness of the film depends basically on the concentration and molecular weight of the polymer solution and the rotating speed. Thus, in this case the choice of the solvent is of extreme importance. The desired solvent characteristics include that it has to be a good solvent for the polymer and it should evaporate rather easily to facilitate its final removal from the sample. However, there is a compromise in the solvent evaporation rate. If the solvent evaporates too fast, the formation of bubbles becomes a problem even at low spin rates. In the case of this research, chloroform was the best solvent found for the polymeric system under study. However, due to the relatively low boiling point of this solvent, the formation of bubbles persisted for all the experimental conditions of temperature and spinning rates evaluated. Therefore, the films obtained by the spin-casting technique were not satisfactory for the gas permeation characterization measurements.

The selected film preparation technique was the "Dr. blade" method (see Section II.C for experimental details). With this procedure and using chloroform as the solvent, standard deviations in thickness of 3 to 5 percent after 56 film thickness readings were obtained.

III.E. Gas Permeability Results.

The gas permeability experiments were performed using "Labtech Notebook" software for process controlling and data acquisition. The detailed description of the procedure was previously described in Section II.E. The permselectivity calculations were carried out with the BASIC program "ANALYZE.BAS" (Appendix D).

The gas permeabilities reported here are the results of 2 to 3 experiments for each gas/polymer pair. The experiments were performed at 30°C and 1 atm gauge and five gases of different sizes and shapes were evaluated: (1) Helium, (2) Oxygen, (3) Nitrogen, (4) Methane and (5) Carbon Dioxide.

The gas permeability data is summarized in a series of figures to illustrate (a) the permeation order of the five gases evaluated (Figures 27 to 33), (b) the effect of the films thermal treatment @ 250°C on the permeabilities of each gas (Figures 34 to 45), (c) the O_2/N_2 selectivities for all the MIPEK series evaluated as a result of the thermal treatment represented by the percentage of insolubles in the samples (Figures 46 to 48) and by the Number Average Molecular Weight ($\overline{M}c$) in them (Figure 49), (d) the CO_2/CH_4 selectivities as a function of the insoluble portion in the films (Figures 50 to 53) and of the $\overline{M}c$ (Figure 54).

a. Permeation Order of the Gases

Figures 27 to 31 show the permeability of the five gases evaluated for each one of the MIPEK blends. These figures are semi-log plots of permeability as a function of the percentage of insolubles in the films.

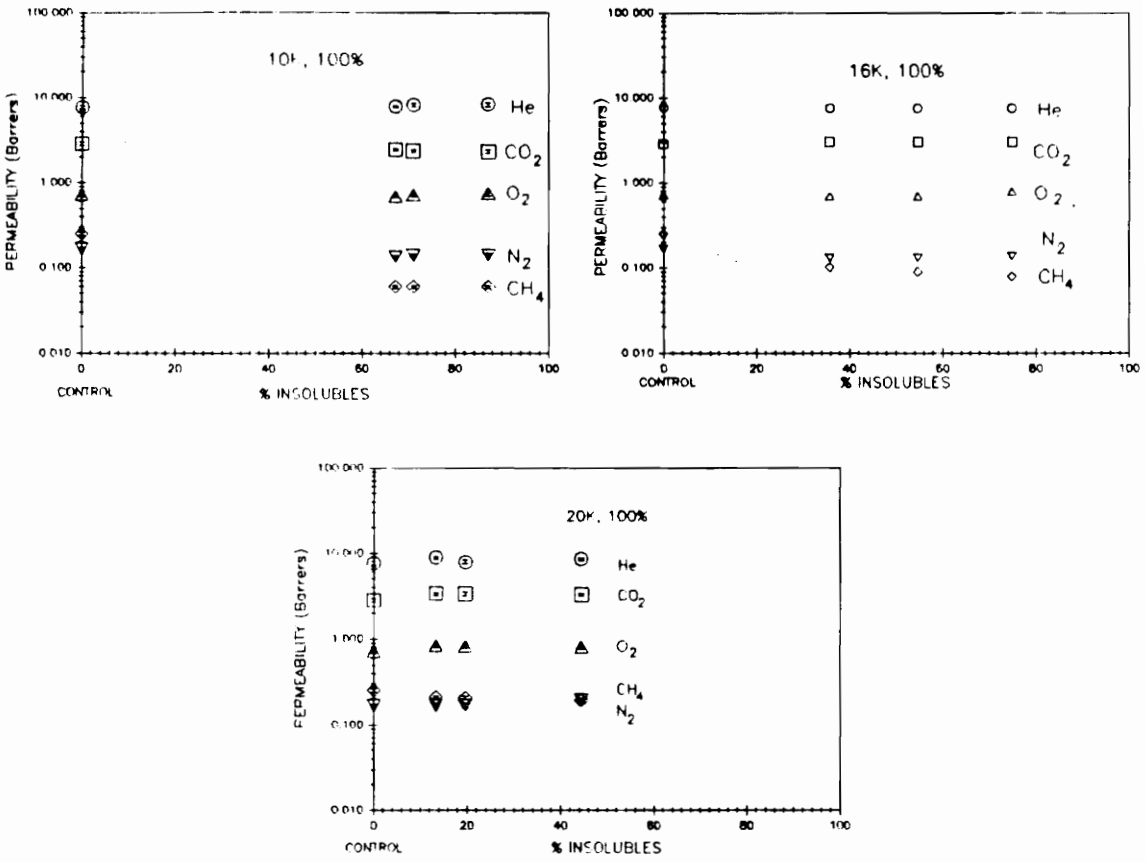

Figure 27. Gas Permeabilities for MIPEK 10K, 16K and 20K. (@ 30°C & 1 atmg)

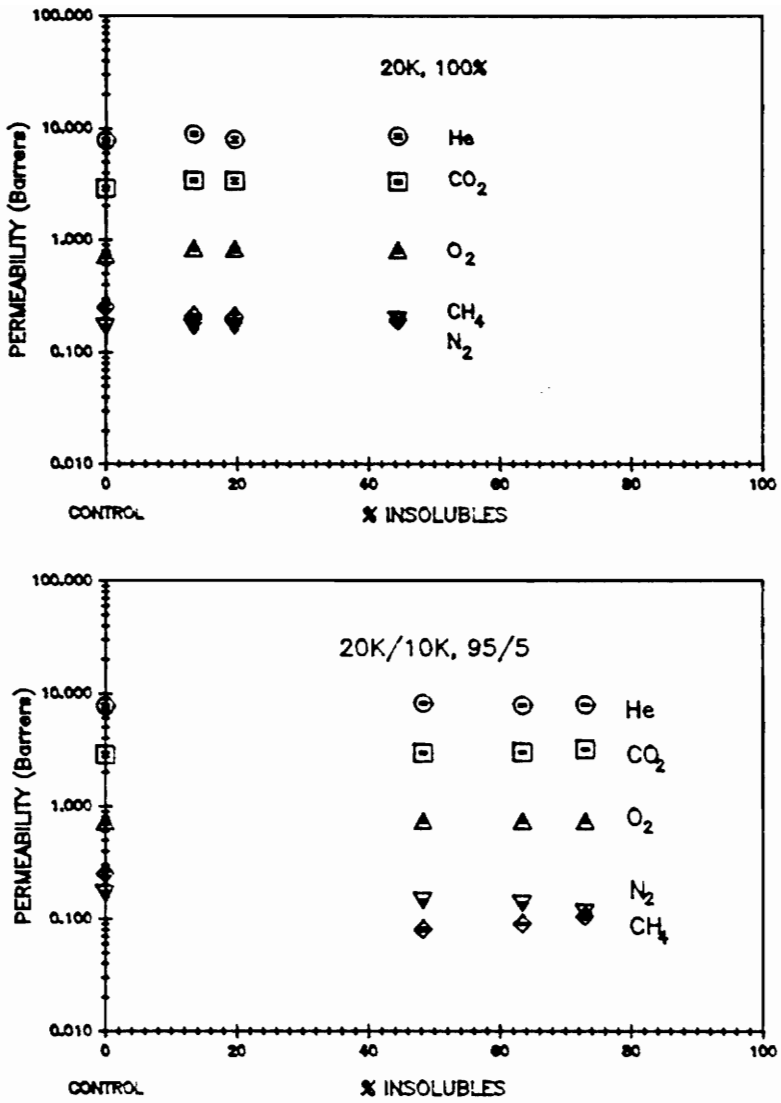

Figure 28. Gas Permeabilities for Series of MIPEK.

(@ 30°C & 1 atmg)

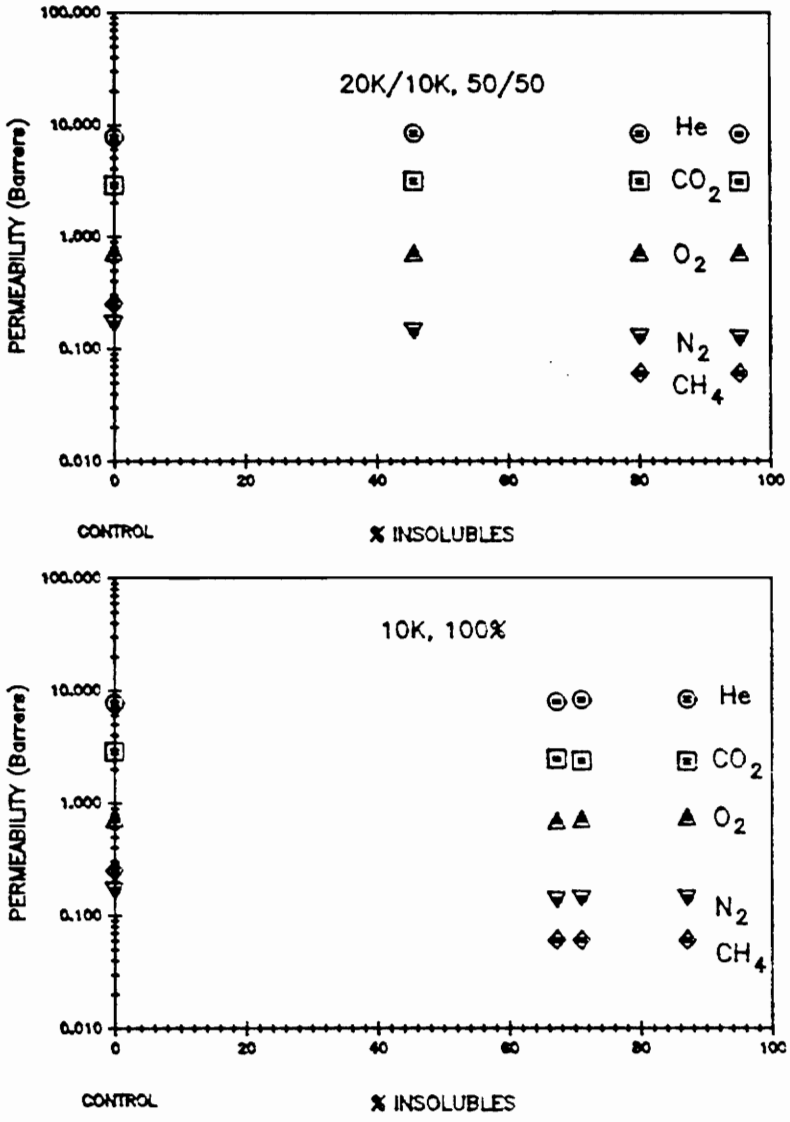

Figure 29. Gas Permeabilities for Series of MIPEK.

(@ 30°C & 1 atmg)

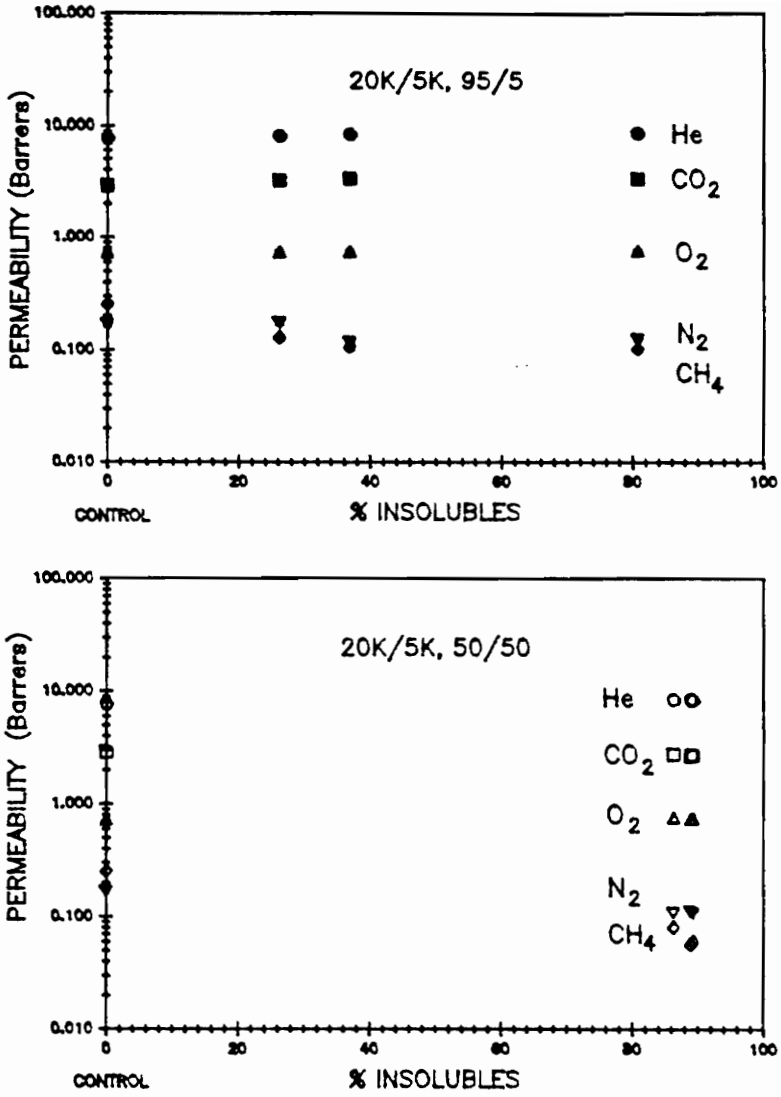

Figure 30. Gas Permeabilities for MIPEK 20K/5K Series.

(@ 30°C & 1 atmg)

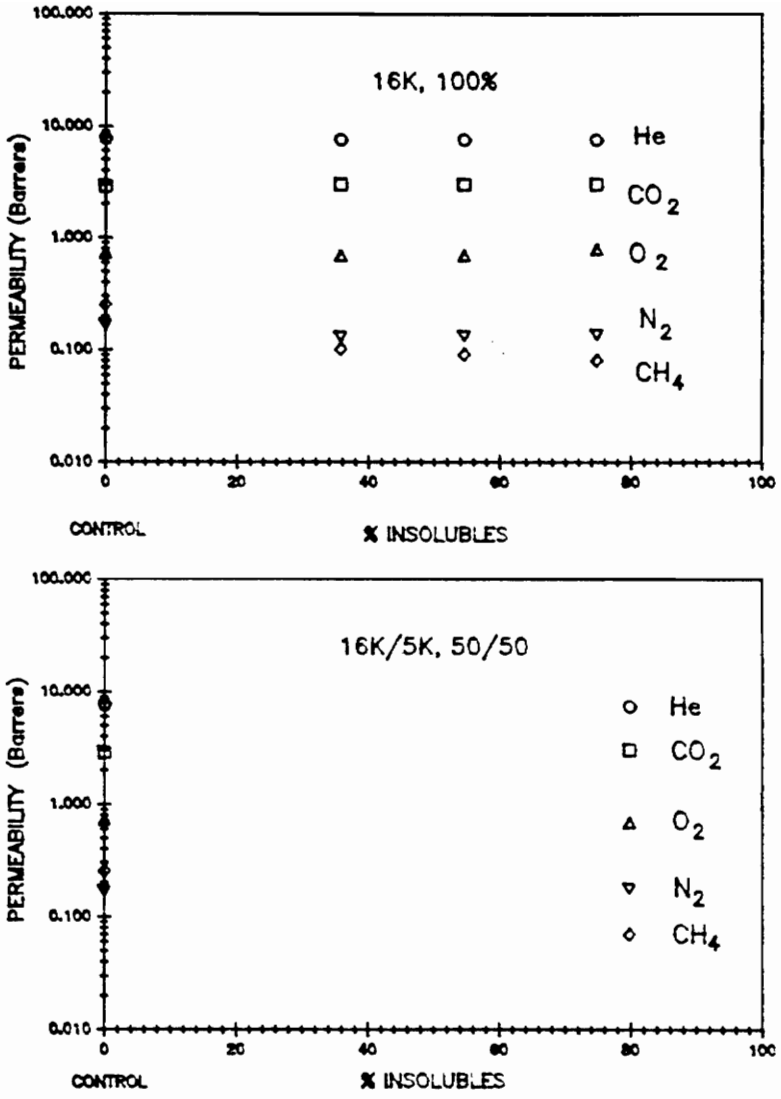

Figure 31. Gas Permeabilities for MIPEK 16K/5K Series.

(@ 30°C & 1 atmg)

The zero percentage of insolubles represents the gas permeability results for the uncrosslinked polymer (PEK or control).

For all the MIPEK blends studied, helium was the faster permeating gas whereas CH_4 was the slower penetrant. The following order of permeation was observed for all the series: $He > CO_2 > O_2 > N_2 > CH_4$ with the exception of the 20K, 100% blend for which the permeabilities for N_2 and CH_4 were approximately the same. These results are not surprising and can be explained by selective effect of the polymer network for penetrants of different sizes and shapes. In order to explain this effect, the permeability coefficient (P) can be expressed as a function of three variables [12]:

$$P = ABC$$

where:

A = f(membrane's physical and chemical structure)

B = f(gas properties such as size shape and polarity)

C = f(membrane - gas interaction)

A and B determine the diffusional characteristics of a particular penetrant through a given membrane. Then, the diffusion coefficient can be considered as a function of A and B:

$$D = AB$$

whereas C represents the solubility coefficient. Thus, the permeability coefficient is given by:

$$P = DS$$

Then, any effect of penetrant size and shape can be easily interpreted by considering the diffusion coefficients.

Table 14 shows the Van der Waal's volumes and the kinetic diameters for the five gases evaluated. The effect of the differences in penetrant size or shape on the molecular mobility is illustrated in Figure 32. This is a semi-log plot of the apparent diffusion coefficients (calculated from the time-lag permeation method) as a function of the Van der Waal's volumes for the five gases analyzed. The following order of diffusion was experimentally determined: He > O_2> N_2> CO_2> CH_4 which is the expected sequence according to the penetrant volumes.

Helium, showed the highest diffusivity which is consistent with its being the smallest gas molecule and also that it is spherical in shape. Larger non-spherical penetrants such as N_2, O_2 and CO_2 tend to reach a plateau in diffusivity. This behavior has been previously reported and explained by considering the effect of the molecular shape as well as its volume. The cross-sectional area of the gas molecule will determine its capacity to pass through a "molecular void" of a determined size in the polymer [52].

The kinetic diameter of the gases need to be considered in comparing the case of the bulky, spherical CH4 molecule to linear CO_2. The kinetic diameter of a gas can be related to the zeolite window dimension needed to permit the passage of the gas and has been traditionally used to explain this phenomenon [52].

Table 14. Penetrants sizes of Various Gases.

GAS	VAN der WAAL's VOLUME b (cc/mol) [51]	KINETIC DIAMETER (A) [52]
He	23.70	2.58
O_2	31.83	2.9
N_2	39.13	3.65
CO_2	42.67	3.3
CH_4	42.78	3.88

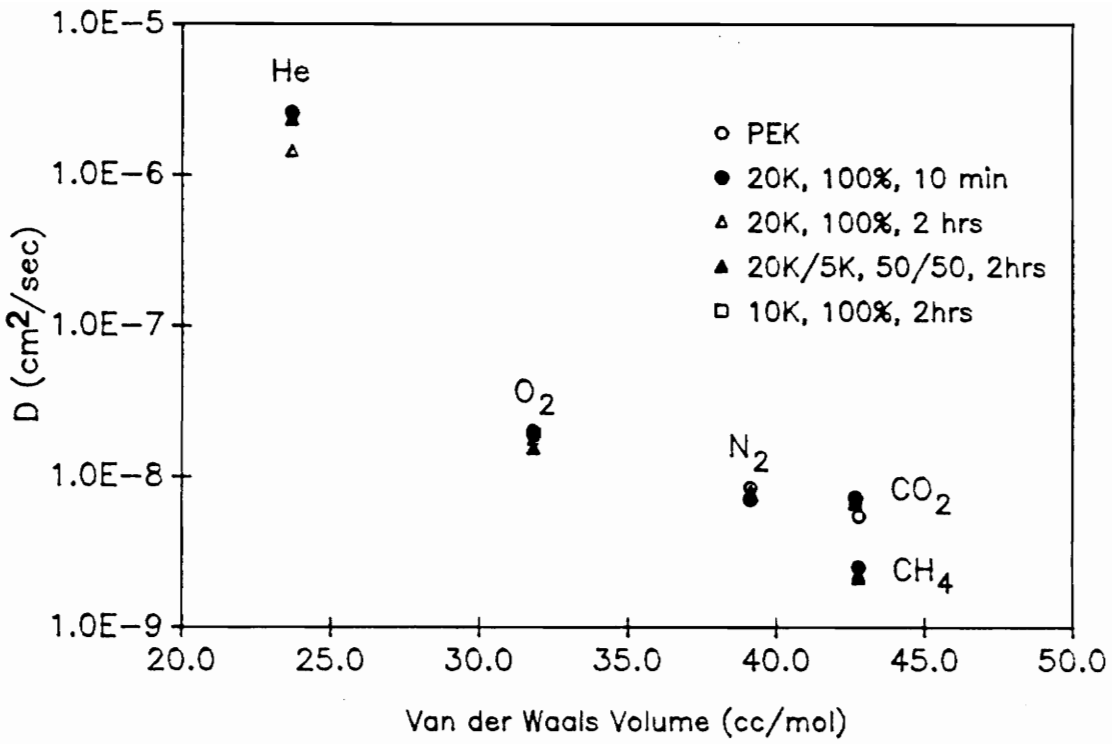

Figure 32. Apparent Diffusion Coefficients for the Different Penetrants in PEK and Crosslinked MIPEK Blends at 30°C for an Upstream Gas Pressure of 1 atmg.

For spherical molecules such as He and CH_4, this dimension is similar to the Lennard-Jones diameter. For the asymmetric molecules O_2,N_2, CO_2, the kinetic diameter represents the minimum diameter of the molecule and the penetrant shape has to be considered. Figure 33 shows the correlation of the apparent diffusion coefficients as a function of the kinetic diameter of the gases. A small difference of about 0.6 Å between the kinetic diameters of CO_2 and CH_4 represents a noticeable difference in the diffusion coefficients observed.

In summary, the experimental orders of diffusivities and permeabilities observed for the different crosslinked MIPEK blends are:

Diffusivity order : $He > O_2 > N_2 > CO_2 > CH_4$

Permeability order: $He > CO_2 > O_2 > N_2 > CH_4$

The apparent anomaly in the observed permeation order which shows a permeability of CO_2 higher than the expected, may be explained by considering the "C" factor or solubility factor in the permeation equation. The apparent solubility coefficients (S) of CO_2 for one of the MIPEK blends is reported in Table 15. The S for CO_2 is by far higher than the S coefficients for the other gases. Thus, the CO_2 molecule due to its high solubility coefficient (and in spite of its relatively large size) tends to permeate faster than O_2, N_2 and CH_4, whose sizes are smaller but also have low solubility coefficients [12].

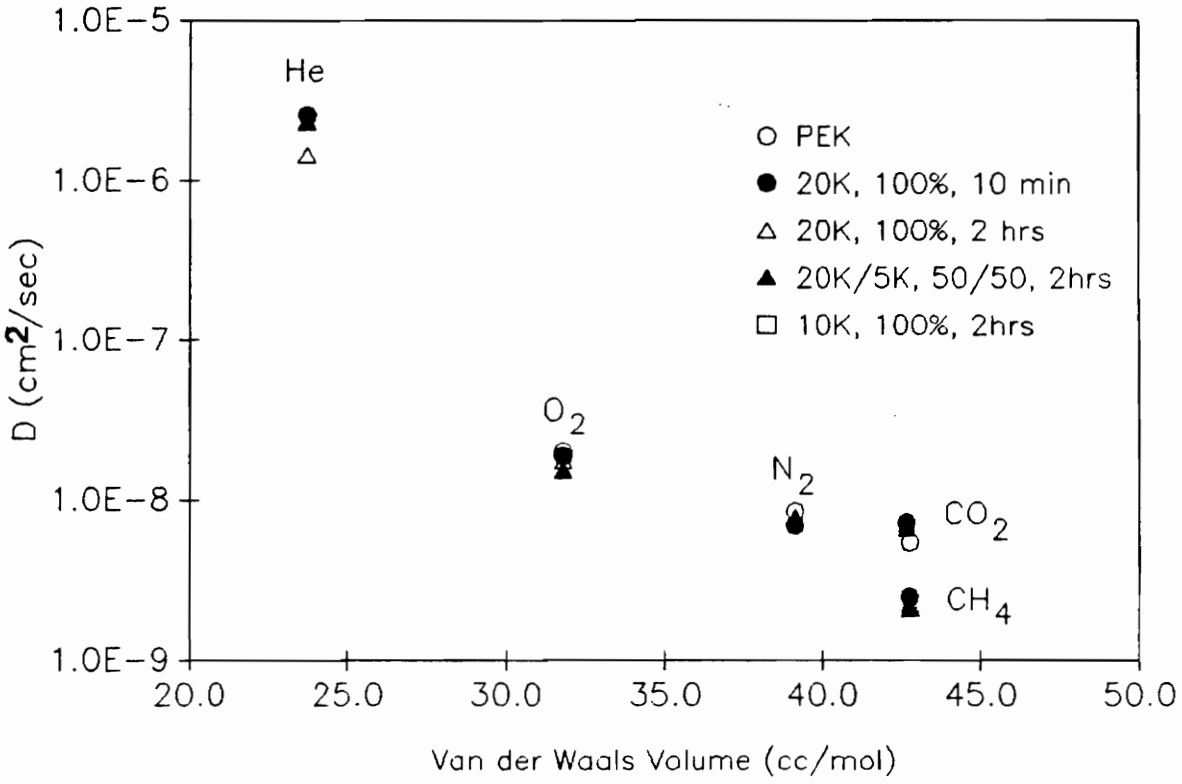

Figure 33. Correlation of the Apparent Diffusion Coefficient and the Kinetic Diameters of the Penetrants in PEK and Crosslinked MIPEK Blends at 30°C for an Upstream Gas Pressure of 1 atmg.

Table 15. Apparent Solubility Coefficients (S) for MIPEK 20K/10K, 50/50, cured for 120 minutes.

GAS	S (STP cc)/ cm. atm
CO_2	3.260
O_2	0.298
N_2	0.179
CH_4	0.156
He	0.030

b. Effect of the Crosslinking Conditions on Gas Permeabilities

The effect of the crosslinking and crosslinking conditions on the permeabilities of the different gases for MIPEK blends is illustrated in Figures 34 to 37. The crosslinking extent are presented here by means of the percentage of insolubles in the samples. This relationship is used here as a first estimate in order to detect the changes in permeabilities and for preliminary identification of the possible causes. Their relationship has already been discussed (Section III.A). The Figures are semi-log plots of the permeabilities versus the insoluble portion in the films.

Figures 34 and 35 show the results for the helium permeabilities. It can be seen that the permeation of helium was not affected by the (gel fraction) crosslinking in the samples. An average permeability of 8.2 Barrers for Helium was calculated from all the blends evaluated with a relative standard deviation (RSD) of 2.3% (less than the experimental error of 5%).

Figures 36 to 37 illustrate the same phenomenon for oxygen. The maximum Oxygen permeability (0.830 ± 0.027 Barrers) was found for a MIPEK blend of 20K, 100% (10 min @ 250°C) and the minimum oxygen permeability (0.686 ± 0.007 Barrers) for the 16K/5K, 50/50 (10 min @ 250°C) blend. An overall decrease in about 0.14 Barrers or 17% was observed. Table 16 summarizes the principal characteristics of these blends. The 20K, 100% (2 hrs @ 250°C) was also included since it shows the second highest

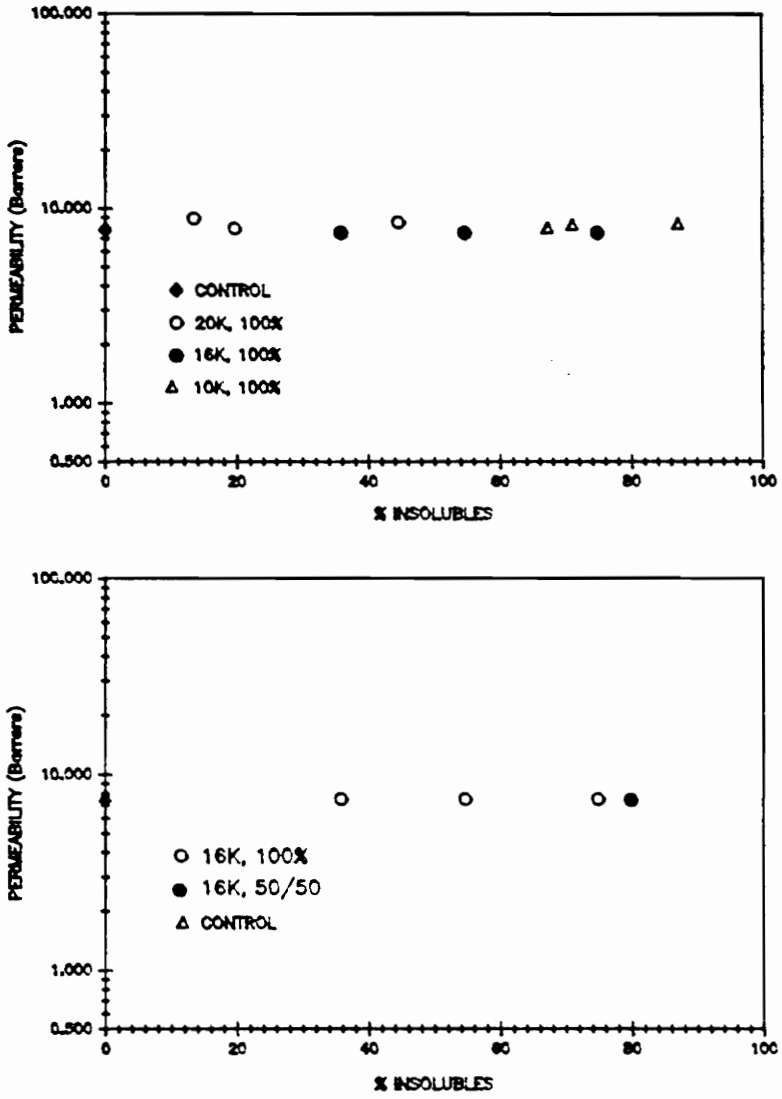

Figure 34. Helium Permeabilities for MIPEK.

(@ 30°C & 1 atmg)

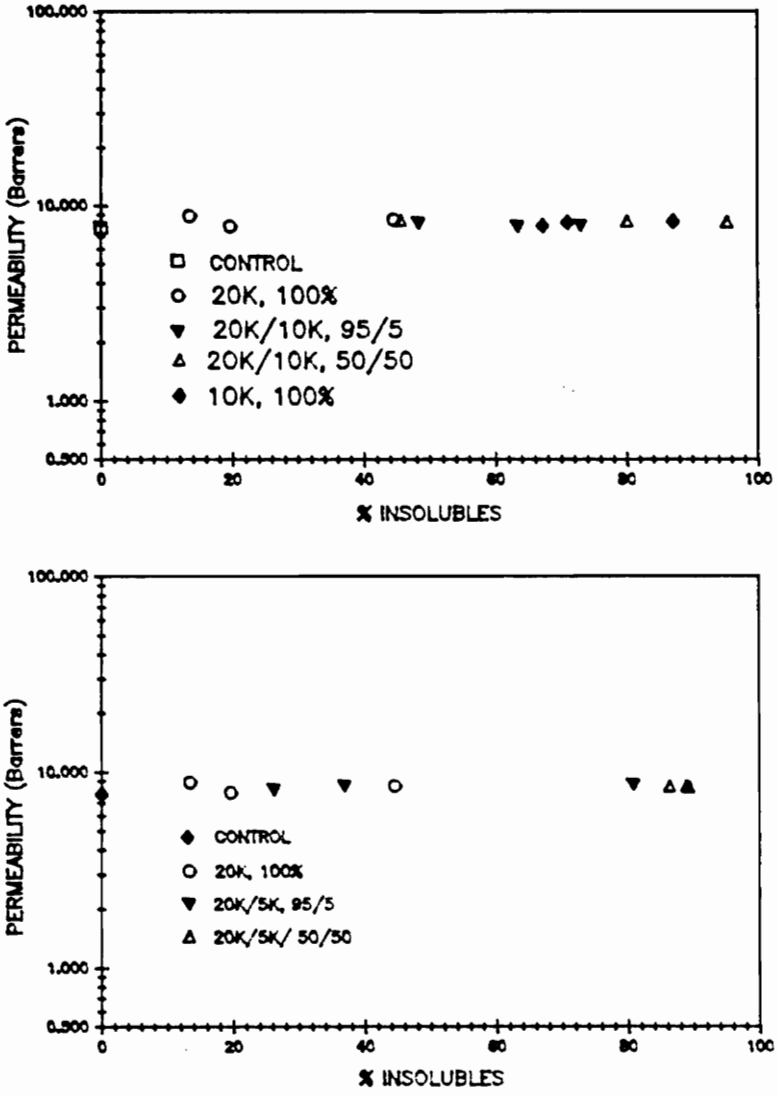

Figure 35. Helium Permeabilities for MIPEK.

(@ 30°C & 1 atmg)

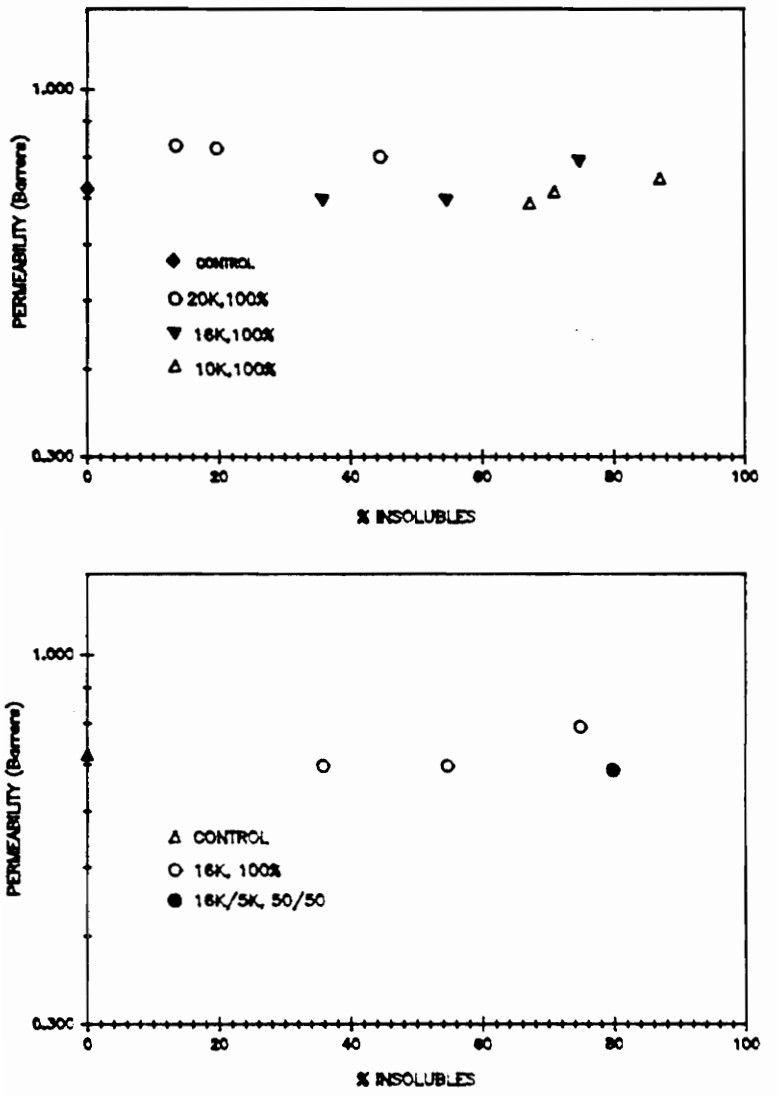

Figure 36. Oxygen Permeabilities for MIPEK.

(@ 30°C & 1 atmg)

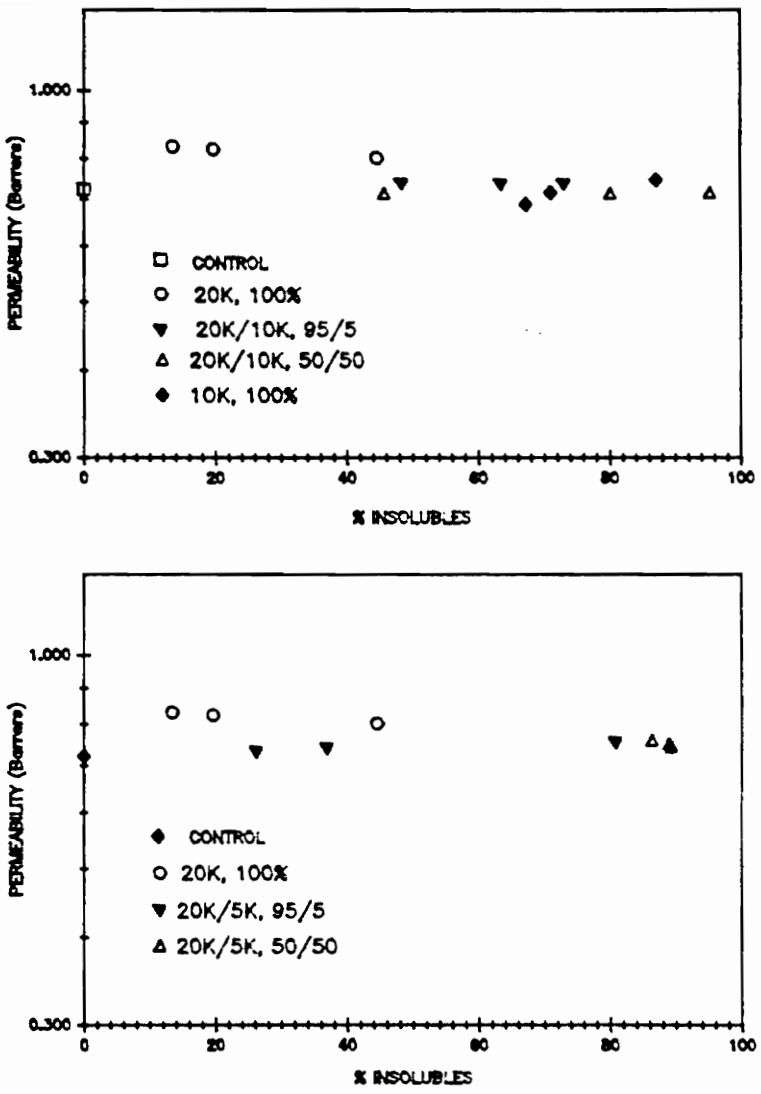

Figure 37. Oxygen Permeabilities for MIPEK.

(@ 30°C & 1 atmg)

Table 16. Oxygen Permeabilities and Sample Characteristics.

SAMPLE CHARACTERISTICS	20K,100% (a)	20K,100% (b)	10K,100% (a)	16K/5K 50/50(a)
P O_2 (Barrers)	0.830± 0.027	0.801± 0.029	0.687± 0.017	0.686± 0.007
% Insolubles	13.4	44.5	67.2	79.8
$\overline{Mc}$ (g/mol)	n.d.(c)	320000(d)	68000	40000
Q	n.d.(c)	43.3	18.4	14.2

a - After 10 minutes @ 250°C.
b - After 2 hours @ 250°C.
c - Was not determined/Film totally dissolved in $CHCl_3$ before reaching constant weight.
d - Too large.

oxygen permeability and because it was possible to determine an experimental value for $\bar{M}c$ (Number Average Molecular Weight of the network chains) from the swelling ratio Q of this sample.

The higher oxygen permeability can be related to the high molecular weight between the crosslinked chains (300K) or to a low dc, whereas the low oxygen permeabilities correspond to low $\bar{M}c$ values (< ~70K).

Figures 38 and 39 show semi-log plots for nitrogen permeabilities as a function of the percentage of insolubles in the samples. The maximum value obtained for nitrogen permeabilities was 0.168 ± 0.006 Barrers for PEK (control polymer) and for 20K, 100% (10 min @ 250°C). The minimum nitrogen permeability observed was 0.107 ± 0.002 Barrers and corresponds to the 20K/5K, 50/50 (10 min to 2 hrs @ 250°C). Thus, a decrease of 0.06 Barrers (or approximately 35%) was observed in the nitrogen permeabilities for the whole range of the evaluated blends.

Table 17 summarizes these results and the corresponding characteristics of the samples. Again, the higher nitrogen permeability corresponds to the largest $\bar{M}c$ values (and Q) and the lower value for the permeation of nitrogen corresponds to $\bar{M}c$ values below 50K (Q = 15).

Figures 40 and 41 illustrate the CO_2 permeabilities which changed from 3.392 ± 0.112 Barrers for 20K, 100% (10 min @ 250°C) to 2.328 ± 0.105 Barrers for 10K, 100% (2 hours @ 250°C), showing a decrease of about 30% (or 1.1 Barrers). These results are summarized in Table 18. On the other hand, the apparent solubility coefficients for the same samples diminished from 3.5 to 2.1 (~ 40%) indicating that the observed

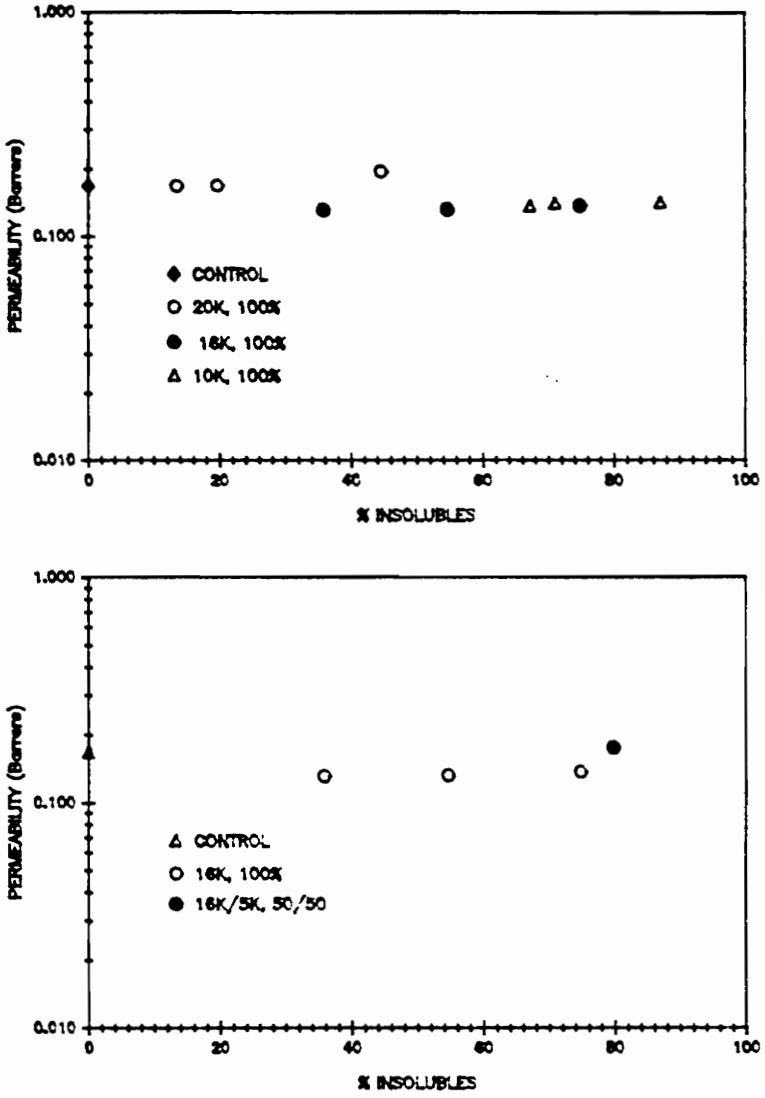

Figure 38. Nitrogen Permeabilities.

(@ 30°C & 1 atmg)

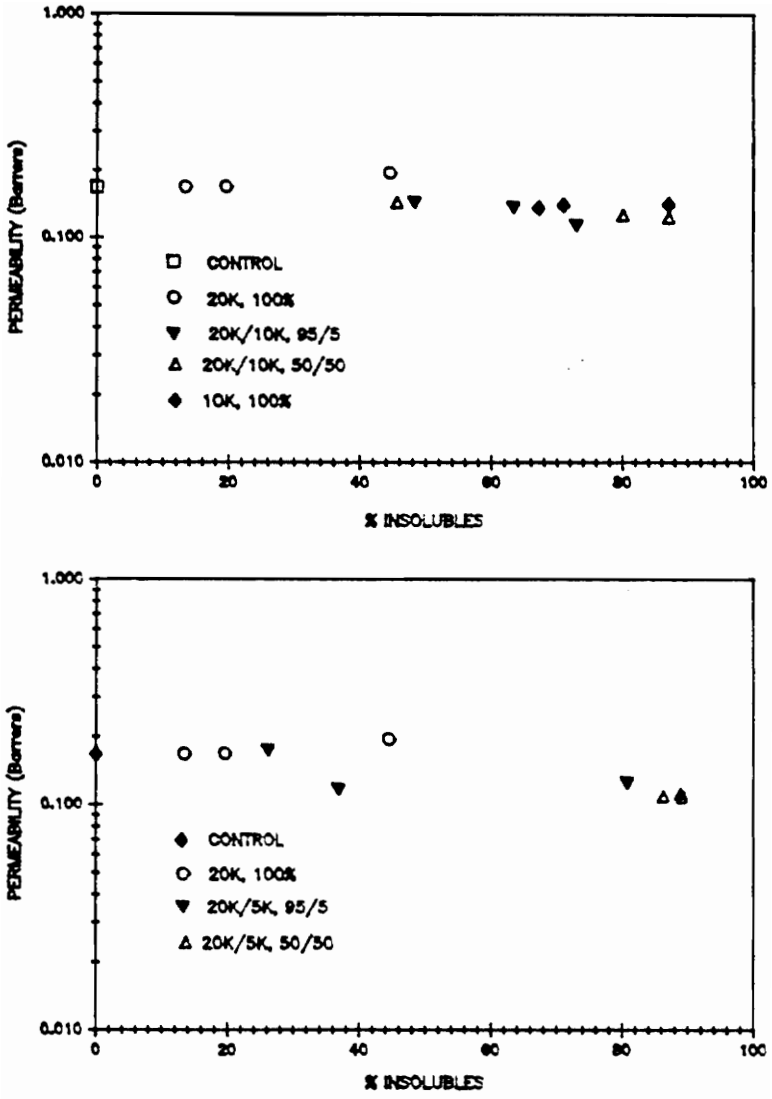

Figure 39. Nitrogen Permeabilities.

(@ 30°C & 1 atmg)

Table 17. Nitrogen Permeabilities and Sample Characteristics.

SAMPLE CHARACTERISTICS	20K,100% (a)	20K,100% (b)	20K/5K 50/50(a)	20K/5K 50/50(b)
P N_2 in Barrers	0.167± 0.006	0.167± 0.007	0.107± 0.002	0.108± 0.004
% Insolubles	13.4	44.5	88.9	86.3
$\bar{M}c$ (g/mole)	n.d.(c)	320000(d)	47000	15000
Q	n.d.(c)	43.3	15.2	8.7

a - After 10 minutes @ 250°C.
b - After 2 hours @ 250°C.
c - Was not determined due to dissolution of the film in $CHCl_3$.
d - Too large.

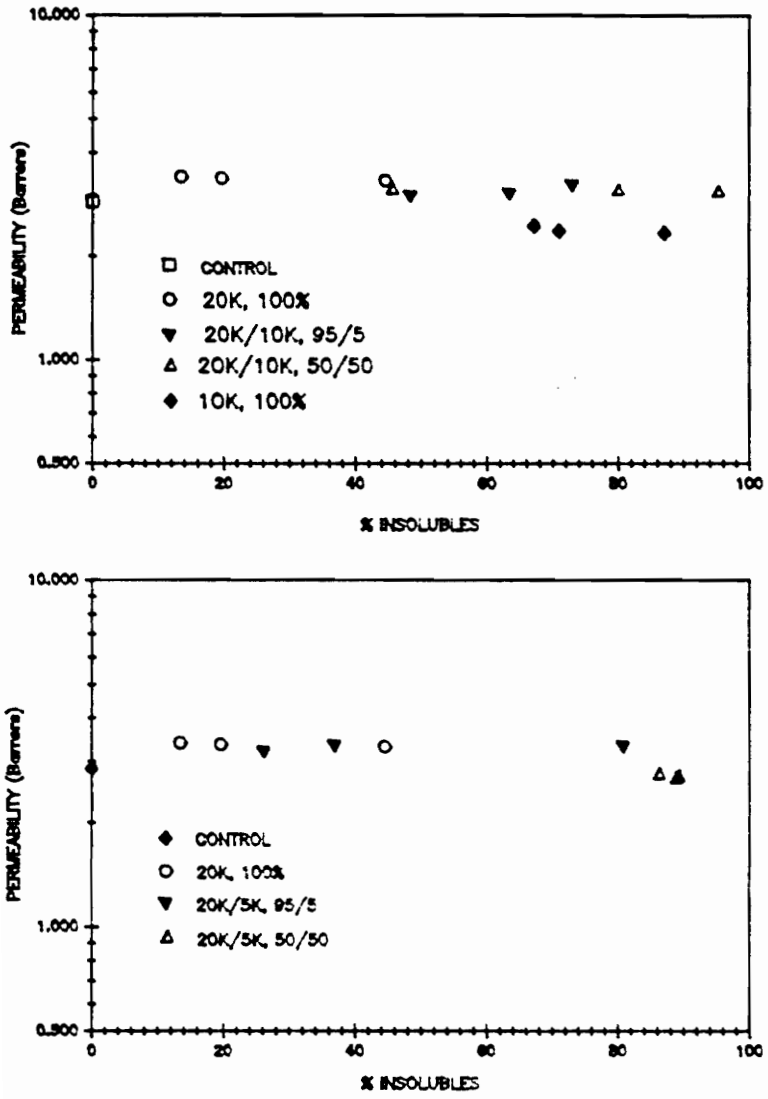

Figure 40. Carbon Dioxide Permeabilities.

(@ 30°C & 1 atmg)

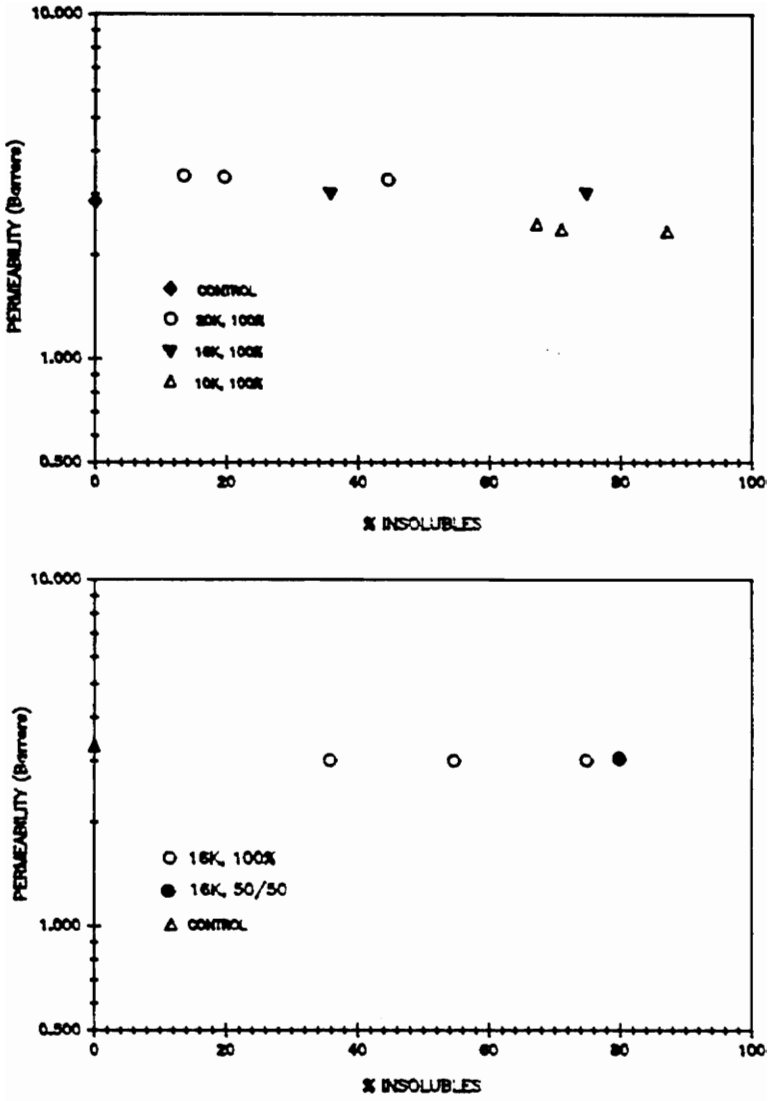

Figure 41. Carbon Dioxide Permeabilities.

(@ 30°C & 1 atmg)

Table 18. CO_2 Permeabilities and Sample Characteristics.

SAMPLE CHARACTERISTICS	20K,100% (a)	20K,100% (b)	10K,100% (b)
P CO_2 in Barrers	3.392± 0.112	3.313± 0.119	2.328± 0.105
% Insolubles	13.4	44.5	87.1
$\overline{Mc}$ (g/mol)	n.d.(c)	320000(d)	30000
Q	n.d.(c)	43.3	11.8
S	3.5	3.6	2.1
D (cm^2/sec)	0.7E-08	0.7E-08	0.7E-08

a - After 10 minutes @ 250°C.
b - After 2 hours @ 250°C.
c - Was not determined due to total dissolution of the sample in $CHCl_3$.
d - Too large.

changes in CO_2 permeabilities were mainly due to changes in the solubility of this gas in the polymer and not due to changes in the mobility properties (the apparent diffusivity factors remained constant). It is important to note however, that the diffusivity and solubility coefficients reported in this work are apparent values calculated from the time-lag permeation method. A way to corroborate these results would be to measure the actual solubility coefficients by equilibrium sorption experiments. Thus, the actual diffusivity coefficients could be calculated from the permeability-solubility quotients.

Figures 42 and 43 show the CH_4 permeabilities. The permeation range observed for CH_4 changed from 0.250 for 20K, 100% to 0.06 Barrers for 10K, 100%. The properties of these samples are tabulated in Table 19. It can be seen that the higher permeability value corresponds to the higher values of $\overline{M}c$ and Q. These correlations are also illustrated in Figure 44 (Permeability versus $\overline{M}c$) and Figure 45 (Permeability versus Q) for all the crosslinking conditions evaluated. As a general trend, a decrease in the Number Average Molecular Weight of the network chain ($\overline{M}c$) is related to a low CH_4 permeability values. The samples that showed the smaller values for CH_4 permeabilities were 10K, 100%, 20K/5K, 50/50 and 16K/5K, 50/50 with $\overline{M}c$ values below than 50K. The same kind of behavior can be observed in Figure 45 for the swelling ratios values for the different films evaluated.

Table 20 summarizes the crosslinking effect on the permeabilities of each one of the gases studied. These effects represent the evaluation of all MIPEK blends and crosslinking conditions that were used in this

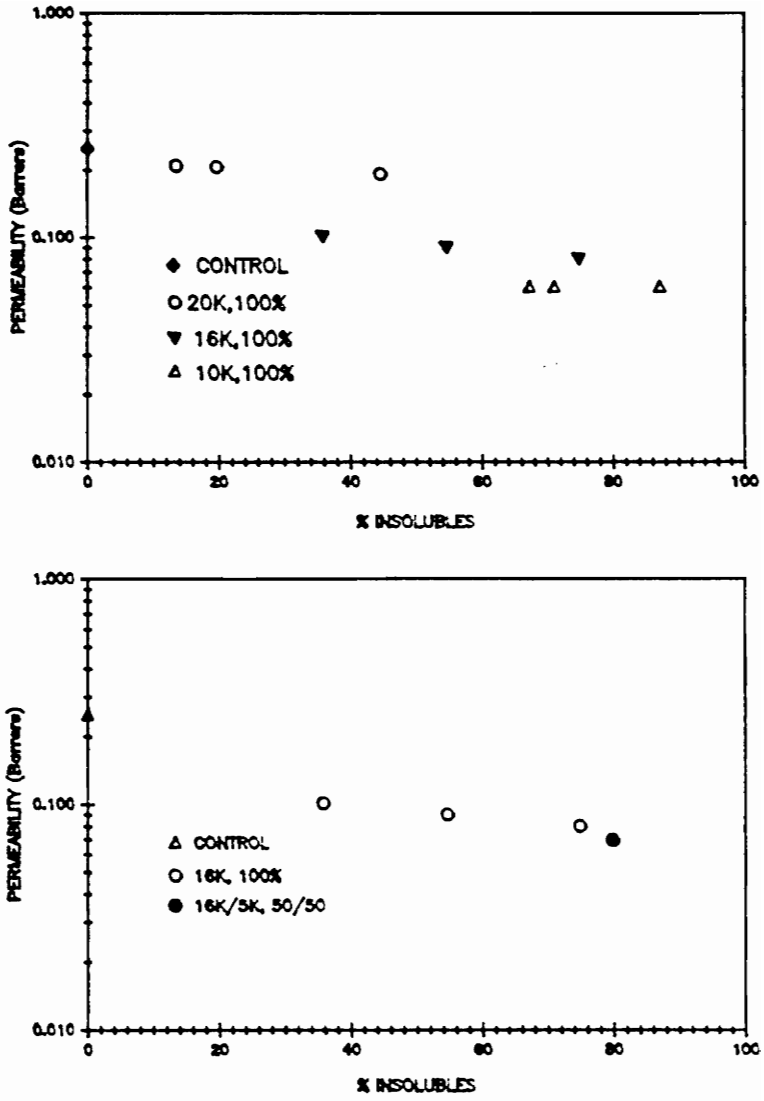

Figure 42. Methane Permeabilities.

(@ 30°C & 1 atmg)

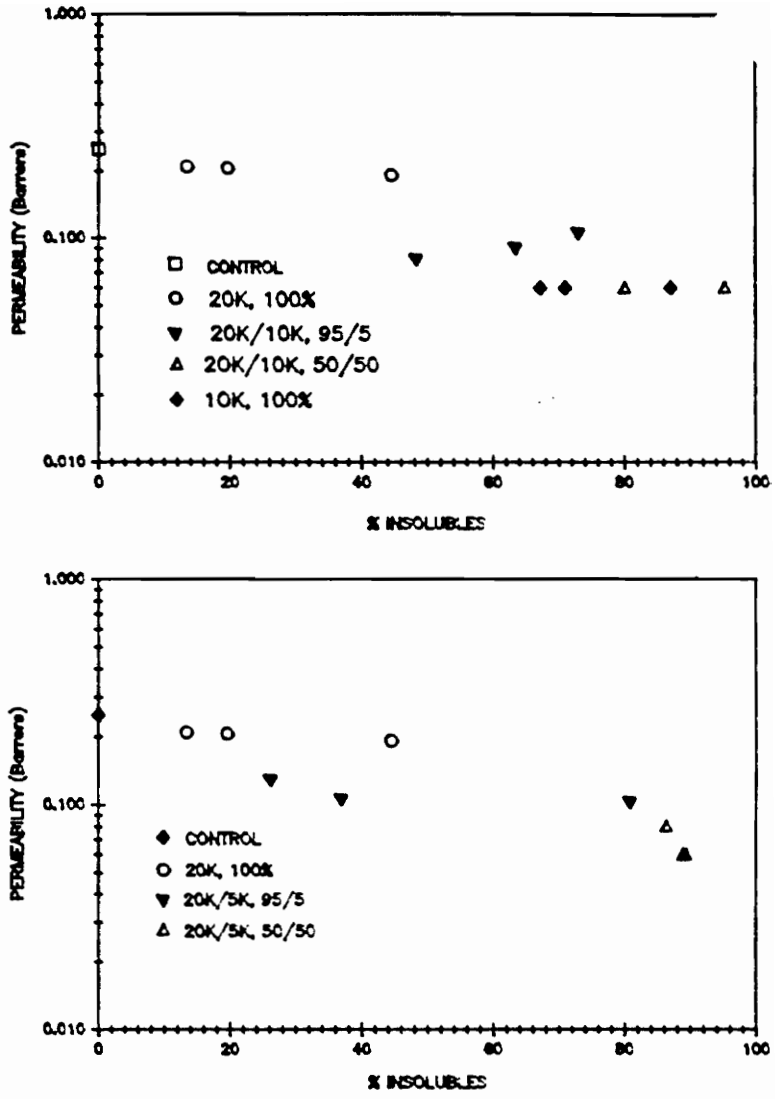

Figure 43. Methane Permeabilities.

(@ 30°C & 1 atmg)

Table 19. CH_4 Permeabilities and Sample Characteristics.

SAMPLE CHARACTERISTICS	20K,100% (a)	10K,100% (a)	20K,100% (b)
P CH_4 in Barrers	0.250± 0.014	0.06± 0.002	0.192± 0.007
% Insolubles	13.4	67.2	44.5
$\overline{Mc}$ (g/mol)	n.d.(c)	68000	320000(d)
Q	n.d.(c)	18.4	43.3
D		0.851E-08	0.20E-08
S		0.18	0.67

a - After 10 minutes @ 250°C.
b - After 2 hours @ 250°C.
c - Not possible to determine.
d - Too large.

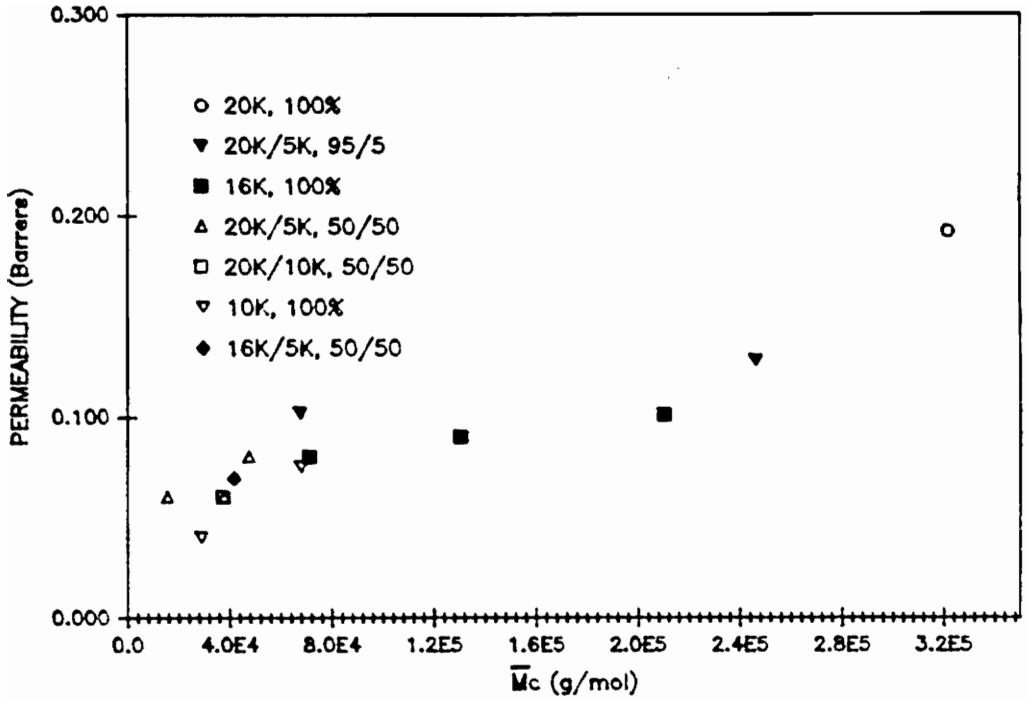

Figure 44. Methane Permeabilities as a Function of $\bar{M}c$.
(@ 30°C & 1 atmg)

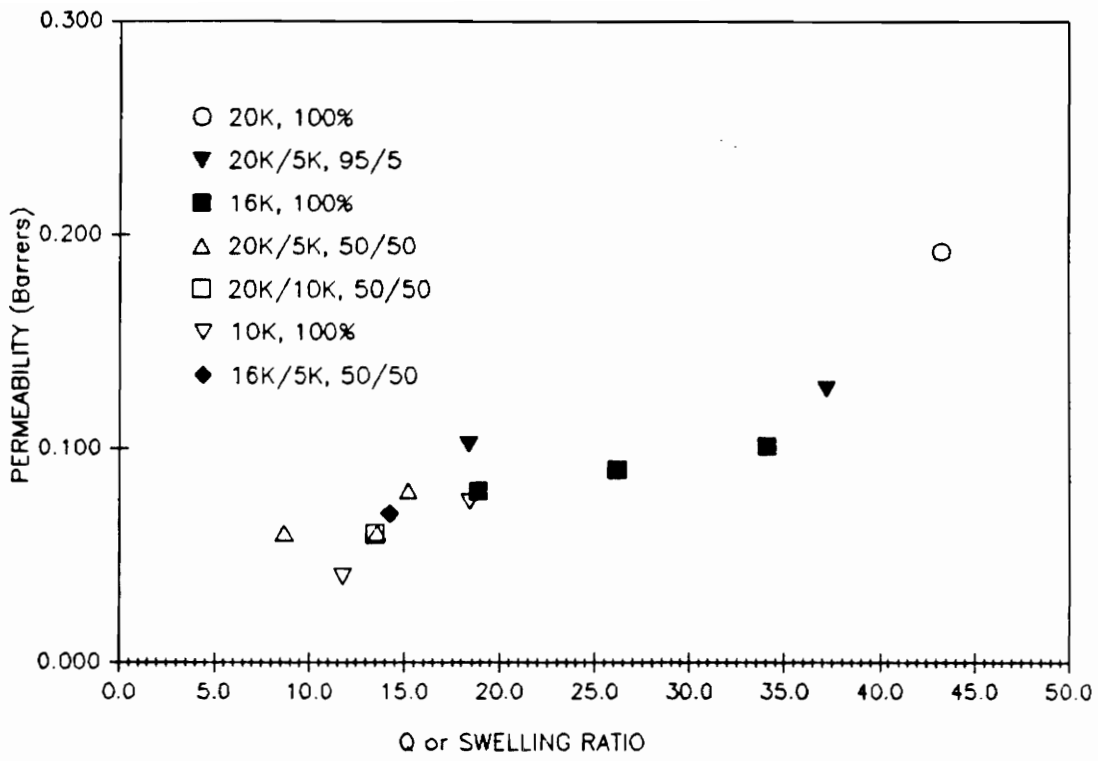

Figure 45. Methane Permeabilities as a Function of the Swelling Ratio.

Table 20. Permeability ranges and overall effect.

GAS	PERMEABILITY RANGE (Barrers) (a)	EFFECT (Decrease)
He	8.2(b)	Constant
O_2	0.83-0.69	0.14 Barrers (~ 15%)
N_2	0.17-0.11	0.06 Barrers (~ 35%)
CO_2	3.39-2.33	1.06 Barrers (~ 30%)
CH_4	0.25-0.06	0.19 Barrers (~ 75%)

a - @ 30°C & 1 atmg.
b - Average value (within the experimental error).

research. Helium permeabilities were not affected whereas the CH_4 permeabilities decreased by c.a. 75% for the degrees of crosslinking evaluated. These effects have already been explained by penetrant size, shape and solubility considerations in Section III.E.a.

c. O_2/N_2 Ideal Permeability Ratios

Figures 46 and 47 illustrate the O_2/N_2 ideal permeability ratios as a function of the percentage of insolubles in the film for different series of MIPEK blends. Figure 48 summarizes the same correlation for all the evaluated samples. The dependance of the O_2/N_2 selectivities on the number average molecular weight of the network chains ($\bar{M}c$) is presented in Figure 49.

O_2/N_2 selectivity increased from 4.8 for 20K, 100% (Q = 43.3) to 7.0 for the 20K/5K, 50/50 blends (Q=8.7) representing an approximately 45% increase in selectivity. Table 21 summarizes these values. The higher O_2/N_2 selectivities correspond to the lower values of $\bar{M}c$.

d. CO_2/CH_4 Ideal Separation Factors

Figures 50 to 52 illustrate the CO_2/CH_4 ideal separation factors as a function of the insoluble fraction in the different series of MIPEK blends and Figure 53 summarizes this dependance for all the evaluated samples. The effect of Mc on the CO_2/CH_4 separation factors is presented in Figure 54 which shows that higher selectivities correspond to the lower values of $\bar{M}c$.

The CO_2/CH_4 ideal selectivities increased from 17 for the blend 20K, 100% (Q = 43.3) to approximately 50 for the 16K/5K, 50/50 and 20K/10K,

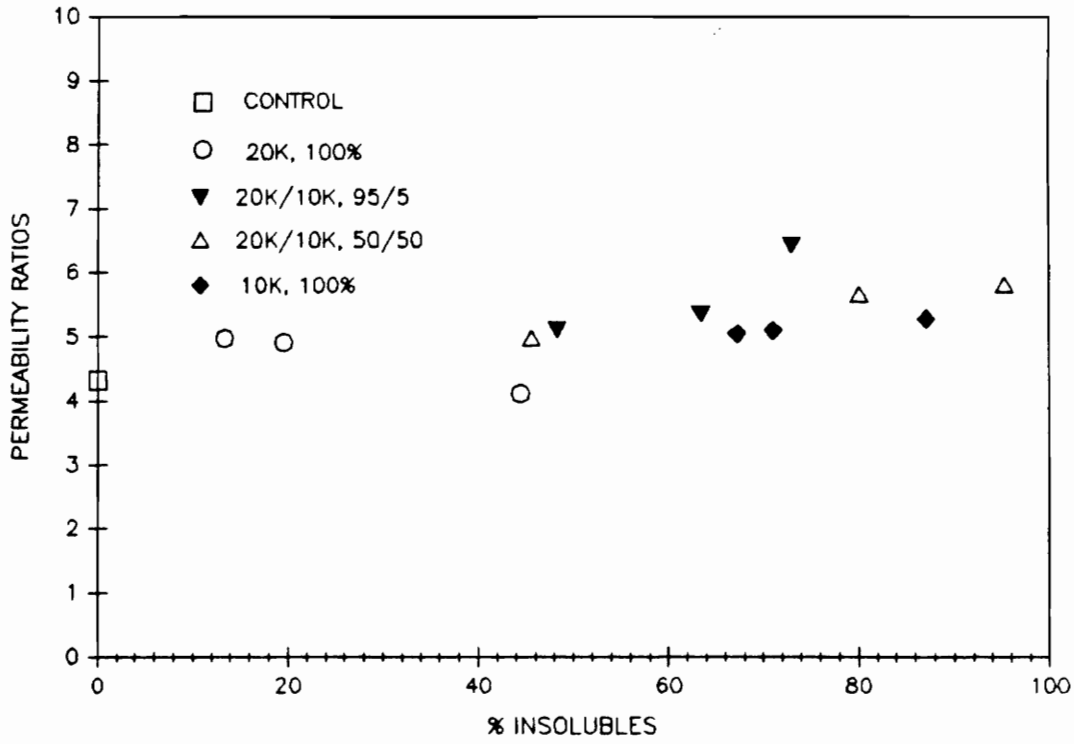

Figure 46. Oxygen/Nitrogen Ideal Permeability Ratios for Series of MIPEK 20K/10K. (@ 30°C & 1 atmg)

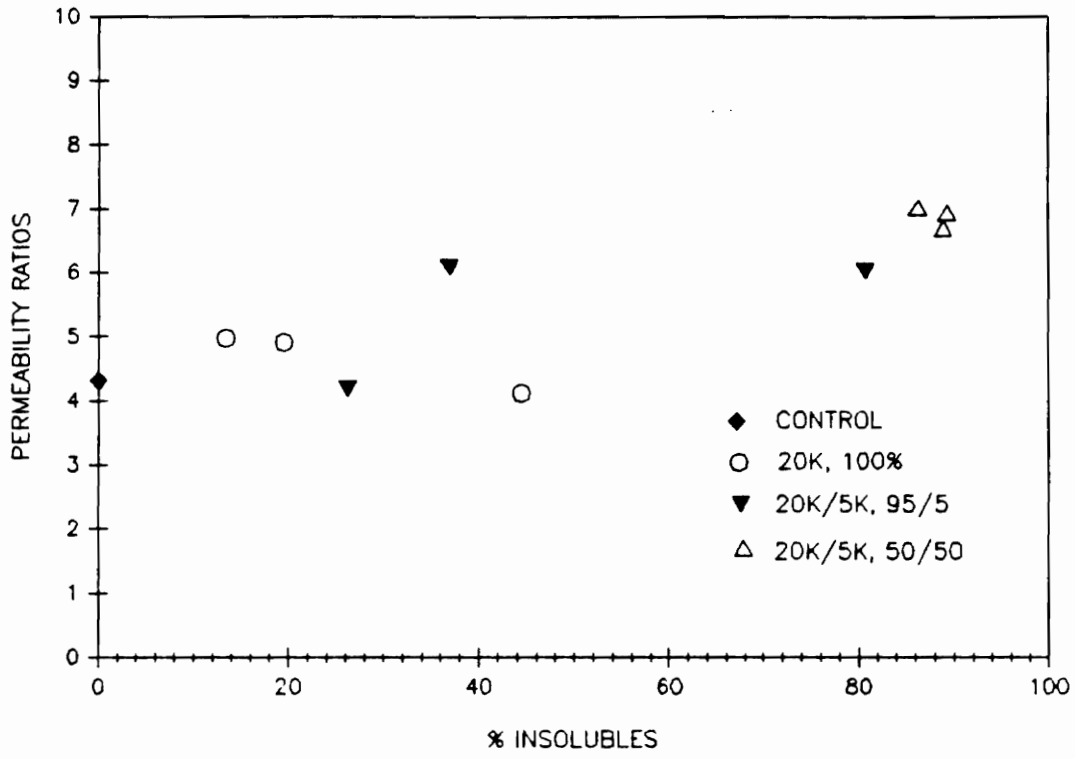

Figure 47. Oxygen/Nitrogen Ideal Permeability Ratios for Series of MIPEK 20K/5K. (@ 30°C & 1 atmg)

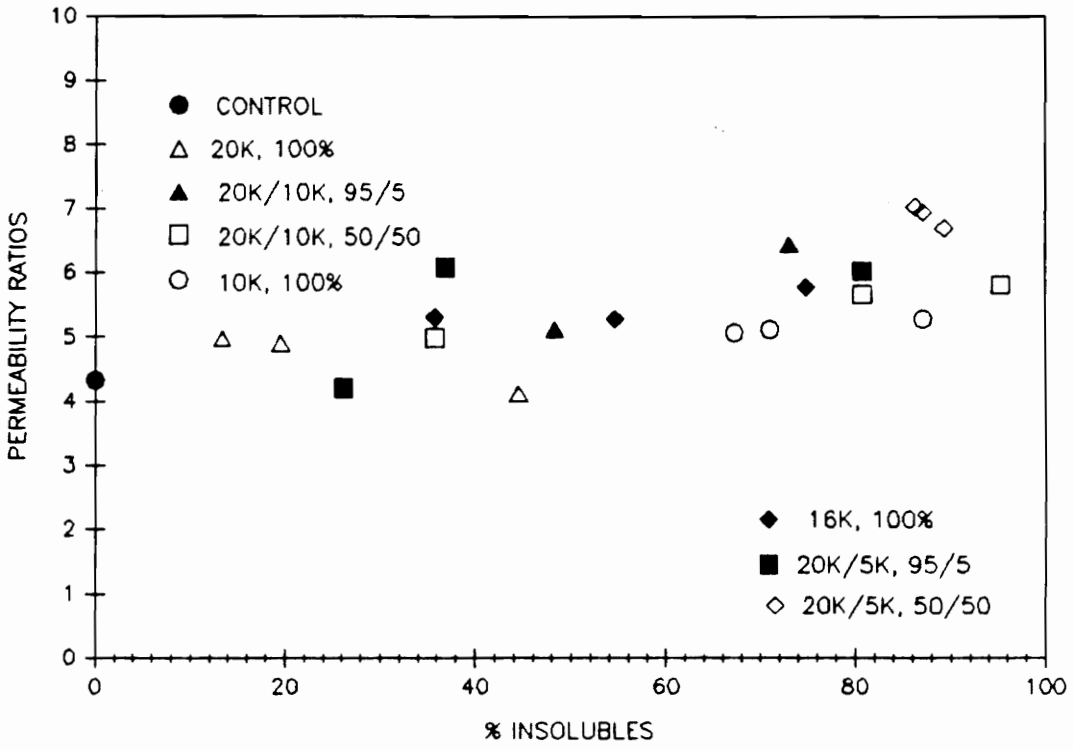

Figure 48. Oxygen/Nitrogen Ideal Permeability Ratios for MIPEK Blends.
(@ 30°C & 1 atmg)

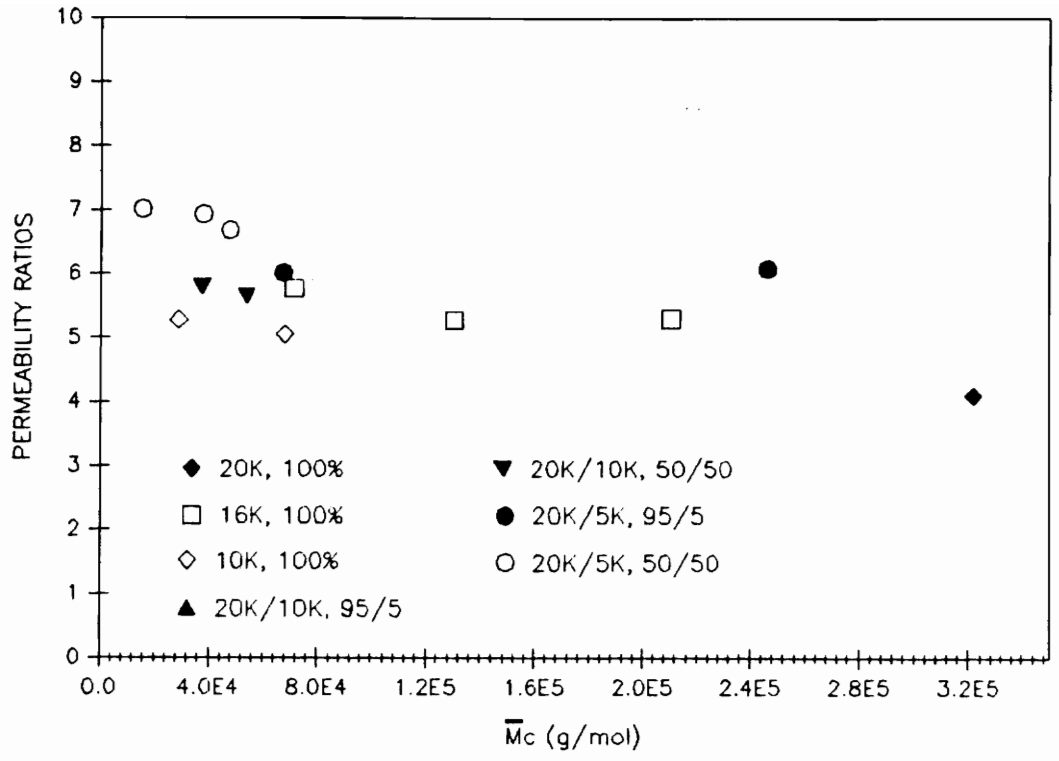

Figure 49. O_2/N_2 Selectivities as a Function of the Number Average Molecular Weight of the Network Chains ($\overline{M}c$).

Table 21. Influence of Crosslink Density on O_2/N_2 Selectivities.

PROPERTY	BLEND 20K/5K,50/50(a)	20K,100%(a)
$\overline{M}c$ (g/mol)	15000	320000(b)
Q	8.7	43.3
P O_2 (Barrers)	0.758	0.801
P N_2 (Barrers)	0.108	0.167
P O_2/ P N_2	7.0	4.8

a - After 2 hours @ 250°C.

b - Too large.

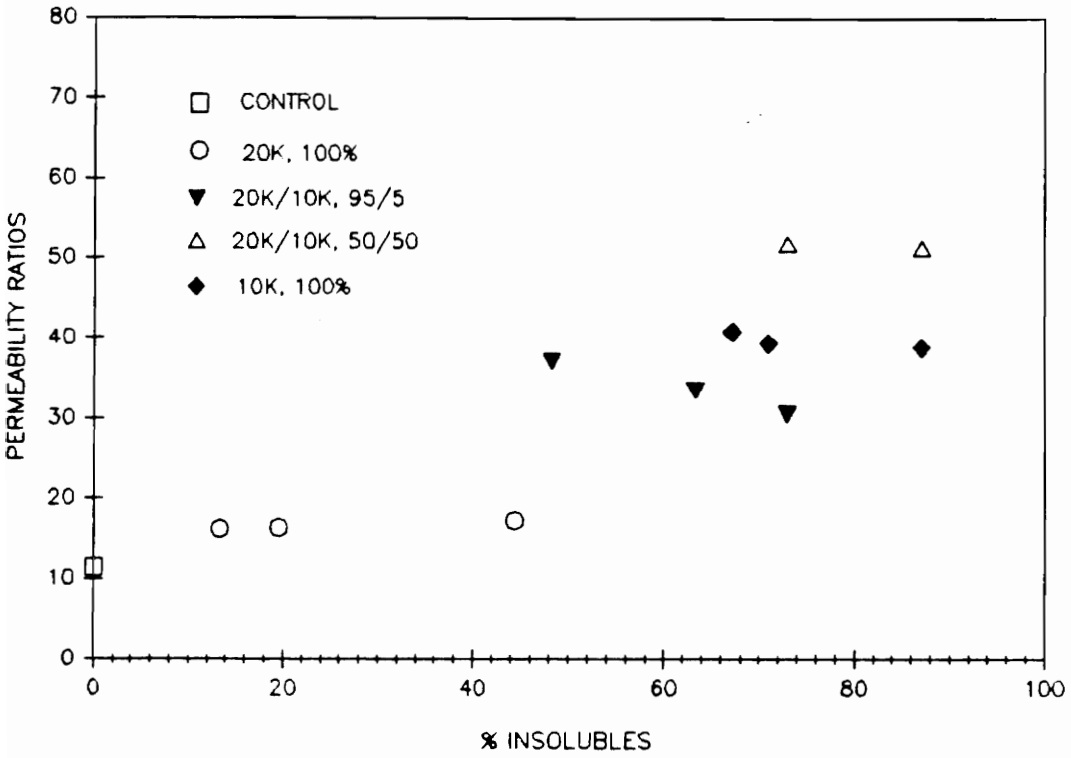

Figure 50. CO_2/CH_4 **Ideal Separation Factors for Series of MIPEK.**
(@ 30°C & 1 atmg)

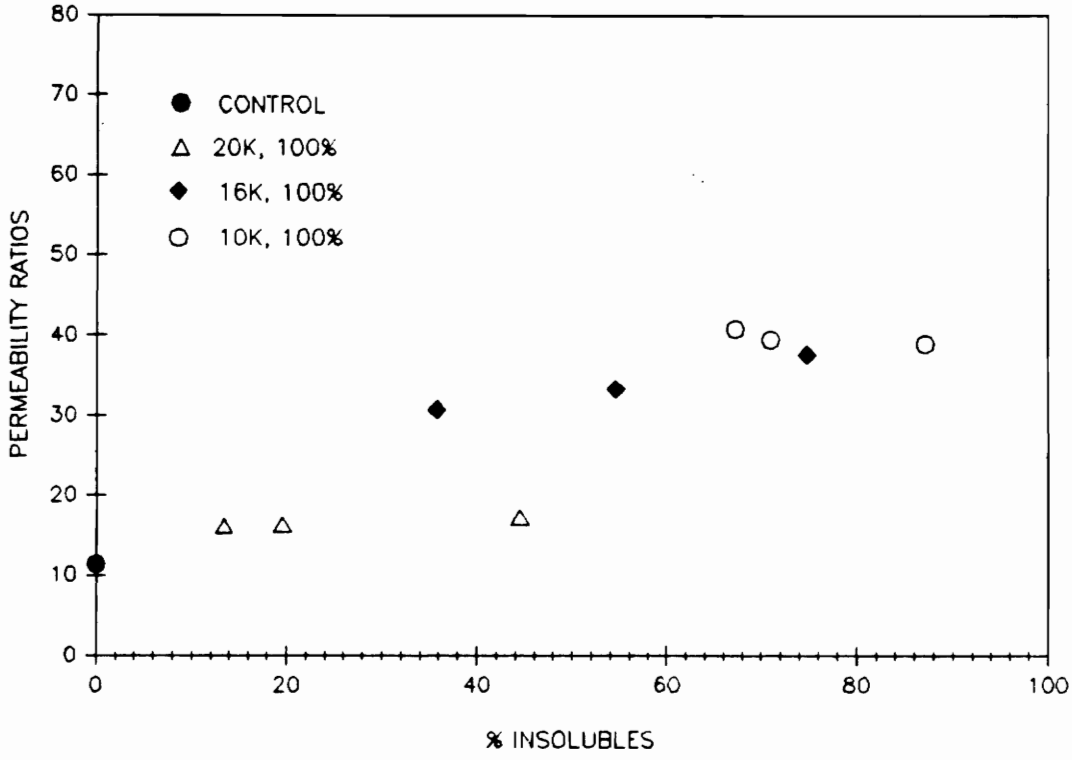

Figure 51. CO_2/CH_4 **Ideal Separation Factors for MIPEK 10K, 16K and 20K.**
(@ 30°C & 1 atmg)

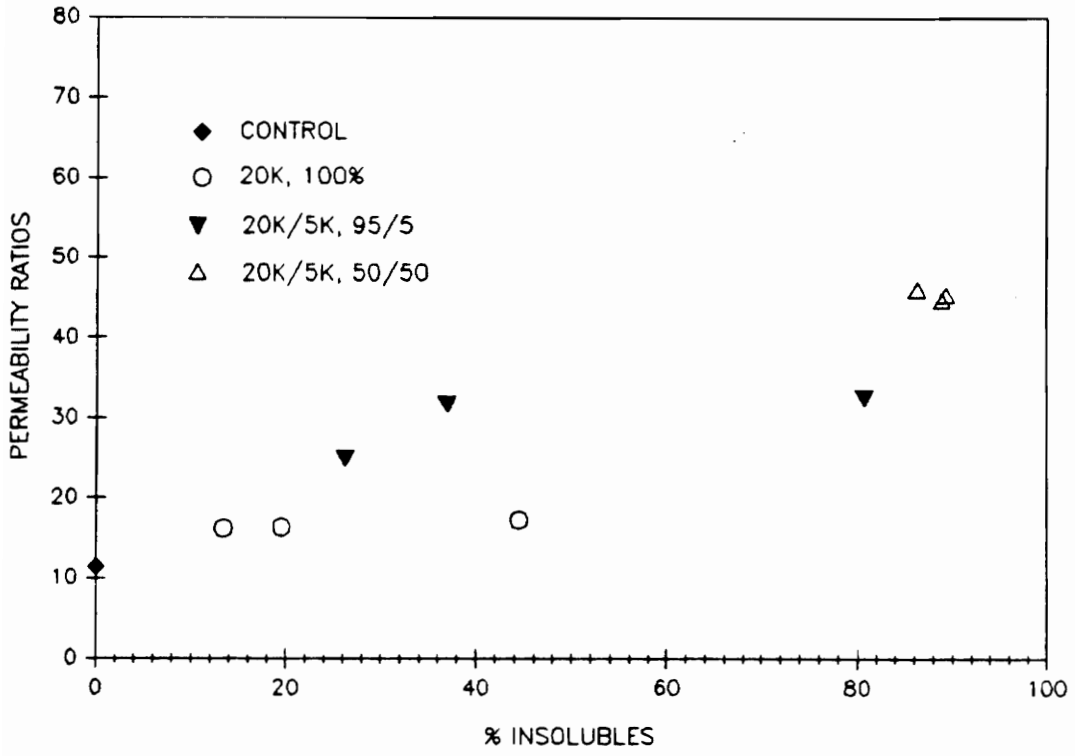

Figure 52. CO_2/CH_4 **Ideal Separation Factors for MIPEK 20K/5K (@ 30°C and 1 atmg).**

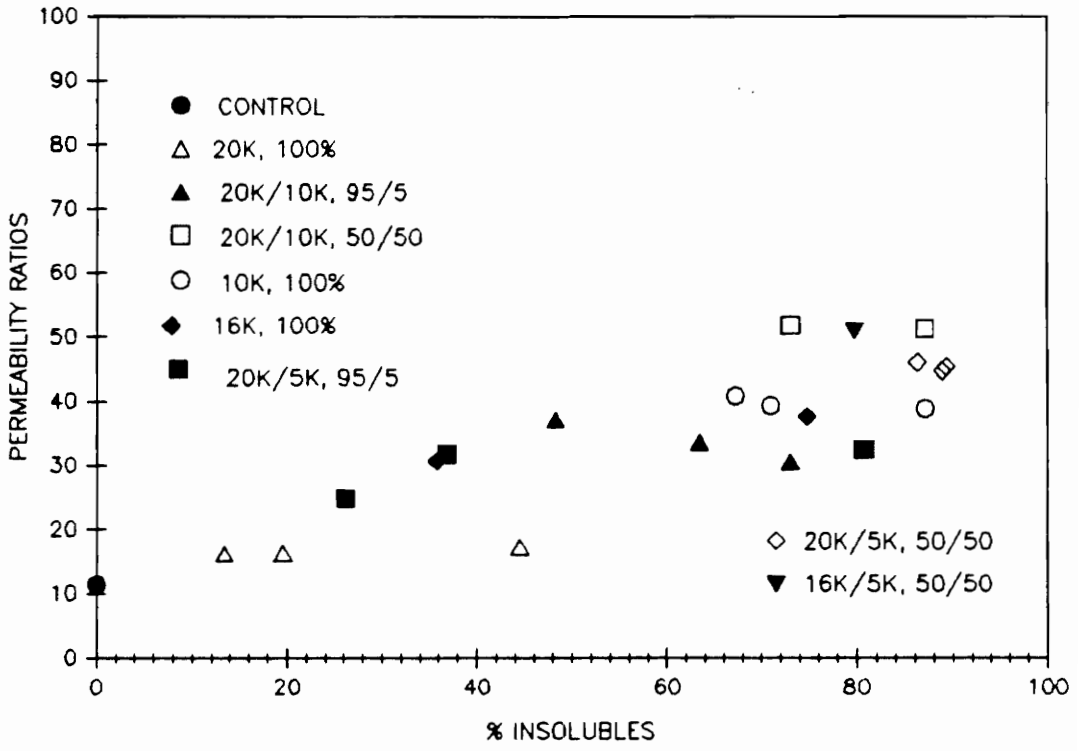

Figure 53. CO_2/CH_4 Ideal Separation Factors for MIPEK Blends (@ 30°C and 1 atmg)

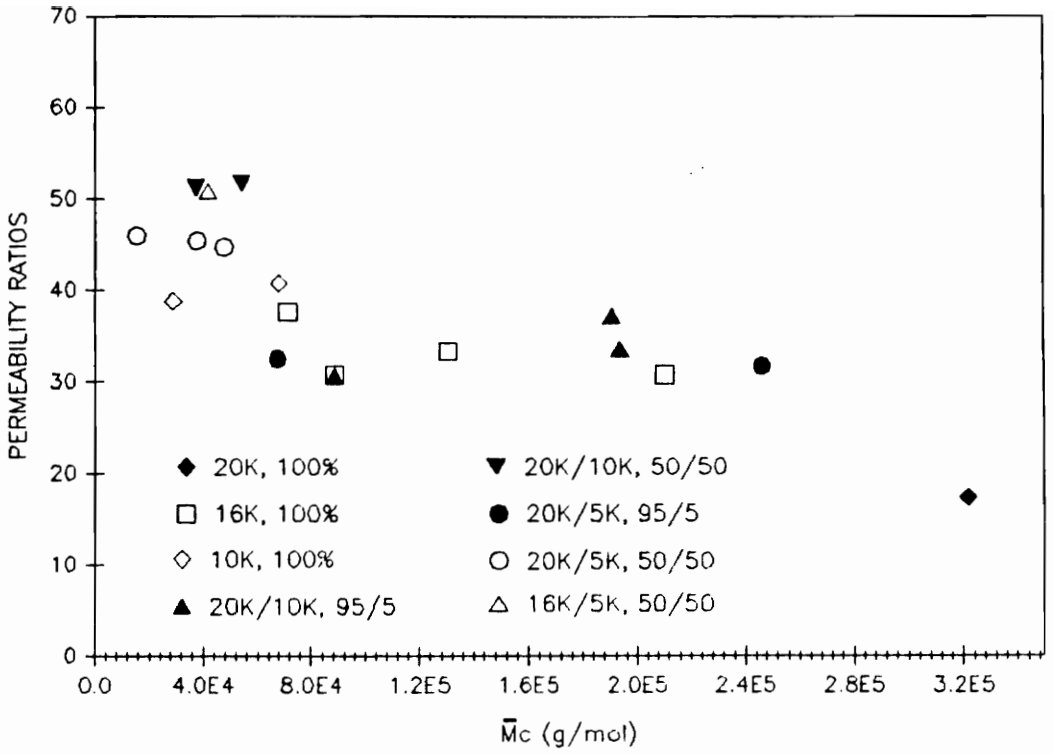

Figure 54. CO_2/CH_4 Ideal Separation Factors as a Function of the Number Average Molecular Weight of the Network Chains ($\overline{M}c$).

50/50 blends (Q = 14). This represents an increase of more than 190% in selectivity. The ideal CO_2/CH_4 permselectivity values are tabulated in Table 22. The diffusivity selectivities and solubility selectivities ratios are also presented. The range of the apparent solubility selectivities ratios (SCO_2/ SCH_4) includes the interval from 5.0 (for 20K, 100%) to 32.3 (for 20K/10K, 50/50), showing a remarkable increase in S as a result of a decrease in the CH_4 solubility when the degree of crosslinking increases. The apparent diffusivity selectivities decreased slightly with an increasing degree of crosslinking.

Considering the validity of using the time-lag method for the diffusion and solubility calculations, it should be recalled that for an average run, the 95% confidence limit on the permeability and diffusion coefficients obtained in this work were ± 5%. The solubility coefficients were subject to a large error since they were calculated from the permeability and diffusion coefficients. Nevertheless, an increase from 5 to 32 in S for CO_2/CH_4 is well above the experimental error. These values should be revised by measuring the solubility coefficients by equilibrium sorption experiments.

It has been reported by several investigators that if the crosslinking decreases the free volume in a polymer, the solubility decreases [53]. It is also known that the effective solubility coefficient of a penetrant varies linearly with the amorphous fraction and that the magnitude of this variation increases sharply with increasing the molecular size of the penetrant, i.e. the change in

Table 22. CO_2/CH_4 Ideal Separation Factors.

PROPERTY	BLEND 20K,100%(a)	20K/10K,50/50(a)
Q	43.3	13.5
D CO_2	0.704E-08	0.716E-08
D CH_4	(0.205E-08)-(0.245E-08)	(0.309E-08)-(0.409E-08)
S CO_2	3.597	3.265
S CH_4	0.716	0.101
P CO_2	3.313	3.074
P CH_4	0.192	0.060
D CO_2/D CH_4 (b)	3.4-2.8	2.3-1.8
S CO_2/S CH_4 (b)	5.0	32.3
P CO_2/P CH_4	17.3	51.2

a - After 2 hours @ 250°C.
b - Apparent values calculated from the time-lag permeation method.

solubility could be appreciable for large molecules such as CH_4 and it may explain the trend observed for the solubility of CH_4.

CHAPTER IV

SUMMARY AND CONCLUSIONS

From the experimental methodology (Section II) and from the discussion of the results (Section III), several conclusions can be made regarding this research.

A methodology was developed for the preparation of films of functionalized crosslinkable MIPEK blends of different number average molecular weights. The technique was appropriate to prepare uniform and defect-free membranes adequate for permeability characterization measurements.

The modification of the surface characteristics of the glass plates by a silanization procedure was employed to obtain films that were easily released from the substrates after thermal treatment at 250°C (@ crosslinking conditions). This methodology solved the problem of the adhesive characteristics developed by the films after the crosslinking procedure, which otherwise made these films impossible to remove from the untreated glass plates.

A scheme was developed to systematically evaluate the effect of crosslinking on gas permeability, which allowed the study of film samples which had a wide range of average molecular weights between the network chains.

The gas permeability characterization measurements showed that for all the crosslinked MIPEK blends evaluated, helium was the fastest permeating gas whereas methane was the slowest one. The permeability of helium was not affected by the crosslinking in the samples but methane was significantly influenced. Thus, methane permeability decreased as much as 75%, which agreed with a decrease of more than 55% in the swelling ratio of the network in chloroform.

The decreasing effect on gas permeability by the crosslinking in the samples affected the permeabilities observed for the separation of O_2/N_2 and CO_2/CH_4. For the O_2/N_2 selectivities, a decrease of 80% in the swelling ratio of the samples increased this selectivity from 4.8 to 7.0. Similarly, a decrease in the permeability of N_2 from 0.167 to 0.108 Barrers was observed. However, these results should be carefully considered due to the low values of the permeabilities involved. A better estimate could perhaps be obtained by studying structures with higher values of permeabilities.

The ideal separation factors for CO_2/CH_4 increased in more than 190% (from 17.3 to 51.2) in the crosslinking range evaluated. This value corresponds to a decrease of about 70% in the swelling ratio and it mainly represents a decrease in the permeability of methane (from 0.192 to 0.06 Barrers). Thus, the general trend observed was that the permselectivity decreases with the increasing degree of swelling or lower degrees of crosslinking, perhaps due to a higher interchain displacement which could decrease the possibility of a separation on the basis of size.

From this observations on the permeability behavior of the crosslinked MIPEK blends, it can be preliminary concluded that the system presented promising O_2/N_2 and CO_2/CH_4 selectivities. In order to detect "true" values of selectivities, the permeability of gas mixtures should be evaluated especially in the case of CO_2 and CH_4 where the presence of either one of them can definitely influence the permeability of the other gas [54].

With the purpose to further determine the potential of this system, a study of structure modified crosslinked Maleimide terminated Poly(arylene ether ketones) could reveal structures with higher permeabilities and hopefully approximately similar selectivities. Such could be the case of substituting Hydrogens by CH_3 groups in the following MIPEK structure [55]:

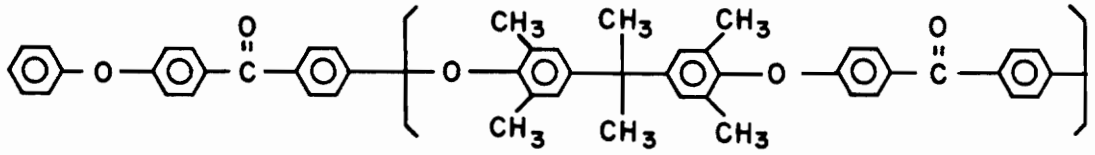

or by starting with more complex structures like [55]:

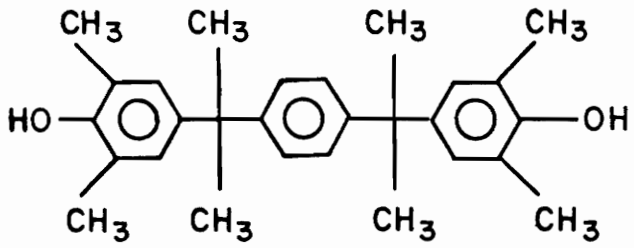

Bis P

and

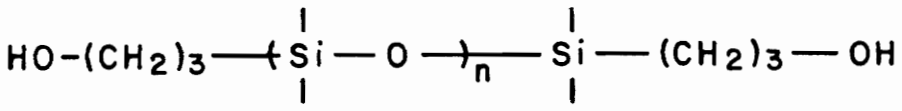

CHAPTER V

REFERENCES

1. P. Meares, The Physical Chemistry of Transport and Separation by Membranes, in Membrane Separation Processes, P. Meares, Edit., Elsevier Scientific Publishing Company, New York, p.2, 1976.
2. W.J.Koros, R.T.Chern, Separation of Gaseous Mixtures Using Polymer Membranes, in Handbook of Separation Process Technology, R.W.Rosseau, Edit., John Wiley & Sons, USA, Chapter 20, pp. 862-874 1987.
3. R.Govind, Definition of a Membrane, in Membrane Technology Course, University of Cincinnati, Cincinnati, p. 1-2, 1989.
4. S.A.Stern, New Developments in Membrane Processes for Gas Separations, in Membrane Technology Course, University of Cincinnati, Cincinnati, p. 5-33, 1989.
5. G.S.Park, Transport Principles-Solution, Diffusion and Permeation in Polymer Membranes, in Membrane Technology Course, University of Cincinnati, Cincinnati, p.7-2, 1989.
6. V.Stannett, Simple Gases-IV. Solubility, Permeability and Some Simple Functional Relationships, in Diffusion in Polymers, J.Crank and G.S. Park, Edit., Academic Press, Inc., London, p.64, 1968.

7. C.E.Rogers, Permeation of Gases and Vapours in Polymers, in Polymer Permeability, J.Comyn, Edit., Elsevier Applied Science, London, pp. 13-21, 1985.

8. V.Stannett, Simple Gases-III. Factors Affecting the Diffusivity of Gases, in Diffusion in Polymers, J.Crank and G.S.Park, Edit., Academic Press, Inc., London, pp. 45-64, 1968.

9. C.E.Rogers, Permeation of Gases and Vapours in Polymers, in Polymer Permeability, J.Comyn, Edit., Elsevier Applied Science, London, pp. 55-67, 1985.

10. R.Govind, Factors Affecting Permeability, in Molecular Level View of Membranes, Membrane Technology Course, University of Cincinnati, Cincinnati, pp. (3-32)-(3-38), 1989.

11. D.R.Lloyd, Membrane Materials Science-An Overview, in Materials Science of Synthetic Membranes, ACS Symposium Series 269, D.R.Lloyd, Edit., American Chemical Society, Washington, D.C., p.1, 1985.

12. R.E.Kesting, Membrane Separation Processes, in Synthetic Polymeric Membranes. A Structural Perspective, R.E.Kesting, Edit., John Wiley & Sons, N.Y., pp.1-81, 1985.

13. R.Govind, Solvent-Cast Films, in Dense Membranes, Membrane Technology Course, University of Cincinnati, Cincinnati, pp. (6-1)-(6-7), 1989.

14. R.Govind, History of Membrane Technology, in Membrane Technology Course, Chapter 4, University of Cincinnati, Cincinnati, pp.(4-2)-(4-3), 1989.

15. D.R.Lloyd, Membrane Materials Science, An Overview, in Materials Science of Synthetic Membranes, ACS Symposium Series 269, D.R.Lloyd, Edit., American Chemical Society, Washington, D.C., pp. 1-21, 1985.

16. W.J.Koros, R.T.Chern, Separation of Gaseous Mixtures Using Polymer Membranes, in Handbook of Separation Process Technology, Chapter 20, R.W.Rosseau, Edit., John Wiley & Sons, USA, pp. 903-916, 1987.

17. C.E.Rogers, Permeation of Gases and Vapours in Polymers, in Polymer Permeability, J.Comyn, Edit., Elsevier Applied Science, London, pp. 35-55, 1985.

18. C.A.Kumins and T.K.Kwei, Free Volume and Other Theories, in Diffusion in Polymers, J.Crank and G.S.Park, Edit., Academic Press, Inc., London, pp.107-140, 1968.

19. J.M.Hoover, Morphological Effects on Gas Transport through Poly(Methylmethacrylate)-Poly(dimethylsiloxane)Graft Copolymers and Instrumentation for their Synthesis and Permeability Characterization, Ph.D. Dissertation Virginia Polytechnic Institute and State University, October, 1987.

20. E.Sada, H.Kumazawa, P.Xu, Some Considerations on the Mechanism of Gas Transport in Glassy Polymer Films, J.Membr.Sci., 35(1), 117-122 (1987).

21. R.T.Chern, W.J.Koros, E.S.Sanders, S.H.Chen, H.B.Hopfenberg, Implications of the Dual-Mode Sorption and Transport Models for Mixed Gas Permeation, ACS Symp. Ser. 223 (Ind. Gas Sep.), 47-73 (1983).

22. T.Nakagawa, Transport Properties of Gases to Polymer Films, Kobunshi, 29(6), 474-478 (1980).

23. P.J.Fenelon, Experimental Support of "Dual Sorption" in Glassy Polymers, Polym. Sci. Technol., 6(Permeability Plast. Films Coat. Gases, Vap., Liq.), 285-299 (1974).

24. P.J.F.Kanitz and R.Y.M.Huang, The Permeation of Gases through Modified Polymer Films. II. Gas Permeability and Separation Characteristics of Gamma Ray-Irradiated Polyethylene, Journal of Applied Polymer Science, 14, 2739-2751 (1970).

25. R.Y.M.Huang and P.J.F.Kanitz, Permeation of Gases through Modified Polymer Films.III. Gas Permeability and Separation Characteristics of Gamma-Irradiated Teflon FEP Copolymer Films, J.Macromol.Sci.-Phys., B5(1), 71-88 (1971).

26. H.Kita, M.Muraoka, K.Tanaka, K.Okamoto, Permeation of Gases through Electron-beam Irradiated Polymer Films, Polym.J.(Tokyo), 20(6), 485-491 (1988).

27. R.M.Barrer, J.A.Barrie and P.S.L.Wong, The Diffusion and Solution of Gases in Highly Crosslinked Copolymers, Polymer, 9, 609 (1968).

28. V.S.Soldatov, V.A.Artamonov, Study of the Gas Permeability of Styrene and m-divinylbenzene Copolymers, Zh.Fiz.Khim., 52(1), 165-168 (1978).

29. K.Yukihiro Saito, M.Yoshimasa, Z.Shiro Asakawa, Selective Gas - Permeable Films, U.S.Patent 4,565,846 (1986).

30. A.V.Nikiforov, A.D.Sobolevskaya, Y.V.Zherdev, A.Y.Korolev, B.A.Kiselev, Diffusion of Gases in Organosilicon Polymers with a

High Degree of Crosslinking, Vysokomol.Soedin., ser.B, 17(3), 238-240 (1975).

31. A.T.Prokof'era, N.V.Maiorova, M.I.Karyakina, V.S.Sporykhina, S.Lavendele, Effect of Crosslink Density on Gas Permeability of Crosslinked Polymers, Modif.Polim.Mater., 12, 101-105 (1984).

32. A.Zampini, R.F.Malon, Cross-linked Polyphenylene Oxide, U.S.Patent 4,468,501 (1984).

33. R.F.Malon, A.Zampini, Amino Ketone Cross-linked Polyphenylene Oxide, U.S.Patent 4,468,500 (1984).

34. A.Zampini, R.F.Malon, Amino Ketone Cross-linked Polyphenylene Oxide, U.S.Patent 4,655,807 (1987).

35. I.Akira Ohmori, T.Nobuyuki Tomihashi, S.Hiroshi Inukai, T.Naoaki Izutani, U.S.Patent 4,655,807 (1987).

36. A.Zampini, Polymeric Membranes with Ammonium Salts, U.S.Patent 4,701,186 (1987).

37. C.R.Robert, P.A.Buri, N.A.Peppas, Effect of Degree of Crosslinking on Water Transport in Polymer Microparticles, J.Appl.Polym.Sci., 30, 301-306 (1985).

38. B.D.Barr-Howell, N.A.Peppas, Structural Analysis of PHEMA Particles, Eur.Poly.J., 23, 591-594 (1987).

39. M.J.Smith, N.A.Peppas, Effect of Degree of Crosslinking on Penetrant Transport in Polystyrene, Polymer, 26, 869-875 (1985).

40. K.G.Urdhal, N.A.Peppas, Amorphous Penetrant Transport in Glassy Polymers. V: Cyclohexane Transport in Polystyrene, J.Appl.Polym.Sci., 33, 2669-2687 (1987).

41. E.R.Lieberman, S.G.Gilbert, Gas Permeation of Collagen Films as Affected by Crosslinkage, Moisture, and Plasticizer Content, J.Polym.Sci., Polym.Symp., 41, 33-43 (1973).

42. G.A.Gordon, A.Ravve, Oxygen Transmission through Highly Cross-linked Polymers, Polymer Engineering and Science, 20, 70 (1980).

43. J.L.Philippart, J.L.Gardette, Analysis of the Photoaging of Polymeric Materials by Evolution of Gas Permeability, Makromol.Chem., 187(7), 1639 (1986).

44. N.A.Peppas, K.G.Urdahl, Anomalous Penetrant Transport in Glassy Polymers. VII. Overshoots in Cyclohexane Uptake in Cross-linked Polystyrene, Polymer Bulletin, 16, 201 (1986).

45. P.Mercea, T.Virag, D.Silipas, S.Baaj, The effect of Ultraviolet Radiation on Gas Permeation through Poly(ethylene terephthalate) Membranes, Polym.Commun., 28(1), 31-33 (1987).

46. S.Yamada, T.Nakagawa, Effect of Ultraviolet Radiation on Gas Permeation through Polystyrene Membranes, Kobunshi Ronbunshu, 39(6), 391-398 (1982).

47. A.L.Andrady, M.D.Sefcik, Mechanical and Gas Transport Properties of Poly-epsilon-Caprolactone Model Networks, J.Appl.Polym.Sci., 29(11), 3561-3568 (1984).

48. G.D.Lyle, J.S.Senger, D.H.Chen, S.Kilic, S.D.Wu, D.K.Mohanty, J.E.McGrath, Synthesis, Curing and Physical Behaviour of Maleimide -Terminated Poly(Ether Ketones), Polymer, 30, 978-985 (1989).

49. J.C. Hedrick, Ph.D. Dissertation, Materials Eng. Sci., Virginia Polytechnic Institute and State University, October, 1990.

50. J.S.Senger, Ph.D. Dissertation, Materials Eng. Sci., Virginia Polytechnic Institute and State University, October, 1990.

51. The Handbook of Chemistry and Physics, 55th Ed., 1974-1975, p. D - 157. CRC. Cleveland, Ohio.

52. R.T.Chern, W.J.Koros, H.B.Hopfenberg, V.T.Stannett, Material Selection for Membrane-Based Gas Separations, in Materials Science of Synthetic Membranes, D.R.Lloyd, Edit., ACS Symposium Series 269, Chapter 2, p. 38, 1985.

53. R.M.Felder and G.S.Huvard, Permeation, Diffusion, and Sorption of Gases and Vapors, in Methods of Experimental Physics: Polymers, Part C: Physical Properties, R.A.Fava, Edit., Academic Press, Inc., N.Y., Vol.16, p. 328-329, 1980.

54. L.A.Pilato, 1.M.Litz, B.Hargitay, R.C.Osborne, A.G.Farnham, J.H.Kawakami, P.E.Fritze, J.E.McGrath, Polymers for Permselective Membrane Gas Separations, Polym.Prep.ACS Div. of Polym.Chem., 16(2), 41 (1975).

55. J.E.McGrath. Personal Communication.

56. The Handbook of Chemistry and Physics, 55th ed., CRC, Cleveland, Ohio, p. F-11, 1974-1975.

57. The Handbook of Chemistry and Physics, 55th ed., CRC, Cleveland, Ohio, p. F-188, 1974-1975.

CHAPTER VI.

APPENDICES

APPENDIX A.

OLIGOMER(S) SOLUTION PREPARATION

Calculation Example:

To prepare a 25% (w/w) solution of 95% (w) of MIPEK 20K and 5% (w) of MIPEK 10K, the following calculation applies:

$$\frac{\text{gms of total solids}}{\text{gms total solids} + \text{ml } CHCl_3 \times \text{d } CHCl_3} \times 100 = 25\%$$

Then, from the previous equation:

$$\text{gms of total solids} = \frac{25 \times \text{ml } CHCl_3 \times \text{d } CHCl_3}{(100 - 25)}$$

where d $CHCl_3$ = 1.473 gms/cc

and normally ml $CHCl_3$ = ~ 30 to 40 ml

gms of MIPEK, 20K for a 95% content = gms total solids x 0.95

gms of MIPEK, 10K for a 5% content = gms total solids x 0.05

APPENDIX B.

EXAMPLE OF A FILM THICKNESS MEASUREMENT

Reading Line #	Measured point (in mils)						
1	1.65	1.66	1.66	1.66	1.65	1.64	1.63
2	1.70	1.67	1.66	1.64	1.62	1.62	1.60
3	1.66	1.64	1.63	1.63	1.62	1.62	1.60
4	1.63	1.64	1.63	1.62	1.63	1.63	1.62
5	1.66	1.65	1.64	1.62	1.62	1.61	1.60
6	1.67	1.66	1.65	1.63	1.61	1.60	1.58
7	1.64	1.63	1.62	1.62	1.61	1.60	1.60
8	1.60	1.62	1.61	1.62	1.63	1.62	1.63

Average reading = X = 1.6304 mils = 0.0414 mm

Standard Deviation = s = 0.0228 mils = 0.0006 mm

Relative Standard Deviation = RSD = 1.45%

Film Thickness = (0.041 ± 0.001) mm

APPENDIX C

PERMSELECTIVITY CALCULATIONS

The following calculations are based in a manometric approach that involves monitoring the gas permeation through the film into an accurately calibrated and thermostated, previously evacuated volume. The rate at which the pressure of the permeated gas increased in this volume is then recorded. The schematic representation of a variable down-stream pressure device is shown in figure C-1.

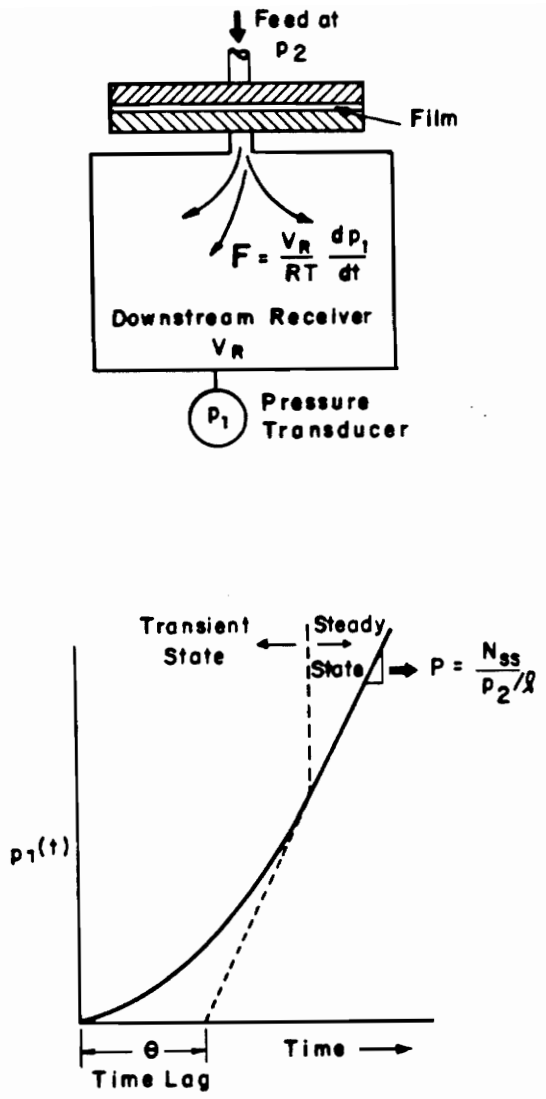

Figure C-1. Variable downstream pressure (manometric device) [2].

APPENDIX C. (CONT.)

PERMEABILITY CALCULATIONS.

1. <u>Molar Flux:</u>

$$F = (Pa/sec) \times 1\ Atm/10^6 Pa \times V/RT\ (=)\ mol/sec$$

slope

2. <u>Permeability:</u>

$$P = (F \times l \times 10^{-10} \times 22414)/(A \times \Delta p)\ (=)\ Barrers\ *$$

where: l : film thickness (cm)

A : membrane area (cm^2)

p : cmHg

* 1 Barrer = $(ccSTP \times 10^{-10})/(cm \times sec \times cmHg)$

3. <u>Diffusivity:</u>

$$D = l^2/6\theta \quad \text{where } \theta = \text{time lag}$$

4. <u>Solubility:</u>

$$S = P/D$$

5. <u>Selectivity:</u>

$$\alpha_{AB} = P_A / P_B$$

APPENDIX D. "ANALYZE" PROGRAM [19]

```
10 REM **********          ANALYZE.BAS          ************
20 REM ***** Questions concerning this Program should be
30 REM ***** directed to Jim Hoover.
40 REM *****       SET-UP INTRODUCTION PAGE
50 COLOR 7,1: KEY OFF: CLS
60 PRINT: PRINT: PRINT: PRINT: SOUND 500, .5
70 PRINT "                    This program analyzes data and
constructs plots"
80 PRINT: SOUND 600, 1
90 PRINT "                    from data files that are stored
in \NOTEBOOK "
100 PRINT: SOUND 700, 1
110 PRINT "                              as a result of data
acquisition runs in"
120 PRINT: SOUND 800, 1
130 PRINT "                                          diffusion
experiments."
140 PRINT: SOUND 900, 1: PRINT: SOUND 1000, 1: PRINT: PRINT:
PRINT: PRINT: PRINT: PRINT: PRINT
150 COLOR 3,1
160 INPUT "                           Do you wish to continue
(Y/N) "; ZAP$
170 REM *****
180 COLOR 7,1: CLS: FOR S = 1000 TO 500 STEP -100: SOUND S,
.5: NEXT S
190 IF ZAP$ = "N" THEN END
200 PRINT: PRINT: COLOR 3,1: REM *****        EXPERIMENTAL
PAGE     ****
210 PRINT "                                   EXPERIMENTAL
INFORMATION"
220 PRINT: PRINT: COLOR 7,1
230 INPUT "                   Enter the filename to read: ",
FILE$
240 PRINT: IF ADD1$ = "Y" THEN GOTO 380
250 PRINT "                             Enter the following
information"
260 PRINT
270 INPUT "                           Membrane Material: ",
MEM$
280 PRINT
290 INPUT "                             Method of Membrane
Preparation: ", PREP$
300 PRINT
310 INPUT "                        Operator: ", OP$
320 PRINT
330 INPUT "                        Comments: ", CMTS$
340 PRINT: PRINT: PRINT: PRINT
350 COLOR 3,1
360 INPUT "                          Do you wish to continue
(Y/N) "; ZAP$
370 REM *****
380 CLS: COLOR 7,1
```

```
390 IF ZAP$ = "N" THEN END
400 PRINT: PRINT: PRINT: PRINT: PRINT
410 COLOR 3,1
420 PRINT "                                READING "; FILE$
430 PRINT: PRINT: PRINT
440 PRINT "                                        PLEASE WAIT"
450 REM *****
460 IF ADD1$ = "Y" THEN GOTO 510
470 REM *****
480 REM *****       SET-UP ARRAYS FOR PRESSURE & TIME DATA
490 REM *****       SET-UP ARRAYS FOR PLOTTER POSITIONS
500  DIM  PRES(1200):  DIM  TM(1200):  DIM  XPOS(1200):  DIM
YPOS(1200): DIM GASP(1200)
510 OPEN FILE$ FOR INPUT AS #1: REM *****    READ DATA FILE
IN
520 H = 1
530 IF EOF(1) THEN GOTO 610
540 LINE INPUT#1, JUNK$(H)
550 H = H + 1
560 IF H >= 7 THEN GOTO 570 ELSE GOTO 530
570 I = 1: N = 1
580 IF EOF(1) THEN GOTO 610
590 INPUT#1, PRES(I), TM(I), GASP(I)
600 I = I + 1: GOTO 580
610 CLOSE #1: REM *****       FINISHED READING DATA
620 REM *****       FIND MAXIMUM PRESSURE AND SUPPLY PRESSURE
630 I = I - 1: AVGASP = 0: AVGAS = 0
640 FOR G = 1 TO I: AVGAS = AVGAS + GASP(G)
650 IF PRES(G) > PRES(N) THEN PMAX = PRES(G): N = G
660 NEXT G
670 AVGASP = AVGAS / I: GPRES = (AVGASP + 14.696)/14.696
680 REM *****       SET-UP FINISHED READING PAGE
690 COLOR 7,1: CLS: PRINT: PRINT: PRINT: BEEP
700 PRINT "                    "; I; " DATA POINTS READ FROM ";
FILE$: PRINT: PRINT
710 PRINT TAB(19): PRINT USING "AVERAGE GAS SUPPLY PRESSURE
IS ###.## psig"; AVGASP
720 REM *****
730 REM *****
740 PRINT: PRINT
750 PRINT "                        MAXIMUM PRESSURE FOUND AT ";
TM(N);" sec ("; CINT(TM(N)/6)/10;" min )"
760 PRINT: PRINT
770 PRINT "                                MAXIMUM PRESSURE IS ";
CINT(PMAX * 100);" Pa"
780 PRINT: PRINT: PRINT
790 COLOR 3,1
800 PRINT "                        INSURE THAT THE PLOTTER IS ON
AND ON-LINE !"
810 PRINT: PRINT: PRINT: COLOR 3,1
820 INPUT "                                        (press ENTER to
continue) ", ZAP$
```

```
830 IF ADD1$ = "Y" THEN GOTO 1080
840 REM *****
850 CLS: PRINT: PRINT: PRINT: PRINT: REM *****      DATA
TREATMENT PAGE
860 PRINT "                    TREATMENT OF DATA IN "; FILE$
870 PRINT: PRINT: PRINT: COLOR 7,1
880 PRINT "                                    A. PLOT RAW DATA"
890 PRINT
900 PRINT "                                B. PERFORM STATISTICAL
ANALYSIS"
910 PRINT
920 PRINT "                                    C. QUIT (return to
basic)"
930 PRINT: PRINT: PRINT: PRINT: PRINT: PRINT
940 COLOR 3,1
950 INPUT "                                  ENTER option desired
(A/B/C) ",  ZAP$
960 IF ZAP$ = "C" THEN COLOR 7,1: CLS: END
970 IF ZAP$ = "B" THEN GOTO 1970
980 CLS: PRINT: PRINT: PRINT: PRINT: COLOR 3,1
990 PRINT "                                    THIS INPUT MUST BE
DIVISIBLE BY 10": PRINT
1000 INPUT "                ENTER TIME (in minutes) OF TIME
AXIS FULL SCALE "; FSTIME: REM *****       SET FULL SCALE
TIME OF PLOT
1010 IF FSTIME/10 <> FIX(FSTIME/10) THEN BEEP: GOTO 980
1020 PRINT: PRINT: PRINT: PRINT
1030 PRINT "                                    THIS INPUT MUST BE
DIVISIBLE BY 5": PRINT
1040 INPUT "              ENTER PRESSURE (IN Pa) OF PRESSURE
AXIS FULL SCALE "; FSPRES
1050 IF FSPRES/5 <> FIX(FSPRES/5) THEN BEEP: GOTO 980
1060 PRINT: PRINT: PRINT: PRINT
1070 INPUT "                          ANNOTATE PLOT WITH SAMPLE
INFORMATION (Y/N)"; SINFO$
1080 REM *****
1090 CLS: COLOR 3,1: PRINT
1100 PRINT: PRINT: PRINT: PRINT: PRINT TAB(29) "PLOTTER PEN
SELECTIONS": PRINT
1110 COLOR 7,1: PRINT: IF ADD1$ = "Y" THEN GOTO 1160
1120  PRINT  TAB(22):  INPUT  "SELECT  PEN  TO  DRAW  BORDER
(1/2/3/4) ", BPEN: PRINT
1130 PRINT TAB(22): INPUT "SELECT PEN TO DRAW AXES (1/2/3/4)
", AXPEN: PRINT
1140  PRINT  TAB(22):  INPUT  "SELECT  PEN  TO  DRAW  LABELS
(1/2/3/4) ", LPEN: PRINT
1150 PRINT TAB(22): INPUT "SELECT PEN TO DRAW KEYS (1/2/3/4)
", KPEN: PRINT
1160 PRINT TAB(22): INPUT "SELECT PEN TO DRAW DATA (1/2/3/4)
", DPEN: PRINT
1170 COLOR 3,1: PRINT: PRINT TAB(28): INPUT "PRESS <ENTER>
TO CONTINUE ", ZAP$
```

```
1180 REM *****
1190 REM *****
1200 CLS: PRINT: PRINT: PRINT: PRINT: PRINT: PRINT: PRINT:
PRINT: COLOR 3,1
1210 PRINT "                                PLOTTING RAW DATA -
PLEASE WAIT"
1220 REM *****
1230 IF ADD1$ = "Y" THEN GOTO 1710
1240 REM *****       INITIALIZE PLOTTER
1250 LPRINT "IN"
1260 REM *****       CHANGE PENS AND DRAW THE BORDER
1270 LPRINT "SP"; BPEN
1280 LPRINT "MA 0, 110"
1290 LPRINT "OR"
1300 LPRINT "DA 2390, 0, 2390, 1760, 0, 1760, 0, 0"
1310 REM *****       CHANGE PENS AND DRAW THE AXES
1320 LPRINT "SP"; AXPEN
1330 LPRINT "MA 200, 200"
1340 LPRINT "OR": LPRINT "SI 35,28
1350 LPRINT "AX 3, 2000, 10, 1, 0,"; FSTIME;" 30, 0
1360 LPRINT "HO"
1370 LPRINT "AX 2, 1400, 5, 1, 0,"; FSPRES;" 30, 0
1380 REM *****       SET CHARACTER SIZE AND DO LABELS
1390 LPRINT "SP"; AXPEN: LPRINT "SI 50, 40"
1400 LPRINT "MA 780, -150"
1410 LPRINT "LA TIME (min)"
1420 LPRINT "MA 205, 1450"
1430 LPRINT "LA PERMEABILITY ANALYSIS - RAW DATA CURVE"
1440 LPRINT "MA -100, 410"
1450 LPRINT "DI 900"
1460 LPRINT "LA PRESSURE (Pa)": LPRINT "DI 0"
1470 IF SINFO$ = "N" THEN GOTO 1710
1480 REM *****       DRAW AND LABEL THE KEY
1490 LPRINT "SP"; KPEN
1500 LPRINT "MA 1300,90"
1510 LPRINT "DA 2100, 90, 2100, 600, 1300, 600, 1300, 90"
1520 LPRINT "MA 1300, 470
1530 LPRINT "DA 2100, 470
1540 LPRINT "SP"; KPEN: LPRINT "SI 35, 28
1550 LPRINT "MA 1425, 520" : LPRINT "DI 0"
1560 LPRINT "LA SAMPLE INFORMATION"
1570 LPRINT "MA 1330, 390"
1580 LPRINT "SI 30,20"
1590 LPRINT "LA DATA FILE: "; FILE$
1600 LPRINT "MA 1330, 340"
1610 LPRINT "LA DATE: ";DATE$
1620 LPRINT "MA 1330, 290"
1630 LPRINT "LA SAMPLE: "; MEM$
1640 LPRINT "MA 1330, 240"
1650 LPRINT "LA PREPARATION: "; PREP$
1660 LPRINT "MA 1330, 190"
1670 LPRINT "LA OPERATOR: "; OP$
```

```
1680 LPRINT "MA 1330, 140"
1690 LPRINT "LA COMMENTS: "; CMTS$
1700 REM *****
1710 REM *****       SCALE AND PLOT THE DATA
1720 LPRINT "SP"; DPEN
1730 XSTRT = TM(1) / FSTIME / 60 * 2000
1740 YSTRT = (PRES(1) / FSPRES * 100) * 1400
1750 LPRINT "MA"; XSTRT, YSTRT
1760 LASTP = PRES(I): MAXTIME = TM(I)
1770 FOR H = 1 TO I: REM ***** SKIP HEADER LINES OF FILE
1780 XPOS(H) = TM(H) / FSTIME / 60 * 2000
1790 YPOS(H) = (PRES(H) / FSPRES * 100) * 1400
1800 LPRINT "DA"; XPOS(H), YPOS(H)
1810 NEXT H
1820 LPRINT "HO": IF ADD1$ = "Y" THEN ADD1$ = "N"
1830 REM *****
1840 COLOR 3,1: CLS: PRINT: PRINT: PRINT
1850 INPUT "                                Replot last analysis
(N/Y) "; RLA$
1860 IF RLA$ = "Y" THEN GOTO 1870 ELSE GOTO 1970
1870 PRINT: PRINT: PRINT
1880 COLOR 7,1
1890 PRINT "                             Insert a new page in the
plotter and"
1900 PRINT
1910 INPUT "                                        Press ENTER to
continue ", ZAP$
1920 REM *****
1930 CLS: GOTO 1090
1940 REM *****
1950 REM *****       SET-UP STATISTICAL ANALYSIS PAGES
1960 REM *****
1970 CLS
1980 PRINT: PRINT: PRINT: PRINT: PRINT: COLOR 3,1
1990 PRINT "                                          STATISTICAL
ANALYSIS"
2000 PRINT: PRINT: COLOR 7,1
2010 PRINT "                      A. LINEAR REGRESSION ANALYSIS
(by least squares)"
2020 PRINT: PRINT
2030 PRINT "                         B. HIGHER ORDER MODEL (not
yet available)"
2040 PRINT: PRINT
2050 PRINT "                                   C. QUIT (return to
BASIC)"
2060 PRINT: PRINT: COLOR 3,1
2070 INPUT "                                      ENTER AN OPTION
(A/B/C) ", ZAP$
2080 IF ZAP$ = "C" THEN COLOR 7,1: CLS: END
2090 IF ZAP$ = "B" THEN COLOR 4,1: BEEP: LOCATE 18,10: INPUT
"            THIS OPTION NOT YET AVAILABLE (press ENTER to
continue)", ZAP$: CLS: GOTO 1980
```

```
2100 REM *****       LIMITS OF LINEAR REGRESSION ANALYSIS
2110 COLOR 3,1: CLS: PRINT: PRINT: PRINT: PRINT
2120 PRINT "                    LINEAR REGRESSION ANALYSIS BY
METHOD OF LEAST SQUARES"
2130 COLOR 7,1: PRINT: PRINT: PRINT
2140 INPUT "              1. ENTER TIME (in minutes) AT WHICH
TO BEGIN ANALYSIS  ", LRSTRT
2150 PRINT: PRINT: PRINT
2160 INPUT "              2. ENTER TIME (in minutes) AT WHICH
TO STOP ANALYSIS  ", LRSTOP
2170 PRINT: PRINT: PRINT
2180 DATAFQ = 1 / (TM(2) - TM(1))
2190 PRINT "                                    (DATA ACQUISITION
FREQUENCY ="; DATAFQ;"Hz)"
2200 PRINT: PRINT: PRINT: PRINT
2210 INPUT "                              IS THE ABOVE INFORMATION
CORRECT ? (Y/N) ",ZAP$
2220 IF ZAP$ = "N" THEN GOTO 2110
2230 REM *****
2240 COLOR 3,1: CLS: PRINT: PRINT: PRINT: PRINT: PRINT:
PRINT: PRINT: PRINT
2250 PRINT "                         PERFORMING LINEAR REGRESSION
ANALYSIS - PLEASE WAIT"
2260 REM *****
2270 REM *****       SUM EQUATIONS FROM STATISTICS TEXT (OTT)
2280 REM *****       LR1 & LR2 DATA POINT INDICES
2290 REM *****       LOOP TO COMPUTE SUMS FOR REGRESSION
2300 LR1 = LRSTRT * 60 * DATAFQ + 1: LR2 = LRSTOP * 60 *
DATAFQ + 1
2310 REM *****
2320 IF LRSTOP > TM(I) / 60 THEN LR2 = TM(I) * DATAFQ + 1
2330 SUMXSQ = 0: SUMX = 0: SUMXY = 0: SUMY = 0: SUMYSQ = 0:
AVGAS = 0: AVGASP = 0
2340 FOR L = LR1 TO LR2
2350 SUMXSQ = SUMXSQ + TM(L) * TM(L)
2360 SUMX = SUMX + TM(L)
2370 SUMXY = SUMXY + TM(L) * PRES(L)
2380 SUMY = SUMY + PRES(L)
2390 SUMYSQ = SUMYSQ + PRES(L) * PRES(L)
2400 AVGAS = AVGAS + GASP(L)
2410 NEXT L
2420 SUMYSQ = SUMYSQ * 10000
2430 SUMXY = SUMXY * 100: SUMY = SUMY * 100
2440 REM *****       LRN IS NUMBER OF POINTS EVALUATED
2450 REM *****
2460 LRN = LR2 - LR1 + 1
2470 AVGASP = AVGAS/LRN: GPRES = (AVGASP + 14.696)/14.696
2480 SXX = SUMXSQ - SUMX * SUMX / LRN
2490 SXY = SUMXY - SUMX * SUMY / LRN
2500 SYY = SUMYSQ - SUMY * SUMY / LRN
2510 BETA1 = SXY / SXX: SLOPE = BETA1
2520 BETA0 = SUMY / LRN - BETA1 * SUMX / LRN
```

```
2530 ONSET = -1 * BETA0 / BETA1: INCPT = BETA0
2540 CC = SXY / SQR(SXX * SYY)
2550 REM *****       UNITS OF BETA0 & BETA1 ARE Pa & Pa/s
2560 REM *****       LOOP FOR COMPUTING VARIANCE
2570 VARY = 0
2580 FOR M = LR1 TO LR2
2590 VARY1 = ((BETA1 * TM(M) + BETA0) - PRES(M)) ^ 2
2600 VARY = VARY + VARY1
2610 NEXT M
2620 VARY = VARY / (LRN - 2)
2630 STDDEV = SQR(VARY)
2640 REM *****       STANDARD ERROR CALCULATIONS
2650 SSE = SYY - (BETA1 * SXY)
2660 SE = SQR(ABS(SSE)/ (LRN - 2))
2670 SEBETA0 = SE * SQR(SUMXSQ / LRN / SXX)
2680 SEBETA1 = SE / SQR(SXX)
2690 REM *****
2700 REM *****       END OF ANALYSIS ROUTINES
2710 REM *****
2720 REM *****       LINEAR REGRESSION ANALYSIS REPORT
2730 COLOR 3,1: CLS: PRINT: PRINT: BEEP
2740 PRINT "                  LINEAR REGRESSION RESULTS ON ";
FILE$
2750 PRINT: COLOR 7,1
2760 PRINT "                              "; LRN; " OBSERVATIONS
ANALYZED"
2770 PRINT
2780 PRINT "                        SUPPLY PRESSURE = "; GPRES;
"atm absolute"
2790 PRINT
2800  PRINT "                                        SLOPE = ";
SLOPE;"Pa/sec"
2810 PRINT
2820 PRINT "                       STANDARD ERROR IN SLOPE = ";
SEBETA1;"Pa/s"
2830 PRINT
2840 PRINT "                                   Y-INTERCEPT = ";
INCPT; "Pa"
2850 PRINT
2860 PRINT "                      STANDARD ERROR IN INTERCEPT =
"; SEBETA0;"Pa"
2870 PRINT
2880 PRINT "                                     TIME LAG = ";
ONSET;"sec"
2890 PRINT
2900 PRINT "                                STANDARD ERROR = ";
SE;"Pa"
2910 PRINT
2920 PRINT "                                        CORRELATION
COEFFICIENT = "; CC
2930 PRINT: COLOR 3,1
2940 INPUT "                                    (press ENTER to
```

```
continue) ", ZAP$
2950 REM *****
2960 COLOR 3,1: CLS: PRINT: PRINT: PRINT
2970 PRINT "                                    SELECT ONE OF THE
FOLLOWING OPTIONS"
2980 PRINT: PRINT: COLOR 7,1
2990 PRINT "                                  A. ANNOTATE RAW DATA
PLOT
3000 PRINT
3010 PRINT "                                     B. PERMEABILITY
ANALYSIS"
3020 PRINT
3030 PRINT "                                C. RETURN TO INPUT DATA
FILE
3040 PRINT
3050 PRINT "                               D. RETURN TO STATISTICAL
ANALYSIS"
3060 PRINT
3070 PRINT "                                E. ADD ANOTHER CURVE TO
SAME PLOT"
3080 PRINT
3090 PRINT "                                F. ANNOTATE PLOT WITH A
KEY"
3100 PRINT
3110 PRINT "                                   G. QUIT (return to
basic)
3120 PRINT: PRINT: COLOR 3,1
3130 INPUT "                                  ENTER option desired
(A/B/C/D/E) ", OPT$
3140 COLOR 7,1: CLS
3150 IF OPT$ = "B" THEN GOTO 3600
3160 IF OPT$ = "C" THEN GOTO 180
3170 IF OPT$ = "D" THEN GOTO 1970
3180 IF OPT$ = "E" THEN ADD1$ = "Y": GOTO 180
3190 IF OPT$ = "F" THEN GOTO 5530
3200 IF OPT$ = "G" THEN COLOR 7,1: CLS: END
3210 REM *****
3220 REM *****       PLOT ANNOTATION PAGE
3230 PRINT: PRINT: PRINT: COLOR 3,1
3240 PRINT "                                 ANNOTATION OF RAW DATA
PLOT WITH"
3250 PRINT
3260 PRINT "                                    LINEAR REGRESSION
FIT"
3270 PRINT: PRINT: PRINT: COLOR 3,1
3280 PRINT "                                                ENTER line
type:"
3290 PRINT: COLOR 7,1
3300 INPUT "                    0 for SOLID LINE     or     1
for DASHED LINE ", LTYPE
3310 PRINT: PRINT: PRINT: COLOR 3,1
3320 PRINT "                                                ENTER line
```

```
color:"
3330 PRINT: COLOR 7,1
3340 PRINT TAB(29): INPUT "SELECT PEN 1,2,3 OR 4 ", LCLR
3350 PRINT: PRINT: PRINT: COLOR 3,1
3360 INPUT "                                press ENTER to construct
regression line ", ZAP
3370 REM *****
3380 REM *****       LOOP TO DRAW REGRESSION LINE
3390 REM *****
3400 L1X = MAXTIME / 60 / FSTIME * 2000
3410 MARK1X = LR2 / DATAFQ / 60 / FSTIME * 2000
3420 MARK2X = LR1 / DATAFQ / 60 / FSTIME * 2000
3430 L1Y = (MAXTIME * BETA1 + BETA0) / FSPRES * 1400
3440 MARK1Y = ((LR2 / DATAFQ * BETA1 + BETA0) / FSPRES *
1400) + 15
3450 MARK2Y = ((LR1 / DATAFQ * BETA1 + BETA0) / FSPRES *
1400) + 15
3460 IF INCPT < 0 THEN L2X = ONSET / FSTIME / 60 * 2000 ELSE
L2X = 0
3470 IF INCPT > 0 THEN L2Y = BETA0 / FSPRES * 1400 ELSE L2Y
= 0
3480 LPRINT "LT"; LTYPE
3490 LPRINT "SP"; LCLR
3500 LPRINT "MA"; L1X, L1Y
3510 LPRINT "DA"; L2X, L2Y
3520 LPRINT "MA"; MARK1X, MARK1Y
3530 LPRINT "LT0"
3540 LPRINT "DR 0, -30"
3550 LPRINT "MA"; MARK2X, MARK2Y
3560 LPRINT "DR 0, -30"
3570 LPRINT "HO"
3580 GOTO 2960
3590 REM *****
3600 REM *****
3610 REM *****       PERMEABILITY ANALYSIS INFO INPUT
3620 COLOR 3,1: CLS: PRINT: PRINT
3630 PRINT "                                        PERMEABILITY
ANALYSIS"
3640 PRINT: COLOR 7,1
3650 PRINT "                                  ENTER THE FOLLOWING
INFORMATION"
3660 PRINT: PRINT
3670 INPUT "                                          PROBE GAS
(HE/N2/O2/CO2/CH4): ", PG$
3680 PRINT
3690 INPUT "                               CONTROL VOLUME (1 or 2):
", CVNUM
3700 PRINT
3710 INPUT "                                  BATH TEMPERATURE (in
degrees C): ", TEMP
3720 PRINT
3730 INPUT "                                SYSTEM TEMPERATURE (in
```

```
degrees C): ", SYTEMP
3740 PRINT
3750 INPUT "                                    FRACTION OF SYSTEM @
BATH TEMP: ", CVFR
3760 IF CVFR > 1 OR CVFR < 0 THEN BEEP: GOTO 3620
3770 SYTEMPK = SYTEMP + 273.15
3780 PRINT: TEMPK = TEMP + 273.15
3790 MAREA = 45.96: REM ***** UNITS = CM
3800 INPUT "                                   MEMBRANE THICKNESS (in
mm): ", THK
3810 PRINT: IF CVNUM = 1 THEN CV = 32.33 ELSE CV = 204!: REM
***** UNITS = ML
3820 INPUT "                                   LEAK RATE (in Pa/sec):
", LR
3830 PRINT: COLOR 3,1
3840 PRINT
3850 INPUT "                                  Do you wish to continue
(Y/N) "; ZAP$
3860 REM *****
3870 COLOR 7,1: CLS
3880 IF ZAP$ = "N" THEN GOTO 3620
3890 REM *****
3900 REM *****
3910 REM *****       VAN DER WAALS CONSTANTS (CRC)
3920 IF PG$ = "HE" THEN A = .03412: B = .0237
3930 IF PG$ = "N2" THEN A = 1.39: B = .03913
3940 IF PG$ = "O2" THEN A = 1.36: B = .03183
3950 IF PG$ = "CO2" THEN A = 3.592: B = .04267
3960 IF PG$ = "CH4" THEN A = 2.253: B = .04278
3970 REM *****       NOT USED - IDEAL GAS LAW GOOD ENOUGH
3980 REM *****       NBS SRM 1470 CONSTANTS AND FLUX
3990 IF PG$ = "HE" THEN PG = 13.79: BG = .02872
4000 IF PG$ = "N2" THEN PG = .0421: BG = .05211
4010 IF PG$ = "CO2" THEN PG = 1.722: BG = .03089
4020 IF PG$ = "O2" THEN PG = .352: BG = .03762
4030 PA = 101325! * GPRES
4040 STDPG = PG * EXP(BG * (TEMPK - 296.15)) / 10000 * PA *
1E-12
4050 REM *****
4060 REM *****       FLUX AND PERMEABILITY CALCULATIONS
4070 CSLOPE = SLOPE - LR
4080 MOLFLUX = SLOPE / 101325! / .0820575 / (TEMPK * CVFR +
SYTEMPK * (1 - CVFR)) * CV / 1000 / MAREA
4090 REM *****
4100 REM *****    MOLFLUX in units of (mol / s / cm^2)
4110 REM *****
4120 PERM = MOLFLUX * THK * 22414 * .1 / GPRES / 76 * 1E+10
4130 DFICK = THK * THK / 6 / 100 / ONSET: REM ***** UNITS =
CM^2/S
4140 SOLUB = PERM / 1E+10 * 76 / DFICK: REM ***** UNITS =
STP CM^3/CM^3/ATM
4150 REM *****
```

```
4160 REM *****     PERM in units of BARRERS
4170 REM *****     1 BARRER = 10^-10 * STP cc * cm / cm^2 / s
/ cm Hg
4180 REM *****
4190 PRINT: PRINT: PRINT: COLOR 3,1
4200 PRINT "                              RESULTS OF PERMEABILITY
ANALYSIS"
4210 PRINT: PRINT: COLOR 7,1
4220 PRINT "                          ON DATA FILE: "; FILE$
4230 PRINT: PRINT
4240 PRINT "                                FLUX = "; MOLFLUX;"
mol/s/cm^2"
4250 PRINT
4260 IF CMTS$ = "NBS SRM 1470" THEN PRINT "
    PREDICTED FLUX = "; STDPG;" mol/s/cm^2": PRINT
4270 PRINT "                             PERMEABILITY = "; PERM;"
barrers"
4280 PRINT
4290 PRINT "                DIFFUSIVITY (from time lag) = ";
DFICK;" cm^2/s"
4300 PRINT
4310 PRINT "                SOLUBILITY (from time lag) = ";
SOLUB;" (STP cm^3)/cm^2/atm"
4320 PRINT: COLOR 3,1: PRINT
4330 INPUT "                                    (press ENTER to
continue) ", ZAP$
4340 REM *****
4350 COLOR 3,1: CLS: PRINT: PRINT: PRINT
4360 PRINT "                                  SELECT ONE OF THE
FOLLOWING OPTIONS"
4370 PRINT: PRINT: COLOR 7,1
4380 PRINT "                  A. SEND EXPERIMENTAL RESULTS TO
PRINTER"
4390 PRINT
4400 PRINT "                           B. ANNOTATE PLOT WITH
STATISTICAL RESULTS"
4410 PRINT
4420 PRINT "                           C. ANNOTATE PLOT WITH
EXPERIMENTAL PARAMETERS
4430 PRINT
4440 PRINT "                       D. RETURN TO PERMEABILITY
ANALYSIS"
4450 PRINT
4460 PRINT "                   E. QUIT (return to basic)"
4470 PRINT: PRINT: COLOR 3,1
4480 INPUT "                              ENTER OPTION DESIRED
(A/B/C/D/E) ", OPT$
4490 COLOR 7,1: CLS
4500 IF OPT$ = "B" OR OPT$ = "C" THEN GOTO 4540
4510 IF OPT$ = "D" THEN GOTO 3620
4520 IF OPT$ = "E" THEN END
4530 GOTO 5070
```

```
4540 REM *****
4550 REM *****       WARNING FOR PLOTTER ON
4560 PRINT: PRINT: PRINT: PRINT: COLOR 4,1: BEEP
4570 PRINT "                    INSURE THAT PLOTTER IS ON AND
ON-LINE !!!"
4580 PRINT: PRINT: PRINT: PRINT: PRINT: PRINT: PRINT: PRINT:
COLOR 7,1
4590 INPUT "                                    (press ENTER to
continue) ", ZAP$
4600 REM *****
4610 CLS: PRINT: PRINT: PRINT: PRINT: COLOR 4,1
4620 PRINT "                          ANNOTATING PLOT - PLEASE
WAIT"
4630 IF OPT$ = "C" THEN GOTO 4780
4640 REM *****
4650 REM *****       ANNOTATE PLOT WITH REGRESSION RESULTS
4660 LPRINT "SP"; LCLR
4670 LPRINT "MA 0, -150"
4680 LPRINT "SI 35, 28
4690 LPRINT "LATIME LAG ="; CINT(ONSET * 10)/10;"s"
4700 LPRINT "MA 1200, 1360
4710 LPRINT "LASTANDARD ERROR ="; CINT(SE * 100)/100;"Pa"
4720 LPRINT "MA 1200, 1300
4730  LPRINT  "LACORRELATION  COEFFICIENT  =";(CINT((CC  *
100000!)-90000!) + 90000!)/100000!
4740 LPRINT "MA 1420, -150"
4750 LPRINT "LA   SLOPE ="; CINT(SLOPE * 1000)/1000;"Pa/s"
4760 LPRINT "HO"
4770 GOTO 4350
4780  REM  *****          ANNOTATE  PLOT  WITH  EXPERIMENTAL
INFORMATION     ***
4790 LPRINT "SP"; KPEN: LPRINT "LT 0"
4800 LPRINT "MA 100, 1400
4810 LPRINT "DA 100, 810, 820, 810, 820, 1400, 100, 1400
4820 LPRINT "MA 100, 1270
4830 LPRINT "DA 820, 1270
4840 LPRINT "MA 100, 990
4850 LPRINT "DA 820, 990
4860 LPRINT "SP"; KPEN
4870 LPRINT "MA 160, 1320
4880 LPRINT "SI 35, 25
4890 LPRINT "LAEXPERIMENTAL INFORMATION
4900 LPRINT "MA 120, 1190": LPRINT "SI 30, 20"
4910 LPRINT "LA PROBE GAS: "; PG$
4920 LPRINT "MA 120, 1140
4930  LPRINT  "LA  GAS  PRESSURE:  ";  CINT(100  *  (AVGASP  +
14.696) / 14.696) / 100; "ATMA"
4940 LPRINT "MA 120, 1090
4950 LPRINT "LA TEMPERATURE: "; TEMP;"C"
4960 LPRINT "MA 120, 1040
4970 LPRINT "LA MEMBRANE THICKNESS: "; THK; "MM"
4980 LPRINT "MA 120, 910
```

```
4990 LPRINT "LA FLUX: "; MOLFLUX; "MOL/CM^2/S
5000 LPRINT "MA 120, 860
5010  LPRINT  "LA  PERMEABILITY:  ";  CINT(PERM  *  100)/100;
"BARRERS"
5020 LPRINT "HO"
5030 REM *****
5040 REM *****
5050 REM *****
5060 GOTO 4350
5070 REM *****       PRINT ALL EXPERIMENTAL RESULTS
5080 BEEP: COLOR 3,1: CLS: PRINT: PRINT: PRINT: PRINT: PRINT
5090 PRINT "                    INSURE THAT PRINTER IS ON AND
ON-LINE !!"
5100 PRINT: PRINT: PRINT: COLOR 7,1
5110 BEEP: INPUT "                                  (press ENTER to
continue) ", ZAP$
5120 REM *****
5130  COLOR  3,1:  CLS:  PRINT:  PRINT:  PRINT:  PRINT:  PRINT:
PRINT: PRINT
5140  PRINT  "                              PRINTING  REPORT  FOR
PERMEABILITY EXPERIMENT"
5150 PRINT: PRINT: PRINT
5160 PRINT"                                     PLEASE WAIT"
5170 LPRINT
5180  LPRINT  "                      CONDITIONS  AND  RESULTS  OF
PERMEABILITY EXPERIMENT"
5190 LPRINT: LPRINT
5200 LPRINT "             SAMPLE INFORMATION": LPRINT
5210 LPRINT "                    DATA FILE: "; FILE$: LPRINT
5220 LPRINT "                    SAMPLE: "; MEM$: LPRINT
5230  LPRINT  "                         SAMPLE PREPARATION: ";
PREP$: LPRINT
5240 LPRINT "                    OPERATOR: "; OP$: LPRINT
5250 LPRINT "                    COMMENTS: "; CMTS$
5260 LPRINT
5270 LPRINT "             EXPERIMENTAL CONDITIONS": LPRINT
5280 LPRINT USING "                      MEMBRANE THICKNESS =
#.#### mm"; THK: LPRINT
5290 LPRINT USING "                      MEMBRANE AREA = ##.#
cm^2"; MAREA: LPRINT
5300 LPRINT "                    PROBE GAS: "; PG$: LPRINT
5310 LPRINT USING "                      GAS PRESSURE = ###.#
psig"; AVGASP: LPRINT
5320 LPRINT USING "                        CELL TEMPERATURE =
##.# C"; TEMP: LPRINT
5330 LPRINT USING "                        CELL VOLUME = ##.#
ml"; CV: LPRINT
5340 LPRINT USING "                        LEAK RATE = #.####
Pa/s"; LR
5350 LPRINT
5360 LPRINT "             RESULTS OF EXPERIMENT": LPRINT
5370 LPRINT USING "                          FLUX = ##.###^^^^
```

```
mol/s/cm^2"; MOLFLUX: LPRINT
5380 IF CMTS$ = "NBS SRM 1470" THEN LPRINT USING "
        PREDICTED   FLUX   =   ##.##^^^^   mol/s/cm^2";   STDPG:
LPRINT
5390 LPRINT USING "                                    PERMEABILITY =
##.##^^^^ barrers"; PERM
5400 LPRINT
5410 LPRINT "              RESULTS OF STASTISTICAL ANALYSIS":
LPRINT
5420 LPRINT "                                      REGRESSION LINE
CHARACTERISTICS:": LPRINT
5430 LPRINT USING "                               SLOPE = ##.##^^^^
Pa/s"; CSLOPE: LPRINT
5440 LPRINT USING "                               STANDARD ERROR IN
SLOPE = ##.##^^^^ Pa/s"; SEBETA1: LPRINT
5450 LPRINT USING "                            TIME LAG = ##.##^^^^
s"; ONSET: LPRINT
5460 LPRINT USING "                                  Y-INTERCEPT =
##.##^^^^ Pa"; INCPT: LPRINT
5470 LPRINT USING "                               STANDARD ERROR IN
INTERCEPT = ##.##^^^^ Pa"; SEBETA0: LPRINT
5480 LPRINT USING "                                STANDARD ERROR =
##.##^^^^ Pa"; SE: LPRINT
5490 LPRINT USING "                                       CORRELATION
COEFFICIENT = #.#####"; CC
5500 FOR S = 1 TO 9: LPRINT: NEXT
5510 GOTO 4350
5520 REM *****
5530 COLOR 3,1: CLS: PRINT: PRINT: PRINT: PRINT
5540 NKEYL% = 0: L = 0: M = 0
5550 FOR A = 1 TO 10: LIN$(A) = "0": NEXT
5560  PRINT  TAB(24)  "Annotation  of  Data  Plot  with  Key":
PRINT: PRINT: COLOR 7,1
5570 PRINT TAB(26): INPUT "Enter number of lines in key: ",
NKEYL%: PRINT: COLOR 3,1: PRINT
5580 PRINT TAB(28) "Location of Key on Plot": PRINT
5590 PRINT TAB(13) "1: upper left     2: upper center     3:
upper right"
5600 PRINT TAB(13) "4: lower left     5: lower center     6:
lower right"
5610 COLOR 7,1: PRINT: PRINT TAB(27): INPUT "Enter location
to draw key: ", KEYLOC: PRINT
5620 PRINT TAB(18): INPUT "Select pen to draw and label key
(1/2/3/4): ", KEYPEN:CLS: COLOR 3,1: PRINT: PRINT: PRINT:
PRINT
5630 PRINT TAB(27) "Information to Place in Key": PRINT:
COLOR 7,1
5640 FOR L = 1 TO NKEYL%
5650 PRINT TAB(13) "line"; L;":"
5660 LOCATE 6+L, 23: INPUT "", LIN$(L): NEXT L
5670 PRINT: COLOR 3,1: PRINT: PRINT TAB(21): INPUT "Press
<ENTER> to continue or R to redo ", AGAIN$
```

```
5680 IF AGAIN$ = "R" THEN GOTO 5530
5690 CLS: FOR H = 1 TO 8: PRINT: NEXT
5700 COLOR 7,1: PRINT TAB(28) "DRAWING KEY - PLEASE WAIT"
5710 REM *****
5720 REM *****
5730 LINMAX = LEN(LIN$(1))
5740 IF NKEYL% = 1 THEN GOTO 5790
5750 FOR M = 1 TO NKEYL%-1
5760 IF LEN(LIN$(M+1)) > LINMAX THEN LINMAX = LEN(LIN$(M+1))
5770 NEXT M
5780 REM *****
5790 LPRINT "SP"; KEYPEN: LPRINT "SI 40,32"
5800 IF KEYLOC = 1 THEN LPRINT "MA 100,1300": GOTO 5870
5810 IF KEYLOC = 2 THEN LPRINT "MA"; 1000 - LINMAX * 16 -
50, 1300: GOTO 5870
5820 IF KEYLOC = 3 THEN LPRINT "MA"; 2000 - LINMAX * 32 -
100, 1300: GOTO 5870
5830 IF KEYLOC = 4 THEN LPRINT "MA 100,"; 100 + L * 40 + 50
+ (L-1) * 20: GOTO 5870
5840 IF KEYLOC = 5 THEN LPRINT "MA"; 950 - 16 * LINMAX, 150
+ 40 * L + (L-1) * 20: GOTO 5870
5850 IF KEYLOC = 6 THEN LPRINT "MA"; 1900 - 32 * LINMAX, 150
+ 40 * L + (L-1) * 20: GOTO 5870
5860 GOTO 5530
5870 REM *****
5880 REM *****
5890 Y2 = -40-40*L-(L-1)*20: X3 = 90+32*LINMAX: Y4 =
40+40*L+(L-1)*20: X5 = - 32*LINMAX-90: X2 = 0: Y3 = 0: X4 =
0: Y5 = 0
5900 LPRINT "DR"; X2;","; Y2;","; X3;","; Y3;","; X4;",";
Y4;","; X5;","; Y5
5910 LPRINT "MR 50,-90": LPRINT "LA"; LIN$(1)
5920 IF NKEYL% = 1 THEN GOTO 5970
5930 FOR N = 1 TO NKEYL%-1
5940 LPRINT "MR"; -LEN(LIN$(N)) * 32, -60
5950 LPRINT "LA"; LIN$(N+1)
5960 NEXT N
5970 LPRINT "HO"
5980 GOTO 2960
5990 REM *****
6000 END
```

APPENDIX E

DIFFERENTIAL PRESSURE TRANSDUCER

CALIBRATION CALCULATIONS

The theoretical slope value was calculated using the density of water at 24°C and the acceleration of gravity at an altitude of 600 meters:

d H_2O @ 24°C = 0.997327 gm/cc [56]

g at latitude 37° [57] = 979.908 cm/sec^2

correction of g at 600 meters:

- 0.0003086 cm/sec x 600 = - 0.1852 cm/sec^2

g at 600 meters and 37 latitude = 979.723 cm/sec^2

$P = d \cdot g \cdot h$

P = 0.0977104 x h (in cm of water) [=] kPa

Then, the theoretical slope is:

kPa = 0.0977104 x cm H_2O

and the values for the theoretical curve are:

APPENDIX E (CONT.)

cm H_2O	kPa (theoretical)
53.8	5.25
44.1	4.30
34.2	3.33
24.3	2.38
14.6	1.42
4.7	0.45

The appreciation of the water manometer (in cm) was up to the first decimal figure (e.g. 44.1 cm). The experimental pressure was recorded with two decimal figures (e.g. 4.30 kPa).

APPENDIX F

TABLE F.1. NUMBER AVERAGE MOLECULAR WEIGHT OF THE NETWORK CHAINS ($\overline{M}c$)

BLEND	% INSOLUBLES	W_o (gms) (a)	W_s (gms) (b)	$\overline{M}c$ (c) (gm/mol)
20K,100%,120 min	44.5	0.1982	8.58	321819
20K/10K,95/5				
10 min	48.3	0.1398	4.51	190576
30 min	63.4	0.1995	6.49	193451
120 min	73.0	0.3205	6.79	88453
20K/10K,50/50				
10 min	40.8	0.113	3.27	156634
30 min	80.1	0.4075	6.63	53857
120 min	94.5	0.291	3.92	37460
10K,100%				
10 min	67.2	0.3035	5.59	68105
120 min	87.1	0.5727	6.76	28915
20K/5K,95/5				
30 min	36.9	0.1698	6.32	246290
120 min	80.8	0.3234	5.94	67751
20K/5K,75/25				
10 min	56	0.250	4.42	63050
30 min	82	0.280	4.25	47169
120 min	83	0.153	1.78	28097
20K/5K,50/50				
10 min	88.9	0.3465	5.28	47523
30 min	89.3	0.3781	5.13	37987
120 min	86.3	0.2872	2.49	15509
16K,100%				
10 min	35.8	0.1024	3.49	210432
30 min	54.6	0.1497	3.92	130609
120 min	74.8	0.1764	3.33	71317
16K/5K,50/50				
10 min	79.8	0.2577	3.67	41721
30 min	90.1	0.2760	3.63	35754

a - W_o = Initial Weight (unswollen polymer) in gms.
b - W_s = Weight of Swollen Polymer in gms.
c - $\overline{M}c$ = Average Molecular Weight of network chains.

APPENDIX F (CONT.)

TABLE F.2. CROSSLINK DENSITY AND SWELLING RATIO.

BLEND	dc (chains/cc)	Q
20K,100%,120 min	0.23E19	43.29
20K/10K,95/5		
10 min	0.40E19	32.26
30 min	0.39E19	32.53
120 min	0.85E19	21.19
20K/10K,50/50		
10 min	0.48E19	28.94
30 min	1.4E19	16.27
120 min	2.01E19	13.47
10K,100%		
10 min	1.11E19	18.42
120 min	2.6E19	11.80
20K/5K,95/5		
30 min	0.31E19	37.22
120 min	1.11E19	18.37
20K/5K,75/25		
10 min	1.2E19	17.68
30 min	1.6E19	15.18
120 min	2.68E19	11.63
20K/5K,50/50		
10 min	1.58E19	15.23
30 min	1.98E19	13.57
120 min	4.85E19	8.67
16K,100%		
10 min	0.36E19	34.08
30 min	0.58E19	26.19
120 min	1.06E19	18.88
16K/5K,50/50		
10 min	1.8E19	14.24
30 min	2.1E19	13.15

a - dc= Crosslink Density.
b - Q = Swelling Ratio = W_s/W_o

VITA

Silvia Parisi Skischally was born on November 30, 1955 and raised in Buenos Aires (Argentina) and Caracas (Venezuela). In 1980 she graduated from "Universidad Simón Bolivar" receiving a "Licenciatura" in Chemistry. In 1981 she was employed at INTEVEP, S.A. (Venezuelan Petroleum Institute for Research and Development, filial of PDVSA). At this company, she worked on enhanced oil recovery and natural gas separation projects. In 1987, she was sponsored by INTEVEP, S.A. to enter the graduate level program at Virginia Tech, with emphasis in membrane technology. Under the direction of Professor James E. McGrath, she received her M.Sc. degree in Chemistry (Polymer Science) in 1990. Silvia is currently employed at INTEVEP, S.A. in Caracas, Venezuela.